ANTICIPATING NATIONWIDE RISKS TO DRINKING WATER: PREDICTING LOCAL SCALE CONTAMINATION OF COMMUNITY SUPPLY WELLS BY GASOLINE ADDITIVES

by

J. Samuel Arey

B.S., Public Policy and Environmental Science
Indiana University, Bloomington
(1998)

Submitted to the Department of Civil and Environmental Engineering in partial fulfillment of the requirements for the Degree of

MASTER OF SCIENCE
in Civil and Environmental Engineering
at the

Massachusetts Institute of Technology

June 2001

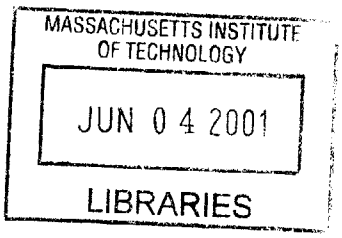

Signature of Author_____
Department of Civil and Environmental Engineering
25 May, 2001

Certified by _____
Philip M. Gschwend
Professor of Civil and Environmental Engineering
Thesis Supervisor

Accepted by ____
Oral Buyukozturk
Chairman, Departmental Committee of Graduate Studies

ANTICIPATING NATIONWIDE RISKS TO DRINKING WATER: PREDICTING LOCAL SCALE CONTAMINATION OF COMMUNITY SUPPLY WELLS BY GASOLINE ADDITIVES

by

J. Samuel Arey

Submitted to the Department of Civil and Environmental Engineering on
May 25, 2001 in partial fulfillment of the requirements for the
Degree of Master of Science in Civil and Environmental Engineering

ABSTRACT

Only ten years after the increased addition of methyl-*tert*-butylether (MTBE) to U.S. gasolines, nationwide MTBE contamination of thousands of drinking water supply wells has been widely documented, reflecting enormous environmental and economic costs. Due to its abundance in gasoline, high aqueous solubility, and slow degradation rate in aquifers, MTBE has migrated in significant quantities from subsurface gasoline spills to a substantial number of community and private drinking water wells in a short period of time. For the purposes of this project, it was hypothesized that the tendency for gasoline additives to contaminate subsurface drinking water resources could be accurately predicted *a priori* using a generalized transport model.

A screening method was developed to predict both the migration times of gasoline constituents from a leaking underground fuel tank (LUFT) to a community drinking water supply well and expected contaminant levels in the well. A review of literature revealed that U.S. municipal drinking water supplies are typically found in shallow sand and gravel aquifers. A subsurface transport model was parameterized based on the proximity of community supply wells to LUFTs (1000 m); probable characteristics of sand and gravel aquifers; typical pumping rates of community supply wells (80 to 400 gal/min); and reasonable gasoline spill volumes from LUFTs (100 to 1000 gal). The transport model was tailored to individual solutes based on their estimated abundances in gasoline, gasoline–water partition coefficients (K_{gw}), and estimated organic matter–water partition coefficients (K_{om}).

Transport calculations were conducted for 17 polar and four nonpolar compounds currently proposed for or found in contemporary U.S. gasolines, including MTBE, ethanol, and methanol. Subsurface degradation processes were not considered. The transport model predicted MTBE concentrations of 40 to 500 ppb in municipal wells, which compared favorably with observed well concentrations at a significant proportion of sites in the U.S. The transport model therefore captured the order of magnitude of observed MTBE contamination of municipal wells without any use of adjustable or "fitted" parameters.

Subsurface transport calculations of gasoline constituents required prior knowledge or estimation of their gasoline–water partition coefficient and organic matter–water partition coefficients. In anticipation of the need to conduct transport calculations for novel or previously unstudied compounds, a review of methods for calculating or predicting solute partition coefficients in gasoline–water, organic matter–water, and octanol–water systems was conducted. Additionally, a new linear solvation energy relationship (LSER) was developed for estimating gasoline–water partition coefficients of organic compounds, having an estimated standard error of 0.22 log K_{gw} units.

Thesis Supervisor: Dr. Philip M. Gschwend

Title: Professor of Civil and Environmental Engineering

Acknowledgments

This research was supported by the Martin Family Society of Fellows for Sustainability, the Alliance for Global Sustainability, the Ralph M. Parsons Fellowship Foundation, the Schoettler Scholarship Fund, and the Ford Scholarly Allowance.

Charles Harvey, Fatih Eltahir, Kris McNeill, John MacFarlane, Bill Green, Eleanor Kane, Ico san Martini, and the Gschwend laboratory research group at MIT all deserve my thanks for their criticism and assistance regarding chemical and hydrogeologic modelling, statistical analysis, equipment and model support, and writing revisions.

Additional thanks go to Al Leo (BioByte Corp.), Jim Landmeyer (USGS) Torsten Schmidt and Stephan Haderlein at the Swiss Federal Institute (ETH), Katsuya Kawamoto (Kanto Gakuin University), Toby Avery (Mobil-Exxon Corp.), Curt Stanley, Bruce Bauman, and Gerry Raabe at the American Petroleum Institute (API), and John Brophy and Jim Caldwell at the EPA for their contributions to my data gathering efforts, legislative interpretations, model design and "real world" perspective.

I could not have completed this project without the continual support of my friends and parents. I am especially grateful for the guidance and endless enthusiasm provided by Phil Gschwend.

Table of Contents

List of Tables

List of Figures

Chapter 1

Introduction. Assessing the Impact of Fuel Additives on National Drinking Water Resources: Development of a Transport Modeling Methodology

1-1. Motivation and purpose

Accumulated experience with environmental contamination has continually led western society to reconsider questions about anthropogenic compounds, including the following: (1) How much of the contaminant is released into the environment? (2) Once in the environment, how does the contaminant transport and transform, thereby controlling exposures to humans and ecosystems? (3) When these exposures occur, what health effects will result? The answers to these questions generate the basis for estimating the social costs of environmental contaminants of interest.

These inquiries are not all feasibly addressed for most chemicals. Question 1 is usually the easiest to answer. In the case of groundwater contamination by fuels, the characteristics of releases are directly related to the estimated number of leaking fuel storage tanks and spillage releases from automobiles during refuelling. Question 3 is probably the hardest to answer: health effects studies are expensive and frequently inconclusive, and usually give information about only certain types of toxicity effects.

Since toxicity and health effects of a contaminant are difficult to address, heavy scientific focus is frequently placed on question 2, the environmental behavior of a contaminant: *how does the compound travel and react in the environment, thereby resulting in human and ecological exposures?* When this critical issue is resolved, the level of need for aggressive health effects testing and envionmental monitoring can be established. For example, although gasoline is composed of hundreds of compounds, toxicity testing and environmental monitoring is only relevant for the few components that may produce significant exposures in the environment.

This preliminary environmental assessment raises a more salient and useful point, however. The transport and reaction behavior of a chemical could be studied before it is introduced to society on a large scale. This pre-emptive modeling could avert future environmental and human health damage and properly focus nationwide contaminant characterization and health effects testing.

In other words, if the environmental transport and reaction behavior of compounds such as tetraethyllead (TEL) and methyl-*tert*-butylether (MTBE) had been studied before they were added to gasoline, the massive environmental, human health, and economic costs incurred by their use might have been avoided. Industrial lead use has increased ambient atmospheric lead concentrations by a factor of 300 [1], and the use of TEL in U.S. gasoline has been linked to child lead poisoning on a national scale [1]. MTBE use in gasolines has resulted in the closure of thousands of drinking water supplies in the U.S. over only a few years, thereby constituting enormous economic and environmental setbacks for society [2-8].

Literally thousands of compounds are used or imported at quantities greater than 1 million lbs per year in the U.S., but basic toxicity data exist for only 10% of these [9]. Over 70,000 synthetic chemicals are now commercially used in the U.S., and about 1000 new compounds are developed for industrial or commercial use every year [10]. In light of accelerating chemical production, the ability to *a priori* assess the environmental transport behaviors of proposed commercial compounds clearly has enormous potential benefits in terms of future human health and ecological and economic cost avoidance. Specifically, the development of a modeling tool to predict the exposure levels of future gasoline additives is an important need, based on past experience with TEL and MTBE.

The **purpose** of this study was therefore to address the following problem. Given a hypothetical newly proposed organic gasoline additive, can one: (1) predict the subsurface transport behavior and drinking water exposures that will result, on a nationwide scale; and (2) tailor these predictions to individual compounds based on physical property estimation methods? *If feasible and accurate, such calculations would allow the threat of future proposed gasoline additives to drinking water resources to be rapidly screened before these additives are used nationwide.*

1-2. The "ensemble average" transport modeling approach

How does one go about developing a model to predict a nationwide subsurface contamination problem? General methodologies for the prediction of compound transport in site-specific hydrogeologic settings have been mapped extensively [11-14]. This foundation can be extended to assess the environmental impact of contamination at a multitude, or distribution, of sites.

Clearly, making specific environmental contamination predictions for every leaking underground fuel tank (LUFT) site in the U.S. is a cost-prohibitive evaluation of the potential environmental costs of using a newly proposed gasoline additive. If possible, the hydrogeology of these sites must instead be generalized to model an "ensemble average" of probable transport behaviors in various hydrogeologic settings. The ensemble methodology does not specifically predict contaminant behavior at any individual site, but it might predict the order of magnitude effects at many or most sites. In other words, I hope to predict the nationwide drinking water contamination consequences of specific gasoline additives by calculating the average behavior of many gasoline spills.

Fortunately, some common sense can be used to restrict the set of gasoline spills under consideration. Since the receptor of interest is drinking water, it is useful to consider only those gasoline spills that are within reasonable vicinity of a community water supply well. Additionally, as a first approximation, only LUFT sources of contamination will be considered. LUFTs are a considerable source of groundwater contamination by gasoline: over 330,000 confirmed releases from regulated LUFTs were reported to EPA between 1988 and 1998 [15]. Substantial data exist on both LUFT locations and their locations relative to community supply wells [16].

Restricting the ensemble approach to this subset of gasoline spills substantially focuses the scope of the transport problem. Investigation of the literature reveals that if only areas near community supply wells are considered, variability in the transport parameters of the sites is significantly reduced. In other words, under these assumptions, critical hydrogeologic characteristics of the transport problem are somewhat generalizable. This is discussed in greater detail in Chapter 3.

The ensemble approach is intended as a screening tool for regulators concerned about what compounds should be put in gasoline. It is therefore not very useful for modeling individual site contamination. A larger goal of this approach is to lay additional groundwork for the large scale modeling of contamination transport, such as that in urban airsheds, rivers, or lakes [17-20].

1-3. Physical property estimation methods

As stated previously, rapid and accurate estimation of physical properties is desirable in the context of a transport screening model for gasoline additives. The rationale for this is two-fold. First, the whole point of a screening method is that it provides a low-cost tool for quickly determining whether a particular societal activity is likely to cause substantial risks or costs. Generally, laboratory measurement of physical properties relevant to environmental transport requires time and money, whereas a modeling procedure is rapid and inexpensive. Second, the "ensemble" approach is proposed with the larger goal of applicability to many kinds of chemicals in other commercial and industrial contexts.

The current "state of the science" for calculating phase partitioning in pertinent environmental media is therefore reviewed, including estimation methods of octanol–water partition coefficients, gasoline–water partition coefficients, and organic matter–water partition coefficients.

1-4. Outline of thesis work

Chapter 2 addresses the composition of contemporary gasoline and the U.S. regulatory guidelines that protect water supplies from contamination by gasoline components. Although gasoline includes several heteroatomic organic (and hence somewhat water-soluble) compounds, most of these chemicals are not considered in regulatory guidelines, nor are they tested for in drinking water supplies. A set of two dozen relevant compounds found in gasoline was selected to test the physical property estimation methods and the transport modeling approach.

In *Chapter 3*, the transport model is outlined and the basis of the ensemble approach is defended using hydrogeologic data. Transport model parameters were derived and an example calculation is shown.

Chapter 4 is an overview of physical property estimation methods of partition coefficients and some benchmarks describing their accuracy and robustness. This chapter

describes the current state of the science, but it may also give insight into the future of physical property calculation methods.

In *Chapter 5*, the transport method and some physical property estimation methods are applied to several of the heteroatomic organic compounds found in gasoline (from Chapter 2). This chapter thus provides practical examples of the subsurface transport screening model. Additionally, it serves as a preliminary assessment of the potential drinking water impacts of the current (known) formulation of gasoline.

Conclusions and recommendations for future research and policy needs are discussed in *Chapter 6*.

1-5. Citations

1. Misch, A., *Assessing Environmental Health Risks*, in *State of the World, A Worldwatch Institute Report on Progress Toward a Sustainable Society*, L. Brown, Editor. 1994, W W Norton and Co.: New York, NY. p. 119.
2. Squillace, P.J., J.F. Pankow, N.E. Korte, and J.S. Zogorski, *Review of the environmental behavior and fate of methyl tert-butyl ether.* Environmental Toxicology and Chemistry, 1997. **16**(9): p. 1836-1844.
3. Allen, S., *Gas additive debated from Tahoe to Maine.* The Boston Globe, March 1, 1999. p. A1, A8.
4. Giordano, A., *MTBE found in N.H. drinking water, report says.* The Boston Globe, March 1, 1999. p. A8.
5. Lien, D., *Minnesota ethanol industry eager to replace polluting gas additive.* Saint Paul Pioneer Press, January 29, 2000.
6. Staff, *California board wants to eliminate MTBE.* United Press International, February 9, 2000.
7. Staff, *Clinton may act on gas additive.* Associated Press, February 23, 2000.
8. Staff, *Senate panel approves MTBE ban.* Associated Press, September 7, 2000.
9. Johnson, J., *Chemical Testing: Chemical makers volunteer to conduct toxicity tests on commonly used chemicals.* Chemical & Engineering News, March 8, 1999. p. 9.
10. Miller, G.T., *Living in the Environment.* 1996, New York, NY: Wadsworth Publishing Company. p. 18, 550.
11. Kitanidis, P.K., *Prediction by the method of moments of transport in a heterogeneous formation.* Journal of Hydrology, 1988. **102**: p. 453-473.
12. Mackay, D.M., P.V. Roberts, and J.A. Cherry, *Transport of organic contaminants in groundwater.* Environmental Science & Technology, 1985. **19**(5): p. 384-392.
13. Thierrin, J. and P.K. Kitanidis, *Solute dilution at the Borden and Cape Cod groundwater tracer tests.* Water Resources Research, 1994. **30**(11): p. 2883-2890.
14. Charbeneau, R.J., in *Groundwater Hydraulics and Pollutant Transport.* 2000, Prentice Hall: Saddle River, NJ. p. 375-418.
15. Davis, M., J. Brophy, R. Hitzig, F. Kremer, M. Osinski, and J. Prah, *Oxygenates in Water: Critical Information and Research Needs.* 600/R-98/048, Office of Research and Development, U.S. Environmental Protection Agency, 1998. p. 7.
16. Johnson, R., J.F. Pankow, D. Bender, C. Price, and J.S. Zogorski, *MTBE, To what extent will past releases contaminate community water supply wells?* Environmental Science & Technology, 2000. **34**(9): p. 2A-9A.
17. Mackay, D. and E. Webster, *Linking emissions to prevailing concentrations - exposure on a local scale.* Environmetrics, 1998. **9**: p. 541-553.
18. MacFarlane, S. and D. Mackay, *A fugacity-based screening model to assess contamination and remediation of the subsurface containing non-aqueous phase liquids.* Journal of Soil Contamination, 1998. **17**(1): p. 17-46.
19. Mackay, D., A.D. Guardo, S. Paterson, G. Kicsi, and C.E. Cowan, *Assessing the fate of new and existing chemicals: a five stage process.* Environmental Toxicology and Chemistry, 1996. **15**(9): p. 1618-1626.
20. Mackay, D., A.D. Guardo, S. Paterson, G. Kicsi, C.E. Cowan, and D.M. Kane, *Assessment of chemical fate in the environment using evaluative, regional and local-*

scale models: illustrative application to chlorobenzene and linear alkylbenzene sulfonates. Environmental Toxicology and Chemistry, 1996. **15**(9): p. 1638-1648.

Chapter 2

Identification of Current Fuel Additives: The Chemical Structures and Abundances of Polar Compounds Found in Western Gasolines

2-1. Introduction

In an environmental context, fuels are conventionally viewed as a mixture of nonpolar hydrocarbons. A few small, aromatic hydrocarbon components, which are somewhat water-soluble and therefore mobile in aquifers, are considered possible groundwater contaminants, according to regulatory and academic literature. More recently, the oxygenate, methyl-*tert*-butylether (MTBE), has been discovered to widely contaminate municipal water supplies, from leaking gasoline underground storage tanks or spills [1]. Other potential oxygenates have also come under scrutiny as a result [2-4].

In reality, fuels contain a variety of organic compounds with heteroatom-containing (nitrogen, oxygen, or sulfur) substituents. These compounds are generally more polar than hydrocarbon components. As a result, they are more water-soluble and thus more likely to transport rapidly and in significant quantities to drinking water wells. Regulatory and wellhead protection literature neither mentions the presence of heteroatom-containing compounds nor considers them an important threat to groundwater. Consequently, neither municipalities nor regulators are encouraged to analyze community drinking water supplies for them.

The purposes of this chapter were to: (1) briefly discuss how contamination of municipal water supplies by fuel constituents and additives is treated in current regulatory and academic literature; (2) review a list of heteroatomic organic compounds which are either additives or refining byproducts currently found in gasoline; and (3) motivate the development of subsurface transport modeling efforts focused on heteroatomic organic compounds found in gasoline.

2-2. Currently evaluated compounds in fuels

In regulatory guides and associated literature for municipalities regarding water supply contamination, the EPA characterizes gasoline and diesel fuel as posing a contamination threat from either "hydrocarbons," "volatile organic compounds" (VOCs), or "oxygenates" [5-7]. Exactly what compounds do these phrases refer to?

EPA wellhead protection guide literature describes "hydrocarbons" as the following compounds [8]: benzene, toluene, ethylbenzene, xylenes, C_3-substituted benzenes, and naphthalene. "Volatile organic compounds" are described in the Safe Drinking Water Act as [9]: benzene, toluene, ethylbenzene, xylenes, and several other chlorinated compounds (by law, there are no chlorinated compounds in gasoline). Currently used "oxygenates" include MTBE and ethanol, although several other oxygen-containing compounds have been proposed as fuel additives in academic and EPA literature [6].

Thus, according to regulatory literature, only a few oxygenates and aromatic hydrocarbons are considered potential threats to water supplies from leaking underground fuel tanks (LUFTs). Until recently [10, 11], studies which considered water contamination by fuel constituents other than hydrocarbons and oxygenates have generally focused on identifying parties reponsible for fuel-associated subsurface contamination [12, 13].

In federal regulatory code (CFR), rules on the specific chemical composition of fuel constituents and additives are unrestrictive. Fuel additives must be registered with the EPA, with information about their chemical composition or the precise process for their production [14]. EPA approves fuel additive compositions without academic or public oversight, as patent privacy precludes the agency from sharing specific composition information with the public. The only other notable restriction on gasoline, diesel fuel, and fuel additive compositions is that they "contain no elements other than carbon, hydrogen, oxygen, nitrogen, and/or sulfur." Additionally, they must contain less than 1.5 percent wt/wt oxygen and less than 1000 ppm sulfur (the sulfur limit is currently undergoing revision, however) [14]. In summary, heteroatom-containing compounds in gasoline other than those specifically mentioned thus far (i.e., compounds other than MTBE, ethanol, benzene, toluene, ethylbenzene, xylenes, propylbenzene, or naphthalene) are largely unregulated. Their potential impact on human health and the environment as related to fuel spills is entirely unstudied in the public record.

2-3. Gasoline additives (other than oxygenates)

There are several specific compounds intentionally added to gasoline (Table 2-1). These compounds and mixtures improve engine performance, clean and lubricate engine valves, increase the octane number, improve emissions quality, preserve fuels during storage, and perform other functions [10, 15-19]. The concentrations of such compounds are in the 10 to 400 ppm range; lower than the abundances of typically studied gasoline constituents.

Table 2-1. A list of gasoline additives

N,N'-disalicylidene-1,2-diaminopropane [15]
Use: chelating agent used to inactivate copper
C_{fuel} = 5 to 12 ppm

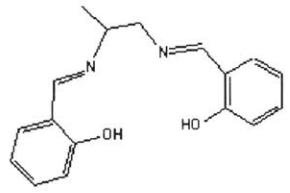

polyisobutylated amines [16]
Use: detergent/dispersant
C_{fuel} = 100 to 250 ppm

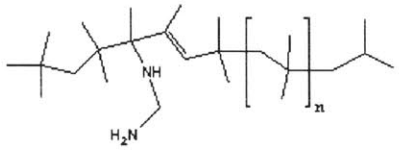

n = 13 to 25

polyisobutylene mannich bases [16]
Use: detergent/dispersant
C_{fuel} = 100 to 250 ppm

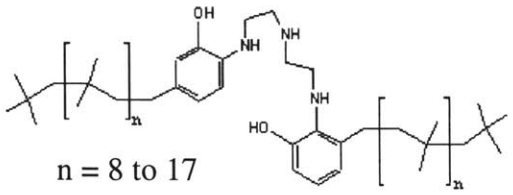

n = 8 to 17

aminated polypropylene oxides [16]
Use: detergent carrier fluid
C_{fuel} = 100 to 250 ppm

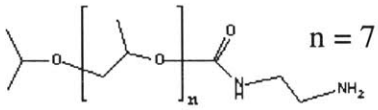

n = 7 to 16

imidazolines [16]
Use: detergent/dispersant
C_{fuel} = 20 to 60 ppm

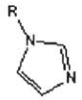

N,N'-disecbutyl-p-phenylenediamine
(N,N'-dialkyl-p-phenylenediamines) [15]
Use: antioxidant (preservative)
C_{fuel} = 5 to 20 ppm

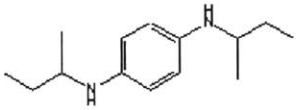

2,4-dimethyl-6-tertbutylphenol [15]
Use: antioxidant (preservative)
C_{fuel} = 5 to 100 ppm

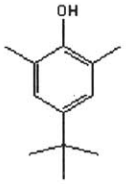

butylated hydroxytoluene (BHT) [15]
Use: antioxidant
C_{fuel} = 5 to 100 ppm

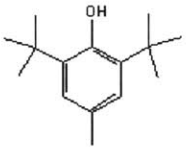

cerium (or other metal) naphthenates [17]
Use: catalyst
C_{fuel} = 25 to 50 ppm

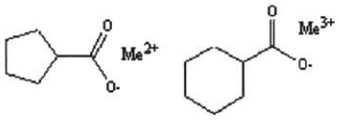

furfural [15]
Use: dye/marker
C_{fuel} = ?

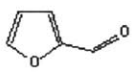

diphenylamine [15]
Use: dye/marker
C_{fuel} = ?

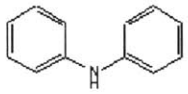

2-4. Other polar compounds found in gasoline

In addition to gasoline additive compounds documented in the literature, there are several heteroatom-containing compounds which have been measured in U.S. and European gasolines (Table 2-2) [10-13, 18, 19]. These compounds may have originated in the crude oil as a result of natural processes, or they may have been formed or added during petroleum refining.

Table 2-2. A list of other polar compounds found in retail gasolines

benzotriazole [10]
C_{fuel} = ?

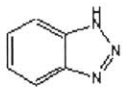

1-methylbenzotriazole [10]
C_{fuel} = ?

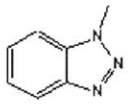

aniline [12, 10, 11, 13]
C_{fuel} = 0.1 to 21 ppm [17]

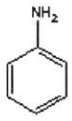

p-toluidine [12, 10, 13]
C_{fuel} = 0.2 to 37 ppm [17]

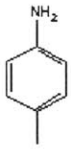

o-toluidine [12, 10, 11]
C_{fuel} = 0.2 to 24 ppm [17]

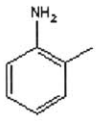

3,4-dimethylaniline [10]
C_{fuel} = est. up to 16 ppm [10]

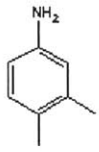

2,6-dimethylaniline [10]
C_{fuel} = est. up to 16 ppm [10]

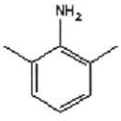

phenol [12, 10, 11, 13]
C_{fuel} = 0.8 to 170 ppm [10]

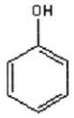

p-cresol [12, 10, 13]
C_{fuel} = 0.3 to 120 ppm [10]

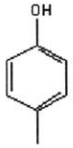

o-cresol [12, 10, 13]
C_{fuel} = 1.5 to 130 ppm [10]

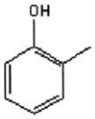

3,4-dimethylphenol [12, 10, 11, 13]
C_{fuel} = est. up to 40 ppm [10]

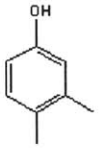

2,6-dimethylphenol [11]
C_{fuel} = est. up to 40 ppm [10]

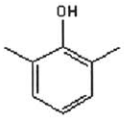

3,4,5-trimethylphenol [12, 10]
C_{fuel} = ?

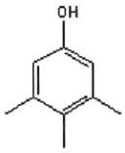

2,4,6-trimethylphenol [12, 10]
C_{fuel} = ?

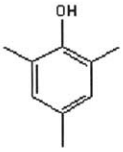

thiophene [18, 19]
C_{fuel} = 18 to 178 ppm [19]

benzothiophene [18, 19]
C_{fuel} = 0 to 385 ppm [19]

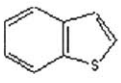

2-5. Discussion and conclusions

Like MTBE, most of the compounds shown in Tables 2-1 and 2-2 are fairly low molecular weight and include one or more heteroatom-containing substituents. As a result, they are likely to be polar, somewhat water-soluble, and poorly retarded in aquifers. The high water solubility of these compounds will enhance their partitioning from fuel non-aqueous phase liquid (NAPL) to groundwater after a subsurface spill or leak. Thus, although many of the heteroatomic organic compounds shown here are present in fuels at low concentrations, they may create high aqueous plume concentrations in aquifers as a result of their partitioning behavior.

Unlike MTBE, the compounds in Tables 2-1 and 2-2 are not generally tested for in municipal water supplies. Whether they are currently contaminating water supplies as prevalently as MTBE is entirely unknown, since they may or may not have the same low "odor threshold" that originally brought MTBE to light as a potential drinking water safety threat [6]. It is important to note that the list of gasoline additives presented here is not necessarily comprehensive. Due to trade privacy barriers, such a compilation would require rigorous experimental analysis of retail gasolines, which is beyond the scope of this study. However, published experimental investigations of gasoline components have generally considered the most light and highly polar compounds, that is, those most likely to solubilize in water [10-13].

The potential problem of water-soluble, highly mobile compounds transporting from fuel leaks to water supplies was the focus of quantitative modeling efforts discussed in subsequent chapters. The goal of these efforts was to propose a general modeling methodology by which proposed gasoline additives might be systematically pre-evaluated before use.

2-6. Citations

1. Johnson, R., J.F. Pankow, D. Bender, C. Price, and J.S. Zogorski, *MTBE, To what extent will past releases contaminate community water supply wells?* Environmental Science & Technology, 2000. **34**(9): p. 2A-9A.
2. Huttenen, H., L.E. Wyness, and P. Kalliokoski, *Identification of environmental hazards of gasoline oxygenate tert-amyl methylether (TAME).* Chemosphere, 1997. **35**: p. 1199-1214.
3. Wallington, T.J., J.M. Andino, A.R. Potts, S.J. Rudy, and W.O. Siegl, *Atmospheric chemistry of automotive fuel additives: diisopropyl ether.* Environmental Science & Technology, 1993. **27**: p. 98-104.
4. Pacheco, M.A. and C.L. Marshall, *Review of dimethyl carbonate (DMC) manufacture and its characteristics as a fuel additive.* Energy & Fuels, 1997. **11**: p. 2-29.
5. Gardner, S. and B. Moore, *Case Studies in Wellhead Protection Area Delineation and Monitoring.* 600/R-93/107, U.S. Environmental Protection Agency, 1993.
6. Davis, M., J. Brophy, R. Hitzig, F. Kremer, M. Osinski, and J. Prah, *Oxygenates in Water: Critical Information and Research Needs.* 600/R-98/048, Office of Research and Development, U.S. Environmental Protection Agency, 1998. p. 7,20,21.
7. Belk, T., J.J. Smith, and J. Trax, *Wellhead Protection, a Guide for Small Communities.* 625/R-93/002, U.S. Environmental Protection Agency, 1993. p. 13.
8. Hoffer, R., *Guidelines for Delineation of Wellhead Protection Areas.* 4405/93/001, U.S. Environmental Protection Agency, 1987. p. 2-16.
9. *Phase I Rule of the Safe Drinking Water Act (SWDA).* 1989, U.S. Code of Federal Regulations 42: Washington, DC.
10. Schmidt, T.C., P. Kleinert, C. Stengel, and S.B. Haderlein, *Polar fuel constituents - compound identification and equilibrium partitioning between non-aqueous phase liquids and water.* 2001.
11. Potter, T., *Analysis of petroleum-contaminated water by GC/FID with direct aqueous injection.* Groundwater Monitoring and Remediation, 1996. **16**(3): p. 157-162.
12. Kanai, H., V. Inouye, R. Goo, L. Yazawa, J. Maka, and C. Chun, *Gas chromatographic/mass spectrometric analysis of polar components in "weathered" gasoline/water matrix as an aid in identifying gasoline.* Analytical Letters, 1991. **24**: p. 115-128.
13. Youngless, T.L., J.T. Swansiger, D.A. Danner, and M. Greco, *Mass spectral characterization of petroleum dyes, tracers, and additives.* Analytical Chemistry, 1985. **57**: p. 1894-1902.
14. *Sections 79.11, 79.21, 79.56(e).* 1997, U.S. Code of Federal Regulations 40: Washington DC.
15. Owen, K., *Gasoline and Diesel Fuel Additives.* 1989: John Wiley & Sons.
16. Avery, T., *Gasoline additive chemistry.* Pers. comm., Exxon-Mobil Corp., (609) 224-2615, September 12, 1998.
17. Kirk-Othmer, *Encyclopedia of Chemical Technology, 4th Edition.* 1994, New York, NY: John Wiley & Sons.
18. Martin, P., F. McCarty, U. Ehrmann, L.D. Lima, N. Carvajal, and A. Rojas, *Characterization and deposit-forming tendency of polar compounds in cracked*

components of gasoline. Identification of phenols and aromatic sulfur compounds. Fuel Science and Technology International, 1994. **12**(2): p. 267-280.

19. Quimby, B.D., V. Giarrocco, J.J. Sullivan, and K.A. McCleary, *Fast analysis of oxygen and sulfur compounds in gasoline.* Journal of High Resolution Chromatography, 1992. **15**: p. 705-709.

Chapter 3

Fugacity and Transport Calculations:
Modeling the Partitioning and Mobility of Gasoline Additives
From Leaking Underground Fuel Tanks (LUFTs)

3-1. Introduction and motivation

In this chapter, fugacity calculations and transport models were used together to describe how compounds in leaked or spilled gasoline: (1) partition from gasoline to water; (2) partition from water to aquifer solids (i.e., sorb); and (3) advect and disperse downgradient with the ambient groundwater flow towards municipal wells or other important water resources. The goal of the modeling approach was to assess the likely non-degraded groundwater concentrations and migration times of fuel constituents at downgradient municipal supply wells. The ultimate objective was to develop a screening methodology for evaluating whether any compound added to gasoline might contaminate significant numbers of municipal wells on a national scale, assuming chemical degradation in the subsurface was negligible.

Fugacity-based modeling assumes chemical equilibrium between all phases of interest, and therefore assumes that time scales of physical phenomena (e.g., groundwater flow) are slow relative to time scales of physical chemistry phenomena (e.g., partitioning between various phases). Fugacity-based models have been used previously to assess compound transport in a number of environmental contexts, including subsurface contamination [1, 2], air-shed modeling [3], and large scale and global transport [4-6].

An entire chapter was devoted to fugacity-driven transport modeling in order to emphasize that the threat of water supply contamination by fuel constituents is primarily controlled by differences in compound physical properties (e.g., the aqueous activity coefficient of naphthalene vs. that of MTBE) rather than variability in hydrogeologic contexts (e.g., alluvial aquifers vs. karst aquifers). There were three primary reasons for this approach to evaluating the mobility of organic compounds in subsurface environments. First, regardless of the specific hydrogeology, compound properties will drastically influence compound mobility and transport. Second, since the general problem of fuel leaks and spills is one that includes literally hundreds of thousands of subsurface systems, it makes little sense to evaluate the threats posed by gasoline components to groundwater with a "site-specific" modeling approach. For example, both MTBE and naphthalene are abundant fuel components exposed to the same set of hydrogeological conditions in fuel spills. However, MTBE, rather than naphthalene, has caused contamination on a large scale (thousands of sites) as a result of its unique physical properties [7, 8]. Finally, this investigation revealed that many hydrogeologic features in the vicinity of municipal water supply wells can be generalized. In other words, there is little variability in the transport parameters of these aquifers. In fact, the geological characteristics common to municipality water supply aquifers make them particularly vulnerable to contamination by highly water-soluble compounds such as those found in fuels (see Chapter 2). Accordingly, a highly relevant hydrogeologic context could be proposed to evaluate fuel additive transport from leaking underground fuel tank (LUFT) spills to municipal water wells.

Since the transport model is intended to screen the potential mobility of anthropogenic organic compounds, biological and chemical attenuation processes were not discussed here. The rates of degradation processes vary widely in different geochemical environments and depend highly on characteristics of local microbial communities and on properties of the compound of interest. As a result, most attenuation processes are difficult to predict even for site specific conditions without accompanying expensive and time-intensive experimental investigation. An important premise of this study is that environmental fugacity and transport behaviors of organic compounds can be more inexpensively and reliably predicted under a wide range of conditions than can environmental degradability. The purpose of this study was therefore to evaluate the potential threat that compounds may pose on the basis of their mobility in the environment. If individual compounds are shown to create significant risks based on their environmental transport behaviors, rigorous studies of their environmental transformation rates should be conducted.

The goals of this chapter were to: (1) describe fugacity calculations of the fuel-water partitioning and aquifer solid-water partitioning of organic compounds and discuss the validity of underlying assumptions; (2) describe a transport modeling approach which computes the advection and dispersion of a contaminant plume as it migrates through the subsurface and dilutes in a municipal supply well; and (3) combine the fugacity and transport calculations to develop a general subsurface transport screening model which reflects probable non-degraded contaminant concentrations at municipal wells downgradient of LUFTs. A "recipe" of complete and succinct instructions for conducting a detailed transport model calculation is given at the end of the Summary and Conclusions part of this chapter (section 3-8).

3-2. Fugacity computations of fuel-water partitioning

Consider a gasoline leak from an underground storage tank (Figure 3-1). As fuel percolates through the vadose (unsaturated) zone, it pools on the water table. Since the aquifers of interest in this study are generally coarse grained and shallow (refer to section 3-4), gasoline transport through the vadose (unsaturated) zone was assumed to occur relatively quickly. Next, individual compounds in the fuel mixture partition into the groundwater. The fuel-water interface was considered equilibrated with respect to chemical partitioning. In other words, partitioning kinetics were assumed fast relative to groundwater flow and dispersion processes on the sub-grain scale. Finally, dissolved compounds are transported downgradient with the groundwater flow and are subject to sorption to aquifer solids (retardation) en route. Sorption kinetics were also treated as fast relative to groundwater flow and sorption equilibrium was therefore assumed, as is discussed later (see section 3-3).

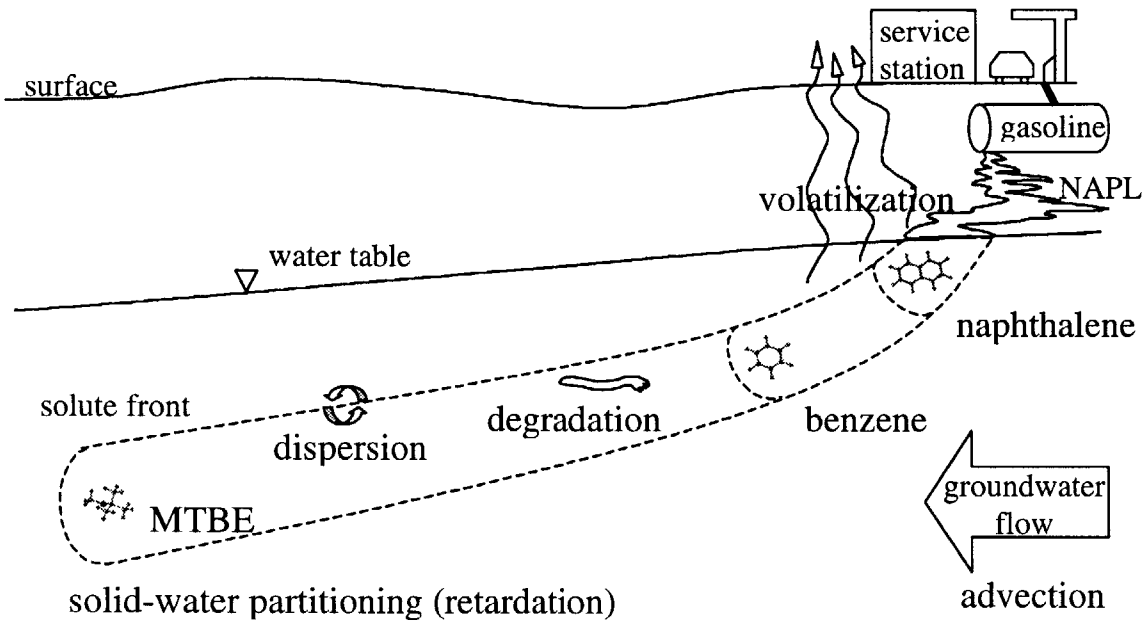

Figure 3-1. Subsurface transport of compounds from a leaking underground storage tank

The fuel-water partition coefficient, K_{fw}, describes the equilibrium concentrations of a compound between two adjacent phases:

$$K_{fw} = C_f/C_w \tag{3-1}$$

where C_f = concentration in fuel [mol L^{-1}], and
C_w = concentration in water [mol L^{-1}].

The partitioning of a solute is governed by the activity coefficients of the solute in different phases:

$$K_{fw} = (\gamma_w V_w)/(\gamma_f V_f) \tag{3-2}$$

where V_f = molar volume of fuel phase (~ 0.12 L mol^{-1}),
V_w = molar volume of aqueous phase (~ 0.018 L mol^{-1}),
γ_f = activity coefficient of solute in fuel [mol_{fuel} mol_{solute}^{-1}], and
γ_w = activity coefficient of solute in water [mol_{water} mol_{solute}^{-1}].

An activity coefficient describes the nonideality of the solute in the phase of interest: the pure liquid phase of the solute itself is considered the "ideal" (reference) state, definitionally having an activity coefficient value of unity. The molar volume of the aqueous phase is treated as equivalent to that of pure water. The molar volume of the fuel phase is formulated as the sum of fractional molar volumes of major fuel components (see section 5-3). The solute activity coefficient is proportional to the exponent of the partial molar excess free energy of solution,

ΔG_s^e. The excess free energy of solubilization represents the energetic cost of transferring the solute to a solution other than its pure liquid state (or reference state, in which $\Delta G_s^e = 0$):

$$\gamma = \exp(\Delta G_s^e/(RT)) \tag{3-3}$$

If the solute activity coefficients, γ_w and γ_f, are known, K_{fw} can be used to approximate the solute concentration in the groundwater immediately adjacent to the fuel, given the fuel concentration of the solute:

$$C_w = C_f/K_{fw} \tag{3-4}$$

The dissolved solute is now subject to the physical and chemical processes of groundwater transport as the solute plume migrates away from the fuel spill. Dispersion in the aquifer matrix will dilute and broaden the contaminant plume, and sorption to aquifer solids will retard its progress as it migrates (advects) with groundwater flow through the subsurface.

3-3. Fugacity modeling of sorption and retardation in the subsurface

The longitudinal velocity of the groundwater flow relative to the average rate of contaminant migration is defined as the retardation factor, R:

$$R = v_{water}/v_{contaminant} \tag{3-5}$$

For non-retarded transport, R = 1. Retardation occurs as a result of sorption of the contaminant to aquifer solids, thereby decreasing the contaminant's effective migration velocity through the subsurface. The retardation factor was formulated assuming that as a contaminant moves through the subsurface, a certain amount of it must spend time being sorbed to aquifer solids to maintain chemical equilibrium. The aqueous mass of the contaminant was considered here to be the portion that can migrate via groundwater flow at any given point in time (i.e., colloid-facilitated transport is ignored). The retardation factor can be expressed [9]:

$$R = 1 + K_d\rho_s(1-\phi)/\phi \tag{3-6}$$

where K_d = sorption coefficient [L water / kg solid],
ρ_s = solids density [kg solid / L solid], and
ϕ = porosity [L water / L bulk aquifer material].

This derivation of the retardation factor (R) assumes that sorption equilibrium is achieved quickly relative to groundwater flow.

Organic compounds may sorb to multiple aquifer solid phases. However, studies have suggested that the organic matter in aquifer materials is the dominant sorbent for most nonpolar organic compounds [10-16]. These studies also suggest that sorption of nonpolar organic compounds to organic matter is approximately linear as a function of solute concentration

[13, 14], and that sorption behavior is similar for different sorbents [10-15]. Linear sorption isotherms suggest that the solute is partitioning between solvent phases (i.e., water and organic matter), rather than sticking to surfaces (adsorption). Adsorption is usually somewhat nonlinear, characterized by limited sorption sites with increased concentration or enhancement of sorption sites with increased concentration [17, 18]. As a modeling simplification, therefore, sorption was assumed here to occur dominantly to organic matter in the aquifer material:

$$K_d = f_{om} K_{om} \tag{3-7}$$

where f_{om} = aquifer solids mass fraction of natural organic matter, and
K_{om} = organic-matter/water partition coefficient.

The retardation factor may now be expressed:

$$R = 1 + f_{om} K_{om} \rho_s (1-\phi)/\phi \tag{3-8}$$

3-4. Advective - diffusive transport in the subsurface

The subsurface transport of a contaminant plume is governed by advection with groundwater (migration), retardation (sorption to solid phases), dispersion in three dimensions, and degradative processes. Representative field dispersivities, relevant hydrogeological characteristics, and length scales to municipal wells were needed.

The hydrologic characterization of nationwide municipal well contamination by LUFTs can only be general. In the derivation of a subsurface transport model, the behavior of the groundwater contamination plume was treated as a longitudinally averaged slug with lateral and vertical Gaussian concentration distributions. This approach begs the question: why wasn't a more mathematically rigorous computational algorithm used, given the physical constraints of the system? A numerical calculation could easily have been devised to produce a three-dimensional plume distribution, with a precisely defined solute peak concentration and plume centroid. However, the level of overall hydrogeologic variability inherent in the thousands of subsurface sites considered here undermines the usefulness of such precision. Kitanidis reports that, especially when the regularity of hydrogeologic morphology is uncertain, the gaussian-like spreading of a plume does not necessarily reflect the extent of dilution of regions within the plume [19]. Clearly, the regularity of geological formations in the distribution of sites under consideration in this work (see section 3-5) is highly variable. The concentration distribution of the plume was therefore treated as a probabilistic, rather than deterministic, entity. Additionally, variability in input parameters (see section 3-5) superimposed still more uncertainty on model results. Therefore, it would have been an exercise in overmodeling to treat subsurface contaminant migration using a highly precise transport algorithm, thereby assuming a higher level of information than was actually available. Accordingly, the 3-dimensional transport problem was solved by simply scaling the transport processes, as is described here. It is important to note that because of the uncertainty inherent in the modeling approach, the calculated municipal well contaminant concentrations must be interpreted as order-of-magnitude estimates. This is discussed further in Chapter 5.

The groundwater velocity (v), retardation (R) of the compound via sorption to aquifer solids, and transport distance (L_x) can be used to estimate the time of arrival (t_{Arr}) of the front of a plug flow (i.e., non-dispersive) plume travelling from a LUST to a municipal well:

$$t_{Arr,\ plug\text{-}flow} = L_x R/v \tag{3-9}$$

In general, however, the time of arrival of the leading edge of the solute front is earlier than that suggested by plug-flow, depending on the extent of longitudinal dispersion of the plume. The longitudinal dispersion of the plume must therefore be characterized before the time of arrival of the solute front can be determined. The solute front is described (eqn 3-10) as the section of the plume that lies a distance $\sigma_{x,\ disp}$ ahead of the plug flow front:

$$t_{Arr,\ front} = (L_x - \sigma_{x,\ disp})R/v \tag{3-10}$$

where $\sigma_{x,\ disp}$ = the square root of longitudinal variance of the dispersion-related plume spread.

The spatial variance (σ_i^2) of the plume in any given direction i can be described as a function of the plume transport time (t) and dispersion coefficient (E_i) [20]:

$$d\sigma_i^2/dt = 2(E_i/R) \tag{3-11}$$

Assuming that dispersion is approximately Fickian (i.e., described as a random walk process), eqn 3-11 can be integrated from t = 0 to the arrival time of the plume at the well ($t = t_{Arr}$) with E_i considered constant [20]:

$$\sigma_i^2 = 2(E_i/R)t_{Arr} \tag{3-12}$$

It is well known that the dispersion coefficient, E_i, is not constant with respect to time in the field, contrary to eqn 3-11. In field studies, it has been shown that E_i is proportional to the size of the plume [Welty, 1989 #21; Chrysikopoulos, 1992 #22; Kitanidis, 1988 #23]. The dispersion coefficients used for modeling purposes here were empirically derived from field studies which assumed constant (time-averaged) Fickian dispersion [21]. This modeling approach is valid because the field studies from which the dispersion coefficient values were calculated involved transport over a spatial scale which was comparable to the transport scale considered here.

In this study, computing the extent of dispersion of the plume has practical value for three reasons. Longitudinal dispersion shortens the amount of time required for the contaminant to reach water supply wells (eqn 3-10). Additionally, longitudinal dispersion increases the spatial variance (or spread) of the plume, and therefore may decrease the average rate at which the contaminant enters the well. Finally, transverse and vertical dispersion determine whether the capture zone of the well is likely to draw the entire depth and breadth of the plume. We computed the probable extent of dispersion in all three dimensions, and addressed the consequences for transport accordingly.

Consider the simple case of a municipal well drawing from the entire depth of a shallow aquifer in a relatively uniform flow field (Figure 3-2). The capture zone width of the well, b, is:

$$b = Q_{well}/(vh\phi) \tag{3-13}$$

where Q_{well} = well pumping rate [m^3/day],
v = ambient groundwater velocity [m/day],
h = depth of the aquifer [m], and
ϕ = aquifer solids porosity (unitless).

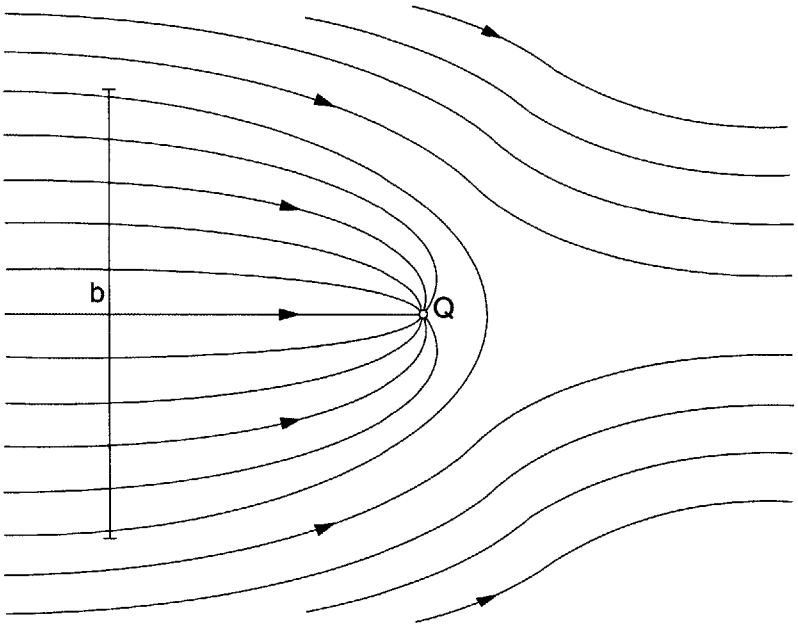

Figure 3-2. Streamline diagram of a well capture zone in a uniform flow field

The rate at which contaminant mass enters the well was calculated by multiplying the total mass of the contaminant in the plume (m_{total}) by the velocity at which the contaminant is transported (v/R), divided by the length of the plume at the well (roughly $2\sigma_{x,\,final}$):

$$dm/dt_{into\ well} = m_{total}v/(2\sigma_{x,\,final}R) \tag{3-14}$$

It is important to note that eqn 3-14 is a poor approximation for the contaminant mass flux into the well if the plume is very long as a result of leaching slowly out of the gasoline spill. In this case, the contaminant mass flux is approximated using the "steady state" transport solution described in section 7 of this chapter (eqns 3-39 and 3-40). The concentration of the compound in the water supply (C_{well}) was determined by the rate at which mass of the compound enters a municipal well, divided by the pumping rate of the well (Q_{well}):

$$C_{well} = (dm/dt_{into\ well})/Q_{well} \tag{3-15}$$

3-5. Realistic field transport parameters

In order to make realistic calculations of contaminants transporting from LUFTs to community supply wells, reasonable field transport parameters were estimated. The choice of each transport parameter value is discussed in detail, based on literature review and a survey of six selected communities in the U.S (Table 3-1). The survey results included too few communities to be very useful as an independent data set and are therefore shown mostly for validation of transport parameter estimates. The field parameters values chosen for the transport model are shown in Table 3-2.

Aquifer characteristics. A brief review of relevant literature demonstrated that municipal and domestic water supply wells are typically (purposefully) located in aquifers with high hydraulic conductivities (10^{-3} to 10^{2} cm/s) and porosities (0.10 to 0.50) [22-24]. In the U.S., the significant majority of water supply wells are drilled in unconsolidated deposits composed of glacial outwash sand/gravel or sedimentary/aeolian sand/silt deposits [22, 23]. To a lesser extent, fractured formation aquifers such as karst or fractured basalt are also exploited [22, 23]. Based on survey data (Table 3-1), we additionally hypothesized that the aquifers in which municipal wells are located generally have low organic carbon levels, with a solids organic matter fraction typically ranging from 0 to 0.005. For modeling purposes, we considered a sand and gravel unconsolidated aquifer with a saturated thickness of about 15 meters (50 feet) and solids organic matter fraction (f_{om}) of 0.001.

Longitudinal groundwater velocity, v, determines the rate of subsurface transport of the contaminant. A review of field studies gives data for ambient groundwater velocities in several sand and gravel aquifers (n = 16) in the U.S. and Europe [21]:

range:	v = 0.0003 to 31 [m/day]
median:	v = 0.75 [m/day]
mean:	v = 4.9 [m/day]

The longitudinal groundwater velocity was therefore assumed to be a constant value of approximately 1 meter per day in a uniform flow field. As shown by the data given above, this is a representative value for unconsolidated materials with high hydraulic conductivities. It is important to recognize that ambient groundwater velocity is a critical transport parameter which is highly variable between sites and regions, and results must be interpreted accordingly.

Distance to municipal wells, L_x, sets the physical scale of the transport problem. In a recent nationwide survey of about 26,000 community water supply wells in 31 states, 35 percent of municipal drinking water wells were found to be within 1,000 meters of at least one reported leaking underground gasoline tank [7]. Therefore, a representative LUFT to well distance of about 1,000 meters was assumed.

Dispersion coefficients E_x, E_y, and E_z represent the scale-dependent tendency for a plume to spread and dilute in the longitudinal (x), transverse (y), and vertical (z) directions. The dispersion coefficients are equivalent to the longitudinal (a_x), transverse (a_y), and vertical (a_z) dispersivities multiplied by the longitudinal component of groundwater velocity, v [20]:

$$E_i = va_i \ [m^2/day] \qquad (3\text{-}16)$$

Dispersivity, a_i, reflects the tendency of a solute plume to dilute and spread during flow through a porous media. In the field, observed dispersivities are determined by the size of the flow regime, since geologic heterogeneities in the aquifer occur on multiple scales [20]. Representative field values of dispersivity in sand and gravel aquifers were obtained from data in a review by Gelhar et al., based on experimental transport distances of 500 to 1,500 meters [21]:

	dispersivity observed in field [21]			
dispersivity	range	average	median	n
a_x [m]	7.6 to 234	50	20	7
a_y [m]	1 to 4.2	3	4	3
a_z [m]	0.31	0.3	0.3	1

For comparison, according to the U.S. Environmental Protection Agency Composite Landfill Model (EPACML), typical subsurface dispersivities for a transport distance of 1000 m would be assigned the following probabilities in a stochastic simulation [20]:

	dispersivity by probability		
dispersivity	p = 0.1	p = 0.6	p = 0.3
a_x [m]	0.078 to 0.78	0.78 to 7.8	0.78 to 78
a_y [m]	0.010 to 0.10	0.10 to 1.0	0.10 to 10
a_z [m]	0.00049 to 0.0049	0.0049 to 0.049	0.0049 to 0.49

The following dispersivity values were considered representative for modeling purposes here:

$a_x = 10$ m $\qquad a_y = 1$ m $\qquad a_z = 0.1$ m

Well Pumping Rate, Q_{well}, can range widely, depending on the needs of the community and the specific hydrologic setting. A survey of several communities suggested a municipal well pumping rate range of 435 to 7620 m^3/day (80 to 1400 gal/min; Table 3-1). A higher pumping rate increases the likelihood that the capture zone will contain an entire contaminant plume, but it also lowers the effective concentration of the contaminant by diluting it with a greater volume of ambient groundwater. A pumping rate value of 2180 m^3/day (400 gal/min) was thought to be reasonable for screening model purposes.

Table 3-1 shows a brief summary of data taken in the field survey. Fuel storage tank distances to community water supply wells (L) were estimated based on known well and service station locations. In a few cases this data was not retrieved. Typical or average well pumping rates (Q_{well}) and well screen depths (d_s) are also listed. Aquifer material fraction organic matter data (f_{om}) is based on measurements taken in studies of local surface aquifers.

Table 3-1. Summary of water supply survey data for 6 randomly chosen U.S. communities

location	aquifer type	L [m]	Q_{well} [gpm]	f_{om}	d_s [m]	citations
Forestdale, MA	sand/gravel	< 200	200-350	0.0003	10-18	[25, 26]
Guymon, OK	silt/sand/clay	300-700	80-900	0-0.01	130	[27, 28]
Columbus, MS	sand/gravel	-	1400	0.0006	300	[29, 30]
Chillicothe, OH	sand/gravel	700-900	900	0.002	20-30	[31, 32]
Brush, CO	alluvium	-	600-1400	0.001	30-40	[33, 34]
College Station, TX	sand	-	200	-	1000	[35]

Table 3-2. Summary of model field transport parameters

aquifer material	sand and gravel	
porosity	ϕ	0.25
fraction of organic matter	f_{om}	0.001
temperature	T	15 °C
aquifer saturated thickness	d	25 m
water table depth	d_w	5 m
ambient groundwater velocity	v	1 m/day
well pumping rate	Q_{well}	2180 m^3/day
calculated capture zone width	b	350 m
distance from LUST to municipal well	L_x	1000 m
longitudinal dispersivity	a_x	10 m
transverse dispersivity	a_y	1 m
vertical dispersivity	a_z	0.1 m

3-6. Estimation of contaminant plume initial conditions

For modeling purposes, a spill volume ($\forall_f$) of about 0.38 m^3 (100 gal) of gasoline was assumed to have reached a shallow water table. The fuel non-aqueous phase liquid (NAPL) was assumed to spread on the water table quickly, relative to the time required for fuel components to leach out of the fuel via dissolution into the groundwater. The groundwater passing by under the fuel NAPL was then assumed to equilibrate a vertical cross section of water with a width equal to that of the NAPL pool (Figure 3-3). The depth (H) of the plume that is equilibrated with the NAPL when it leaves the NAPL pool was assumed equivalent to the square root of the variance of dispersion-related vertical plume spread (i.e., one standard deviation of the dispersion vertical transport term) [36].

$$H = \sigma_z = \sqrt{(2(E_z)(t/R))} = \sqrt{(2(va_z)(L_{spill}/v))} \quad (3\text{-}17)$$

$$H = \sqrt{(2a_z L_{spill})} \quad (3\text{-}18)$$

where H = depth of the equilibrated plume [m], and
L_{spill} = length of the NAPL pool [m].

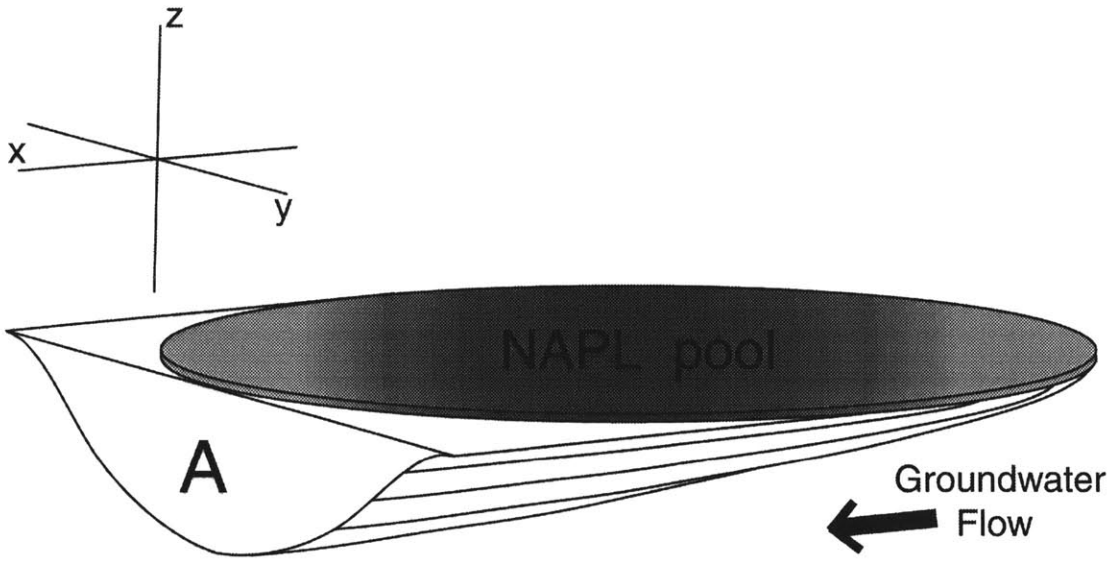

Figure 3-3. Zone of contamination beneath the NAPL phase

If the spill spreads in an approximately circular fashion (Figure 3-3), the length of NAPL spill that passing groundwater is exposed to varies as $2\sqrt{(r^2 - y^2)}$, where r is the radius of the spill. The dimensions of the NAPL pool were chosen so that the saturated thickness of the NAPL lens was about 5 cm. For a 100 gallon spill, this translates into a lens diameter of about 3.1 m, after correcting for aquifer porosity. The cross-sectional area (A) of contamination leaving the NAPL pool was found by integrating the depth of the plume as it leaves the NAPL over the width of the plume:

$$A = \int_{-r}^{r} [\sqrt{(2a_z(\text{length of exposure}))}]dy \tag{3-19}$$

Since A is an even function over –r to r, the integral limits can be simplified:

$$A = 2\int_{0}^{r} [\sqrt{(2a_z(2\sqrt{(r^2 - y^2)}))}]dy \tag{3-20}$$

$$A = [4\sqrt{a_z}]\int_{0}^{r} [\sqrt[4]{(r^2 - y^2)}]dy \tag{3-21}$$

No satisfactory analytical solution to this integral was found. It is a well-behaved function that can be numerically integrated with nominal error. In this work, the midpoint-method numerical integration approximation was used, with N = 1000 intervals [37]. A fitting function was found which empirically relates the computed value of A [m^2] to the NAPL spill radius, r [m]:

$$A = 3.49\, r^{1.50}\sqrt{a_z} \qquad r^2 = 1.000 \qquad (3\text{-}22)$$

A list of the transport model initial conditions is given in Table 3-3, based on the NAPL characteristics described above.

Table 3-3. Summary of estimated transport model initial conditions and NAPL pool parameters

volume of the NAPL gasoline lens	$\forall_f$	0.38 m^3
radius of the NAPL lens	r	1.56 m
vertical dispersivity on a 10 m scale [21]	a_z	0.002 m
initial cross-sectional area of plume	A	0.30 m^2

3-7. Calculation of contaminant plume transport

The plume was assumed to spread in 3 dimensions with a Gaussian distribution as it migrated away from the NAPL spill. The mass leaving rate of the compound from the NAPL pool was approximated as:

$$dm/dt_{\text{out of NAPL}} = -Q_P C_w = -(Av/\phi)C_w \qquad (3\text{-}23)$$

where Q_P = flux of groundwater through area A (Figure 3-3) at the NAPL edge [m^3/day].

The rate at which the fuel spill is depleted was calculated by relating the aqueous concentration of the equilibrated plume with the fuel–water partition coefficient of the compound of interest (eqn 3-4):

$$dm/dt_{\text{out of NAPL}} = -(A/\phi)vC_f/K_{fw} \qquad (3\text{-}24)$$

$$dm/dt_{\text{out of NAPL}} = -(A/\phi)vm/(\forall_f K_{fw}) \qquad (3\text{-}25)$$

where $\forall_f$ = volume of fuel spill [m^3], and
m = mass of compound in fuel [mol].

The mass of the compound in the fuel varies as a function of time, so the compound concentration in the fuel experiences first-order decay:

$$m_{t,\text{fuel}} = m_{0,\text{fuel}} \exp(-Avt/(\phi \forall_f K_{fw})) \qquad (3\text{-}26)$$

$$C_{t,\text{fuel}} = C_{0,\text{fuel}} \exp(-Avt/(\phi \forall_f K_{fw})) \qquad (3\text{-}27)$$

The amount of time required to deplete the fuel of 75% of the compound (i.e., two fuel concentration "half-lives"), excluding a weak plume tail, is therefore:

$$t_{\text{depletion}} = -\phi \forall_f K_{fw} 2\ln(0.5)/(Av) \qquad (3\text{-}28)$$

The initial length of the plume, approximated as a slug of uniform concentration, is therefore:

$$l_{x,\,initial} = vt_{depletion}/R \tag{3-29}$$

Note that the initial plume length cannot be smaller than the original spill, so it is also always true that:

$$l_{x,\,initial} \geq 2r \tag{3-30}$$

The initial lateral concentration distribution was assumed Gaussian. The initial lateral spread reflects the width of the spill (2r):

$$\sigma_{y,\,initial} = r/2 \tag{3-31}$$

The initial vertical spread was calculated based on the length of the spill (2r) and the vertical dispersivity, a_z (see eqn 3-18):

$$\sigma_{z,\,initial} = \sqrt{(2a_z 2r)} \tag{3-32}$$

Clearly, the initial shape of the plume depends highly on the geometry of the NAPL spill (which is unlikely to be circular, as idealized here), heterogeneities in the aquifer material, etc. The methods employed here are intended to capture only the rough magnitude of initial vertical and transverse spread: trial calculations demonstrated that the extent of the initial dispersion did not significantly affect the final vertical and transverse dimensions of the plume.

Two general descriptions were used to characterize the plume transport of different contaminants from the fuel NAPL spill to a water supply well. Some contaminants leach slowly out of the fuel and thereby generate a plume that is long relative to transport-induced longitudinal spreading. These compounds were said to create *steady state* plumes, in which longitudinal spreading does not significantly dilute the contaminant as it travels towards the water supply well. Conversely, a contaminant may transfer quickly to the aqueous phase and generate a shorter *slug* plume which can be effectively diluted by longitudinal dispersion during transport. In both cases, it was assumed that the capture zone of the well draws the entire plume. This is realistic, since, based on the parameters suggested here, the calculated capture zone width (b) is 260 m, and the lateral spread of the plume is on the order of 40 m when it reaches the well (see section 3-9).

The plume behaves approximately as a "slug" as long as the initial length of the plume, $l_{x,initial}$, is less than the extent of longitudinal spreading which occurs during transport:

$$l_{x,initial} < 2\sqrt{(2a_x L_x)} \tag{3-33}$$

But using eqn 3-29, we see that:

$$vt_{depletion}/R < 2\sqrt{(2a_x L_x)} \tag{3-34}$$

Plugging eqn 3-28 into the $t_{depletion}$ term in eqn 3-34 and solving for K_{fw}/R, we find that the condition for a **"slug" plume** is controlled by the ratio of the fuel–water partition coefficient to the retardation factor:

$$K_{fw}/R < - (A\sqrt{(2a_xL_x)})/(\phi\Psi_f \ln(0.5)) \quad (3\text{-}35)$$

Eqn 3-35 implies that the condition for a slug plume is $K_{fw}/R < 644$ (unitless) for a 100 gallon spill and $K_{fw}/R < 175$ for a 1000 gallon spill. In this case, the initial variance of the plume, $\sigma_{x,\,initial}^2$, can be related to the 2nd moment of a slug of uniform concentration, $(l_{x,initial})^2/12$. Using the assumption of Fickian dispersion (eqns 3-11 and 3-12), the final longitudinal variance of the plume was described by summing the initial variance and the transport-induced variance:

$$\sigma_{x,\,final}^2 = \sigma_{x,\,initial}^2 + 2(E_x/R)t_{Arr,\,front} = (l_{x,initial})^2/12 + 2(E_x/R)t_{Arr,\,front} \quad (3\text{-}36)$$

The final longitudinal spread (expressed as the square root of the plume variance) is therefore:

$$\sigma_{x,\,final} = \sqrt{((l_{x,initial})^2/12 + 2(E_x/R)t_{Arr,\,front})} \quad (3\text{-}37)$$

In this case, the mass transfer rate into the well is given by eqn 3-14:

$$dm/dt_{into\ well,\,slug} = m_{total}v/(2\sigma_{x,\,final}R) \quad (3\text{-}38)$$

If the K_{fw}/R value is sufficiently high ($K_{fw}/R > 644$ for a 100 gallon spill and $K_{fw}/R > 175$ for a 1000 gallon spill), the NAPL will generate a **"steady state" plume**. In this event, the plume length is significantly greater than the extent of longitudinal dispersion during transport to the well, or:

$$l_{x,initial} > 2\sqrt{(2a_xL_x)} \quad (3\text{-}39)$$

This implies (from eqn 3-35) that:

$$K_{fw}/R > - (A\sqrt{(2a_xL_x)})/(\phi\Psi_f \ln(0.5)) \quad (3\text{-}40)$$

During steady state plume transport, eqn 3-14 cannot be applied, but it is approximately true that:

$$dm/dt_{into\ well,\,steady\ state} = (dm/dt_{out\ of\ NAPL}) = - (A/\phi)vm/(\Psi_f K_{fw}) \quad (3\text{-}41)$$

Regardless of whether the transport is described as steady state or slug, the arrival time of the leading edge of the solute front at the well may be much earlier than calculated from plug-flow (described by eqn 3-9). The leading edge of the solute front was defined here as the section of the plume that lies ahead of the plug flow front by a length of the square root of the variance of dispersion-related spread (eqn 3-42). The solute front was treated as Gaussian and therefore has a concentration of roughly 1/3 of the steady state plume concentration. Under these conditions, the time of arrival of the solute front is given by:

$$t_{Arr,\,front} = (L_x - \sigma_{x,\,disp})R/v \quad (3\text{-}42)$$

where the longitudinal dispersion is itself a function of $t_{Arr,\,front}$:

$$\sigma_{x,\,disp} = \sqrt{(2(E_x/R)t_{Arr,\,front})} \quad (3\text{-}43)$$

Eqns 3-42 and 3-43 may be coupled to find $t_{Arr,\,front}$ as an explicit function of E_x:

$$t_{Arr,\,front} = L_xR/v - (R/v)(-E_x/v +/- \sqrt{(E_x^2/v^2 + 2E_xL_x/v)}) \quad (3\text{-}44)$$

Finally, the extent of lateral and longitudinal dispersion that the plume displays when it reaches the supply well may be treated as a Fickian process (eqns 3-31 and 3-32):

$$\sigma_{y,\,final} = \sqrt{(\sigma_{y,\,initial}^2 + 2(E_t/R)t_{Arr,\,front})} \quad (3\text{-}45)$$

$$\sigma_{z,\,final} = \sqrt{(\sigma_{z,\,initial}^2 + 2(E_t/R)t_{Arr,\,front})} \quad (3\text{-}46)$$

3-8. Summary and discussion

The fugacity/transport screening model method proposed here allows the user to predict probable arrival times and concentrations of gasoline component solutes in community water supply wells. The theoretical framework is based on physical property data of the compound of interest and a generalized description of the hydrogeology was used to derive a transport, dispersion and dilution calculation.

The relevance of this approach lies in its generality. In principle, any organic compound added to gasoline may be screened for its potential to create significant water supply contamination on a national scale. Data is provided to assess the validity and usefulness of the screening model, in the results section (see Chapter 5).

Understanding the choices of hydrogeologic parameter values is crucial to interpreting the screening model results. The parameter values suggested here were chosen to represent a relatively probable scenario, rather than an unusually 'high risk' scenario. It is important to note that there are many very realistic ways in which the water supply may be at greater risk than proposed here. Fractured-rock aquifers may provide much more rapid transport with less plume spreading and less dilution. Larger spills would result in a higher mass transfer rate and thus higher contaminant concentrations in the water supply. Municipal wells with lower pumping rates (or private wells) would create smaller capture zones and dilute the plume less, thus resulting in higher water supply concentrations. These are only a few examples.

Alternatively, several other factors and processes may serve to mitigate contamination risks to groundwater supplies. In many cases, the ambient groundwater velocity is a fraction of the value suggested here, thereby extending transport times of unretarded contaminants to decades (eqn 3-44) and proportionately decreasing their mass transfer rate into wells (eqns 3-38 and 3-41). Biodegradation, which is not addressed in this work, may attenuate the plume over a

short distance. Many wells draw from deep, confined aquifers, or far enough below the water table to avoid drawing the plume into their capture zone. In many cases, the water table is very deep, so that a significant amount of time is required for the gasoline NAPL to reach the saturated zone, increasing the extent of biological or chemical attenuation.

A complete partitioning and transport calculation based on the concepts developed here involves the following steps:

(1) Estimation of the equilibrium water concentration of the compound, based on the fuel concentration and fuel/water partition coefficient (eqn 3-4).
(2) Estimation of the retardation factor of the compound in aquifer material, based on the organic-matter/water partition coefficient of the compound (eqn 3-8).
(3) Estimation of the time of arrival of the compound at a municipal water supply well, based on the rate of retardation and extent of dispersion (eqn 3-44).
(4) Computation of A, the cross-section of contamination area at the spill (eqn 3-22).
(5) Characterization of the transport process as "slug" or "steady state" (see eqns 3-35 and 3-40).
(6) Estimation of the final lateral and vertical spread of the plume (eqns 3-45 and 3-46, with initial spread values given by eqns 3-31 and 3-32).
(7) Estimation of the concentration of the compound in the water supply well (eqn 3-15), based on the subsurface mass flux of the contaminant (eqn 3-38 or 3-41) and the well pumping rate.

3-9. Example calculation of MTBE transport from a NAPL spill to a municipal well

The following calculation output was produced by a gnu c++ transport program, and is parameterized using the "input file" shown below. The raw program code is included in the appendix, and compiled executables are available for both PC (Windows 98 or Windows NT) and UNIX (Solaris) operating systems. Using the hydrogeologic parameters discussed here with the partitioning properties of MTBE (see Chapter 5 for data), the following input file is constructed:

parameter file for MTBE transport calculation

```
*** transport.c parameter file -- edit with guidance!! ***
   Please edit only the numerical values in this file..

compound properties:

 molecular weight                        88.15
 fuel concentration [ppm]                100000
 Kfw                                     16
 Kom                                     8

spill description:

 NAPL volume [m^3]                       0.38
 NAPL lens thickness [m]                 0.05

hydrogeologic parameters:

 fom                                     0.001
 porosity                                0.25
 aquifer solids density [g/cm^3]         2.5
 groundwater velocity [m/day]            1
 aquifer saturated thickness [m]         25

 a(x) [m]                                10
 a(y) [m]                                1
 a(z) [m]                                0.1

 well pumping rate [m^3/day]             1635
 well distance [m]                       1000
```

The transport program extracts parameter data from the input file, and produces both on-screen output and an output file using the algorithm outlined in this chapter. If multiple runs are conducted, results will be serially appended to the output file. Interpretation of the results is discussed in Chapter 5 of this work.

transport.c on-screen output for MTBE transport calculation

```
                    * * *   * * *
NOTE TO USER:  Welcome to transport.c, a program designed to characterize
the contamination plume created by gasoline components.  Change inputs
using the transparms.dat parameter file.  This program is not exception-
handled and will bail if the parameter file is incorrectly modified.

          - - - PRELIMINARY DATA CHECK - - -

       solute molec wt = 88.15
       solute fuel concentration = 100000 ppm
       solute Kfw = 16
       solute Kom = 8
       NAPL volume = 0.3785 m^3 = 100 gallons
       NAPL thickness = 0.05 m
       fraction of organic matter = 0.001
       porosity = 0.25
       aquifer solids density = 2.5 g/cm^3
       groundwater longitudinal velocity = 1 m/day
       aquifer saturated thickness = 25 m
       dispersivities (in meters) = 10 [x]  1 [y]  0.1 [z]
       well pumping rate = 1635 m^3/day
       distance to the supply well = 1000 m

          - - - TRANSPORT.C FULL RESULTS - - -
     The time of arrival of the solute front is 920 days.
     The plug-flow time of arrival is 1100 days.

     The initial plume length is 6.5 meters

     The initial spread of the plume is:
     [y] 3.1 meters
     [z] 0.79 meters

     The plume transport type is 'slug'.

     The final spread of the plume is:
     [x] 130 meters
     [y] 42 meters
     [z] 13 meters

     The width of the well capture zone is 350 meters.

     The aqueous concentration at the spill is:
     0.053 mol/L or 4700 ppm

     The aqueous concentration in the well is:
     5.3e-07 mol/L or 0.047 ppm
```

transport.out (the transport output file) for MTBE transport calculation

```
                    ** TRANSPORT.C RESULTS SUMMARY **

        t_arr      C_well     C_well     plume dispersion, [m]      transport
run#    [days]     [ppb]        [M]        x       y       z          type
 1       920         47      5.3E-07      130      42      13         slug
```

3-10. Citations

1. MacFarlane, S. and D. Mackay, *A fugacity-based screening model to assess contamination and remediation of the subsurface containing non-aqueous phase liquids.* Journal of Soil Contamination, 1998. **17**(1): p. 17-46.
2. Mackay, D., W.Y. Shiu, A. Maijanen, and S. Feenstra, *Dissolution of non-aqueous phase liquids in groundwater.* Journal of Contaminant Hydrology, 1991. **8**: p. 23-42.
3. Mackay, D. and E. Webster, *Linking emissions to prevailing concentrations - exposure on a local scale.* Environmetrics, 1998. **9**: p. 541-553.
4. Mackay, D., A.D. Guardo, S. Paterson, G. Kicsi, and C.E. Cowan, *Assessing the fate of new and existing chemicals: a five stage process.* Environmental Toxicology and Chemistry, 1996. **15**(9): p. 1618-1626.
5. Mackay, D., A.D. Guardo, S. Paterson, G. Kicsi, C.E. Cowan, and D.M. Kane, *Assessment of chemical fate in the environment using evaluative, regional and local-scale models: illustrative application to chlorobenzene and linear alkylbenzene sulfonates.* Environmental Toxicology and Chemistry, 1996. **15**(9): p. 1638-1648.
6. Wania, F. and D. Mackay, *A global distribution model for persistent organic chemicals.* Science of the Total Environment, 1995. **160/161**: p. 211-232.
7. Johnson, R., J.F. Pankow, D. Bender, C. Price, and J.S. Zogorski, *MTBE, To what extent will past releases contaminate community water supply wells?* Environmental Science & Technology, 2000. **34**(9): p. 2A-9A.
8. Squillace, P.J., M.J. Moran, W.W. Lapham, C.V. Price, R.M. Clawges, and J.S. Zogorski, *Volatile organic compounds in untreated ambient groundwater of the United States.* Environmental Science & Technology, 1999. **33**: p. 4176-4187.
9. Freeze, R.A. and J.A. Cherry, *Groundwater.* 1979, Englewood Cliffs, NJ: Prentice-Hall, Inc. p. 404.
10. Means, J.C., S.G. Wood, J.J. Hassett, and W.L. Banwart, *Sorption of polynuclear aromatic hydrocarbons by sediments and soils.* Environmental Science & Technology, 1980. **14**: p. 1524-1528.
11. Hassett, J.J., J.C. Means, W.L. Banwart, S.G. Wood, S. Ali, and A. Khan, *Sorption of dibenzothiophene by soils and sediments.* Journal of Environmental Quality, 1980. **9**: p. 184-186.
12. Schwarzenbach, R.P. and J. Westall, *Transport of nonpolar organic compounds from surface water to groundwater: Laboratory sorption studies.* Environmental Science & Technology, 1981. **15**: p. 1360-1367.
13. Chiou, C.T., P.E. Porter, and D.W. Schmedding, *Partition equilibria of nonionic organic compounds between soil organic matter and water.* Environmental Science & Technology, 1983. **17**: p. 227-231.
14. Abdul, A.S., T.L. Gibson, and D.N. Rai, *Statistical correlations for predicting the partition coefficient for nonpolar organic contaminants between aquifer organic carbon and water.* Hazardous Waste & Hazardous Materials, 1987. **4**(3): p. 211-222.
15. Paya-Perez, A.B., M. Riaz, and B.R. Larsen, *Soil sorption of 20 PCB congeners and six chlorobenzenes.* Ecotoxicology and Environmental Safety, 1991. **21**: p. 1-17.
16. Lyman, W.J., *Adsorption Coefficient for Soils and Sediments*, in *Handbook of Chemical Property Estimation Methods*, W. Lyman, W. Reehl, and D. Rosenblatt, Editors. 1990, American Chemical Society: Washington D.C. p. 1,2.

17. Schwarzenbach, R.P., P.M. Gschwend, and D.M. Imboden, *Chapter 11, Sorption: Solid-Aqueous Solution Exchange*, in *Environmental Organic Chemistry*. 1993, John Wiley & Sons: New York, NY. p. 258,259.
18. Xia, G.S. and W.P. Ball, *Polyani-based models for the competitive sorption of low polarity organic contaminants on a natural sorbent.* Environmental Science & Technology, 2000. **34**: p. 1246-1253.
19. Kitadinis, P., *The concept of the dilution index.* Water Resources Research, 1994. **30**(7): p. 2011-2026.
20. Charbeneau, R.J., in *Groundwater Hydraulics and Pollutant Transport*. 2000, Prentice Hall: Saddle River, NJ. p. 375, 385, 389, 393, 418.
21. Gelhar, L.W., C. Welty, and K.R. Rehfeldt, *A critical review of data on field-scale dispersion in aquifers.* Water Resources Research, 1992. **28**(7): p. 1955-1974.
22. Campbell, M.D. and J.H. Lehr, in *Water Well Technology, Field Principles of Exploration Drilling and Development of Ground Water and Other Selected Minerals*. 1973, McGraw Hill Book Company: New York, NY. p. 239, 245, 248.
23. Delleur, J.W., *Geological Occurence of Groundwater*, in *The Handbook of Groundwater Engineering*. 1999, CRC Press: Boca Raton. p. 4,5,7-11.
24. Detay, M., in *Water Wells, Implementation, Maintenance, and Restoration*. 1997, John Wiley & Sons: Chichester. p. 7-9,16-18.
25. Crocker, C., *Centerville water supply data.* pers. comm., Centerville Water Dept, (508) 428-6691, October 5, 1999.
26. Barber, L.B., *Sorption of chlorobenzenes to Cape Cod aquifer sediments.* Environmental Science & Technology, 1994. **28**: p. 890-897.
27. Grounds, D., *Guymon water supply data.* pers. comm., City of Guymon, (580) 338-5838, June 29, 1999.
28. McMahon, P.B., *Southwest Kansas aquifer sediment organic carbon data.* pers. comm., NAWQA Study Unit, (303) 236-4882 ext. 286, October 21, 1999.
29. Hayslett, F., *Columbus water supply data.* pers. comm., Columbus Light and Water Dept, (601) 328-7192, October 13, 1999.
30. MacIntyre, W.G., C.P. Antworth, T.B. Stauffer, and R.G. Young, *Heterogeneity of sorption and transport-related properties in a sand-gravel aquifer at Columbus, Mississippi.* Journal of Contaminant Hydrology, 1998. **31**: p. 257-274.
31. Biza, B., *Chillicothe water supply well data.* pers. comm., Supervisor, Chillicothe Water Plant, (740) 773-3435, July 22, 1999.
32. Springer, A.E. and E.S. Bair, *Natural-gradient transport of bromide, atrazine, and alachlor in an organic carbon-rich aquifer.* Journal of Environmental Quality, 1998. **27**: p. 1200-1208.
33. Marymee, D., *Brush water supply data.* pers. comm., Brush City Utilities, (970) 842-5001, October 12, 1999.
34. McMahon, P.B., J.K. Bohlke, and B.W. Bruce, *Denitrification in marine shales in northeastern Colorado.* Water Resources Research, 1999. **35**(5): p. 1629-1642.
35. Goldapp, C., *College Station water supply data.* pers. comm., College Station Public Utilities, (409) 764-3660, October 12, 1999.
36. Weaver, J.W., R.J. Charbeneau, J.D. Tauxe, B.K. Lien, and J.B. Provost, *The Hydrocarbon Spill Screening Model.* EPA/600/R-94/039a, Robert S Kerr Environmental Research Laboratory, Office of Research and Development, US EPA, 1994.

37. Stewart, J., in *Calculus, Early transcendentals*. 1995, Brooks/Cole: Pacific Grove, CA. p. 456.

Chapter 4

Physical Property Estimation Methods Relating to
Subsurface Transport of Gasoline Constituents

4-1. Introduction and motivation

The partition coefficients of organic compounds are the fundamental parameters used in fugacity-based models. In the interest of developing a screening tool, it was useful to examine how these physical properties might be calculated from quantitative structure activity relationships (QSARs), rather than measurements in the laboratory. Accordingly, methods used to predict partition coefficients from chemical structure were briefly evaluated.

A substantial literature exists on the topic of physical chemical property estimation. This review only addressed methods relevant to subsurface transport modeling of fuel solutes. Additionally, I have restricted discussion to those methods which appear the most comprehensive and accurate in their predictive power.

The purpose of this chapter was to: (1) briefly survey and discuss the theory of methods for estimating aqueous activity coefficients, fuel activity coefficients / fuel–water partition coefficients, organic matter–water partition coefficients, octanol–water partition coefficients; and (2) discuss the role of Linear Solvation Energy Relationships (LSERs) and recent developments in *ab initio* calculations of activity coefficients.

4-2. Aqueous activity coefficient estimation

The aqueous activity coefficients of different organic compounds can vary over many orders of magnitude. Since activity coefficients of organic compounds in other phases typically vary much less, the characteristic transport behavior of a particular organic compound from spills in the subsurface is frequently controlled by the value of its aqueous activity coefficient. As a result, the validity of the subsurface mobility prediction is particularly sensitive to the accuracy of this parameter. Theories of aqueous solubilization will therefore be discussed in some detail.

A. The solution theory behind AQUAFAC

A considerable number of methods have been developed to predict aqueous activity coefficients, especially fragment methods and linear free energy relationships (LFERs) with other properties [1-6]. Probably the most accurate and comprehensive fragment method is AQUAFAC, developed in several papers by P.B. Myrdal, S.H. Yalkowsky and many others [7-11]. This method relies on the following conceptualization of the excess free energy of solubilization, which is composed of enthalpic and entropic components [12]:

$$\Delta G_s^e = \Delta H_{mix} - T\Delta S_{iceberg} - T\Delta S_{mix} \qquad (4\text{-}1)$$

where ΔG_s^e = excess free energy of solubilization in water,
ΔH_{mix} = enthalpy of mixing,
$\Delta S_{iceberg}$ = entropy of aqueous ice-crystal formation along the solute surface, and
ΔS_{mix} = entropy of mixing.

The individual components ΔH_{mix} and $\Delta S_{iceberg}$ of the solubilization energy are postulated as the sums of contributions, Σ_i, from i parts, or "fragments," that make up a non-ionic solute molecule:

$$\Delta H_{mix} = \Sigma_i(\tau_{iw}A_i) \quad (4\text{-}2)$$
$$\Delta S_{iceberg} = \Sigma_i(h_iA_i) \quad (4\text{-}3)$$

where τ_{iw} = solute-water interfacial tension per unit area of solute fragment i,
h_i = entropy of ice-crystal formation per unit area of solute fragment i, and
A_i = molecular surface area of fragment i.

Myrdal et al. thus hypothesize that fragments of an organic solute molecule each generate a *characteristic contribution* to the components ΔH_{mix} and $T\Delta S_{iceberg\ [7]}$. The entropy of mixing term, ΔS_{mix}, is derived from combinatorial mixing and solvent volume effects [13]:

$$\Delta S_{mix} = R(-X\ln X - (1-X)\ln(1-X) + X\ln(V_j/V_{mix})) \quad (4\text{-}4)$$

where R = molar gas constant,
X = mole fraction of the solute in water,
V_j = solute molar volume, and
V_{mix} = water-solute mixture molar volume.

Using these approximations, the activity coefficient for any organic solute in water may be calculated, provided that the energetic contributions from all of its individual fragments have been found from the known solubilities of other organic molecules. The aqueous activity coefficient is then:

$$\gamma_w = \exp(\Delta G_s^e/(RT)) \quad (4\text{-}5)$$

This approach can make good approximations. However, the assumption that fragments of the organic solute individually generate constant contributions to the free energy of solubilization is not completely valid for different organic molecules. We can examine this assumption in further detail by looking at its validity for the individual enthalpic and entropic components of ΔG_s^e.

The partial molar enthalpy of mixing ($\Delta H_{mix} = \Sigma_i\tau_{iw}A_i$) represents the enthalpic cost of placing an organic solute in a polar solvent, such as water. τ_{iw} is the interfacial tension of the organic solute in an aqueous solvation cavity: it is the integral of the theoretical solute-water adhesion energy over the aqueously solvated area of the solute. τ_{iw} is represented as a sum over the surface area of the solute because it is presumed to vary over the surface of the solute

molecule. The partial molar enthalpy of mixing of an organic molecule can be approximated using empirically derived molecular fragment contributions, but this is not strictly valid. For example, electron-withdrawing or electron-donating groups on the solute molecule may change the electronic densities of neighboring groups through inductive effects [14]. Additionally, steric effects created by some fragments may reduce the extent to which neighboring fragments are able to interact with the solvent (water) [14]. Consequently, the interfacial tensions of individual parts of the solute molecule depend on the nature of neighboring parts within the solute molecule itself. Thus, calculating the partial molar enthalpy as a sum of independent molecular fragment contributions is only an approximation.

The so-called entropy of iceberg formation derives from the hypothesis that a solvated organic solute causes the surrounding water molecules to form approximately crystalline layers along its hydrophobic surfaces [15]. The entropy of iceberg formation contributes the energetic cost of this increase in solvent organization. Similar to the interfacial surface tension, the extent of iceberg formation probably depends on the steric and electronic environment of individual parts of the surface of the organic solute molecule. For this reason, the entropy of iceberg formation probably cannot be exactly derived as a sum of characteristic contributions from individual solute fragments. However, the success of the AQUAFAC model shows that it is probably a good approximation.

AQUAFAC predicts the aqueous activity coefficient with an absolute average error of a factor of 1.5 to 3, depending the family of compound [7-11]. Regression optimizations have been conducted using many types of organic moieties, so that AQUAFAC can make predictions for a wide variety of compounds.

B. The Mobile Order and Disorder (MOD) theory of solvation

Mobile order and disorder theory predicts the energy of aqueous solvation of organic molecules using a different theoretical approach than AQUAFAC. Huyskens and Siegel argue that the hydrophobic effect mostly results from the decreased domain of mobility of meandering water molecules [16-19]. If correct, their derivations imply that the aqueous activity coefficient, γ_w, is mostly entropic in nature. Huyskens and Siegel propose that, in the liquid phase, the protons of a water molecule spend most of their time "following" an electron-donating (oxygen) group. The water molecule therefore experiences a lower entropy in bulk solution than if its orientation with respect to neighboring molecules was non-preferential (i.e., random). Unlike a solid phase, however, the neighbors of the water molecule physically exchange locations within a short time frame. Huyskins and Siegel refer to this intermediate level of order, in between random orientation and crystalline, as a "mobile order." They argue that when thinking about the entropy loss related to increased solvent order around the solute molecule, it is incorrect to treat the solvating water molecules as a "quasi-lattice" structure.

Huyskens and Siegel derive the entropic cost of "mobile order" in water from only three properties: (1) the fraction of time during which protons are hydrogen-bonded vs. free; (2) the volume that a water molecule could occupy while hydrogen-bonded to one proton donor; and (3) the volume of the standardized domain. The "standardized domain" of a water molecule is

defined as the molar volume of the bulk liquid divided by N, Avogadro's number. The derived entropic cost associated with the mobile order is given as:

$$\Delta S_{\text{mobile order}} = R \ln\{(\gamma^{-\gamma}(1-\gamma)^{\gamma-1})(V_0/\text{Dom})^{1-\gamma}\} \quad (4\text{-}6)$$

where γ = time fraction during which protons are H-bonded vs free,
V_0 = volume that an H-bonding water molecule may occupy, and
Dom = volume of the standardized domain of a water molecule.

Huyskens and Siegel then argue that solvation of an organic solute causes a loss of entropy related purely to the increased standardized domain of adjacent water molecules. This is hypothesized to be the dominant energetic term of the hydrophobic effect.

Additional solubility contributions are derived to formulate a total solubility equation for non-ionic aqueous solutes. The only necessary parameters are the compound molar volume (V_B) and derived solute-solvent specific interaction stability constants (K_{Oi}). The volume fraction solubility (Φ_b) is given as:

$$\Phi_B = B + F + O \quad (4\text{-}7)$$

$$B = 0.5\Phi_W(V_B/V_W - 1) + 0.5\ln(\Phi_B + \Phi_W V_B/V_W)$$
$$F = -r_W\Phi_W V_B/V_W$$
$$O = \Sigma_i \ln(1 + K_{Oi}/V_W)$$

where Φ_B = volume fraction solubility of solute, B,
Φ_W = volume fraction of solvent (water) at solubility,
V_B = molar volume of solute [cm^3/mol],
V_W = molar volume of water [cm^3/mol],
r_W = water "structuration factor," having a value of 2.0 (a water donates two protons),
K_{Oi} = solute-solvent stability constant (a derived parameter for various substructures), and
i = index of solute-solvent interaction sites.

In eqn 4-7, "B" is the correction for the entropy of mixing resulting from the size difference of the solute and solvent molecules. "F" accounts for the hydrogen-bonded chains of water molecules that form around the solute, the proposed origin of the hydrophobic effect [20]. "O" expresses the enthalpic impact of proton-*accepting* sites on the solute. Ruelle has also derived a general expression similar to the "O" term to account for proton-*donating* sites on solutes [21, 22]. V_B can be estimated using a reliable fragment method [23] or molecular simulation calculations, and K_{Oi} is an empirically adjusted parameter.

Using MOD theory, P. Ruelle predicts the solubilities of 531 organic compounds with weak hydrogen bonding capacities with an average absolute error of 2.3-fold in the solubility or 0.37 base-10 log solubility units [20].

4-3. Fuel activity coefficient and fuel–water partition coefficient estimation

A. The UNIQUAC functional-group activity coefficients (UNIFAC) [24]

UNIFAC is a fragment contribution contribution method based on the statistical thermodynamics UNIQUAC (universal quasi-chemical equation [25]) solvation expression and the ASOG (analytical solution-of-groups [26, 27]) model. For a mixture of several solutes, each solute can be composed of individual structural fragments. The excess free energy of solution is assumed to be the sum of independent contributions of fragment pair-wise interactions between solute molecules.

The UNIFAC method requires two adjustable parameters for each fragment-fragment interaction in solution. As a result, comprehensive predictive capability using the approximately 78 proposed fragments in recent UNIFAC revisions requires literally thousands of adjusted parameters from experimental solution data. For a large number of fragment-fragment interactions, parameters have not yet been derived. As a consequence, UNIFAC is frequently unable to make predictions for molecules or mixtures with multiple functional groups. The robustness of UNIFAC lies in its ability to be extended to any solute mixture or system, such as gasoline. The recently modified UNIFAC method also has improved accuracy over a range of temperatures (273 to 413 K), but requires three times as many parameters [28, 29]. Several authors have investigated UNIFAC's predictive accuracy for systems of environmental interest (Table 4-1), citing the absolute average error (AAE) [30-33]. Errors range up to a factor of three in the partition coefficient.

Table 4-1. Previous studies of the accuracy of UNIFAC predicted octanol–water partition coefficients

system parameter	author	N	AAE
K_{ow} (octanol-water)	Park and Back (2000)	39	factor of 0.70 in the K_{ow}
K_{ow} (octanol-water)	Lin and Sandler (1999)	226	factor of 0.41 in the K_{ow}
$\gamma_{octanol}$	Li et al. (1995)	131	factor of 2.0 in the $\gamma_{octanol}$
γ_{water}	Kan and Tomson (1996)	66	factor of 3.2 in the γ_{water}

B. Mobile Order and Disorder Theory

The MOD theory has been used to predict activity coefficients of solutes in organic solvents, as described in several papers by Huyskens, Siegel and Ruelle [16-18, 21, 22]. Unlike UNIFAC, the MOD model is currently derived for binary rather than multicomponent solutions such as fuels. The MOD model is more general than UNIFAC, however, in the sense that it may be applied to any organic solute for a given solvent. Since the MOD theory is not currently formulated to make predictions for mixtures, solute partitioning behavior in nonpolar solvents such as hexane or toluene must be used to approximate solute partitioning in gasoline.

Ruelle fitted MOD parameters for two solvent systems and tested predictions for several non-polar, polar, and hydrogen bonding organic compounds (Table 4-2) [22]. Generally these estimates were accurate within a factor of three.

Table 4-2. Previous studies of the accuracy of MOD predicted partition coefficients [22]

partition coefficient	N	RMSE	r^2
K_{ow} (octanol-water)	1844	factor of 2.9 in the K_{ow}	0.988
K_{hw} (hexane-water)	102	factor of 2.7 in the K_{hw}	0.984

C. Linear free energy relationships (LFERs)

Linear free energy relationships are frequently developed to relate organic compound partitioning in one solvent-solvent system to partioning in another solvent-solvent system. Data from Hansch and Leo yields a LFER between log K_{ow} (octanol-water) and log K_{hw} (hexane-water) for polar and nonpolar compounds with moderate success [34]:

$$\log K_{hw} = 1.66 \log K_{ow} - 2.26 \qquad N = 16 \qquad r^2 = 0.79 \tag{4-8}$$

D. Linear solvation energy relationships (LSERs)

Linear solvation energy relationships are designed to reflect the principle solute-solvent intermolecular interactions responsible for solvation and partitioning behavior. LSERs have substantially advanced the accuracy of partition coefficient calculations. LSER theory postulates that the essential characteristics that will determine the solvation behavior of any compound is captured by the molecular descriptors: R_2, π^H, α^H, β^H and V_x; and that the solvation behavior of any mixture (solvent) is captured by characteristic coefficients: r, s, a, and b, plus a constant, c. The solute and mixture parameters are a linearly related to find the partition coefficient, via:

$$\log K_{i,12} = c_1 - c_2 + (r_1 - r_2)*R_{2,i} + (s_1 - s_2)*\pi^H{}_i + (a_1 - a_2)*\Sigma\alpha^H{}_i + (b_1 - b_2)*\Sigma\beta^H{}_i + (v_1 - v_2)*V_{x,i} \tag{4-9}$$

for any solute i partitioning between mixtures 1 and 2,

where R_2 = solute *excess* sodium D-line molar refraction (not identical to molar refraction) [35],
π^H = solute polarity/polarizability [36],
α^H = experimentally determined solute acidity [37],
β^H = experimentally determined solute basicity [38], and
V_x = solute McGowan molecular volume [39].

The molecular solute parameters used in regression eqn 4-9 may be found in published databases, experimentally determined, or calculated [35-41].

In principle, a partition coefficient can be calculated for any characterized solute partitioning between any two characterized mixtures or solvents. Solute descriptors are related to solute physical properties; mixture coefficients are found via regression from literature partition coefficient values. Many partitioning systems have been characterized, (e.g., examples

in Table 4-3). The largest deviations (AAE ~ 0.25) of the LSERs shown in Table 4-3 correspond to only a factor of 0.78 in the partition coefficients.

Table 4-3. Previous studies of the accuracy of LSER predicted partition coefficients

Partition system	N	r^2	AAE of log K_{sw}	error factor in K_{sw}
octanol-water [40]	613	0.997	0.12	0.32
hexadecane-water [40]	370	0.998	0.12	0.32
cyclohexane-water [40]	170	0.997	0.13	0.35
methanol(dry)-water [42]	93	0.988	0.16	0.45
1-pentanol(dry)-water [42]	59	0.996	0.11	0.29
1-heptanol(dry)-water [42]	38	0.997	0.081	0.21
chloroform-water [43]	335	0.97	0.25	0.78

No previous studies have investigated LSERs for gasoline-water systems. A proposed linear relationship between the base-10 log of the gasoline-water partition coefficient and three solute solvatochromic parameters is developed in Chapter 5 of this work.

4-4. Organic matter-water partition coefficient estimation

There is a substantial literature on the prediction of organic matter–water partitioning (K_{om}) or organic carbon–water partitioning (K_{oc}) of polar and nonpolar organic compounds [44-47]. Generally, the organic matter content of a sediment is believed to be about a factor of 2 greater than the organic carbon content, and a typical approximate conversion is [48]:

$$K_{oc} \sim 2K_{om} \tag{4-10}$$

A recent, comprehensive review of K_{om} and K_{oc} prediction methods by Gawlik et al. categorizes them into four major approaches [46]: estimation from aqueous solubility; estimation from K_{ow}; estimation using reverse-phase HPLC capacity factor; and estimation from molecular parameters, topological indices, and linear solvation energy relationships (LSERs).

Gschwend and Wu have shown, however, that improper analytical approaches for quantifying soil–water partitioning have led to highly biased estimates of the K_{oc} in much of the sorption literature [49]. In particular, these authors find that failure to account for colloidally-bound organic compounds in batch equilibrium partitioning experiments leads to underestimated K_{oc}'s and incorrect conclusions about the nature of the sorption process. Clearly, estimation models based on regressions with poorly derived data are unlikely to accurately reflect soil–water partitioning in nature. Therefore we must carefully consider the data quality of established soil–water partition coefficient regressions before accepting the resulting models.

Predicted K_{om} values must be interpreted with legitimate sources of error in mind. Due to the heterogeneous nature of natural organic matter in sediments, measured K_{om} values for a single organic compound may vary by a factor of two between different sediments [48]. Additionally, linear regressions between K_{om} and other physical properties are generally most

accurate when only specific families of organic compounds are considered [48]. General "heterogeneous" regressions which include many families of compounds are less accurate. Therefore, the best strategy to predict the K_{om} of a novel compound is to use a general heterogeneous estimator only if there is not a family-specific regression appropriate for that compound.

Schwarzenbach et al. have compiled critically reviewed experimentally determined K_{om}'s for different families of hydrophobic (highly water insoluble) and hydrophilic (highly water soluble) organic compounds [48]. These authors find reasonably good predictive LFERs between K_{om} and K_{ow} for several compound families:

aromatic hydrocarbons $\log K_{om} = 1.01 \log K_{ow} - 0.72$ (4-11a)
N = 10 $r^2 = 0.99$

chlorinated hydrocarbons $\log K_{om} = 0.88 \log K_{ow} - 0.27$ (4-11b)
N = 12 $r^2 = 0.97$

chloro-s-triazines $\log K_{om} = 0.37 \log K_{ow} + 1.15$ (4-11c)
N = 6 $r^2 = 0.93$

phenyl ureas $\log K_{om} = 1.12 \log K_{ow} + 0.15$ (4-11d)
N = 6 $r^2 = 0.93$

While the best fits were found for individual families of compounds, a reliable general correlation including all of the compounds in the data set was also found:

all compounds $\log K_{om} = 0.82 \log K_{ow} + 0.14$ (4-12)
N = 34 $r^2 = 0.93$

4-5. Octanol–water partition coefficient estimation

Many reliable methods have been developed to predict K_{ow} [40, 50-53]. The most accurate of the comprehensive methods is probably Hansch and Leo's ClogP fragment/factor contribution method [34]. These authors use a fragment contribution approach, modified with molecular structure factors. The factors improve on the fragment method with additive correction terms for branching, long chains, polyhalogenation, rings, and other structural arrangement details that are not captured by the sum of the fragment contributions. The root mean squared error of K_{ow} values predicted using ClogP version 4.0 corresponds to a factor of 1.9 in the partition coefficient, based on a test against 10,000 published values [54, 55].

4-6. Ab initio approaches to estimating organic and aqueous solvation parameters

A number of *ab initio* approaches to estimating solvation energies have been developed or are in progress. Several *continuum solvation* models focus on computation of the electrostatic interaction energies of organic molecules with aqueous or organic solvents, including the Polarizable Continuum Model (PCM) [56], the Solvation Model (SM) [57, 58], and the Conductor-like Screening Model for Real Solvents (COSMO- RS) [59]. These models present the advantage of theoretically rigorous treatments of the specific interactions of solute and solvent molecules. None of these methods incorporate a general solvation theory into their calculations, however. In recent work, Lin and Sandler rely on statistical mechanics to derive the Group Contribution Solvation (GCS) model based on the UNIQUAC solvation theory and parameterize it using *ab initio* interaction energy calculations [31, 60].

A. The Conductor-like Screening Model for Real Solvents (COSMO-RS)

COSMO-RS is probably the most theoretically justified of the continuum solvation models. Earlier continuum solvation models (PCM, SM) approximate the electrostatic part of the solvation energy as a dielectric field around a solute, and determine the field strength from the corresponding dielectric constant of the solvent. COSMO-RS improves on this approximation by calculating the extent to which a solvent screens the charge density of the solute molecule.

Dielectric models respond linearly to molecular surface electric fields, which is physically unrealistic [61-63]. COSMO-RS initially approximates the solute as ideally screened, or perfectly grounded, and proceeds to optimize the approximation by finding the "misfit energies," or deviations from ideal screening, between the solute and adjacent solvent molecules.

The boundary condition used in COSMO-RS is as follows:

$$\Phi_{tot} = \Phi^{B} + \Phi(q^*) = 0 \qquad (4\text{-}13)$$

The total electric field flux (Φ_{tot}) is the sum of contributions from the solute (B) and screening charges (q*) lining the solute cavity. Φ_{tot} must be net zero. The charges are determined by f(ε), where ε is the dielectric constant:

$$f(\varepsilon) = (\varepsilon - 1)/(\varepsilon + 0.5) \qquad (4\text{-}14)$$

For calculation purposes, the screening charges are discretized into patches along the surface of the solute molecule. The screening charges are set at the ideally screened state and simultaneously optimized until the energy of residual charges from solute/solvent electrostatic interactions is at a minimum. This optimization is performed within the framework of a DMol Density Functional Theory (DFT) molecular orbital energy minimization, used to simultaneously find the optimal electron density of the solute.

The COSMO-RS formulation for the chemical potential of a solute B in solvent S, relative to the ideally screened state, is:

$$\mu_S^B = \int(p^B(\sigma)\mu'(\sigma))_S d\sigma - \lambda kT\ln A^S - kT\ln X^B \quad (4\text{-}15)$$

where σ = the screening charge density,

$p^B(\sigma)$ = the "σ-profile," or distribution of solute surface patches with respect to σ,

$\mu'(\sigma)$ = the "σ-potential of S," or the chemical potential of one additional patch with charge density σ, on a molar basis,

λ = the number of patch sets that are independent, per solute (a fitted parameter),

A^S = the surface area of the solvent molecule, and

X^B = the mole fraction of B in the solvent S.

Finding the change in free energy corresponding to transfer of a solute from its pure phase (B) to a different solvent (S):

$$\Delta G_{soln} = \mu_S^B - \mu_B^B = 0 \quad (4\text{-}16)$$

$$0 = \Delta f(\sigma) - \lambda kT\ln(A^S/A^B) - kT\ln X^B \quad (4\text{-}17)$$

where $\Delta f(\sigma) = \int(p^B(\sigma)\mu'(\sigma))_S d\sigma - \int(p^B(\sigma)\mu'(\sigma))_B d\sigma$

The first term in eqn 4-17 integrates the weighted screening charge potential over the solute surface to find the electrostatic costs of screening of the solute and cavitation of the solvent. The second term is derived from the solvent ensemble derivation, but it does not rigorously account for the combinatorial factors in statistical mechanical treatments of solvation. The third term relates the standard chemical potential to the real chemical potential of the solute via the solute mole fraction. No crystallization energy (melting) cost is considered here, that is, the chemical potential formulation addresses solvation of liquids or hypothetical liquids. Finally, the activity coefficient corresponds to:

$$\gamma = (A^S/A^B)^\lambda \exp(-\Delta f(\sigma)/kT) \quad (4\text{-}18)$$

B. The Group Contribution Solvation (GCS) model

Unlike any methods discussed up to this point, the GCS model integrates a rigorous statistical mechanics solvation framework with quantum mechanical computations of electrostatic interaction energies between solute and solvent molecules. The GCS model uses the Polarizable Continuum Model [64] to calculate the electrostatic and induction interactions and the method of Amovilli and Mennucci [65] to calculate dispersion and repulsion contributions. These methods are used to parameterize UNIQUAC molecular interaction terms for partition coefficients.

The UNIQUAC system is decomposed into two parts: ΔG^{cav}, a sum of terms representing the energetic costs of cavity formation in the solvent; and ΔG^{chg}, a sum of terms representing the energetic contribution of electronic (charge) interactions between the solute and solvent molecules.

The study reveals that a key variable in the quantum calculation, the scale factor, can be parameterized for different structural functionalities in a given solvent. The scale factor represents a correction to the proximity of the dielectric field around the solute molecule. In other words, a scale factor value other than one implies that the solvent does not induce the same dielectric field at the solute surface as it does in the bulk solution (where the average dielectric field is equal to the dielectric constant). It turns out that if a characteristic scale factor is optimized for individual solute structural fragments in a given solvent, solvation energy predictions can be made with high accuracy. This strongly supports the hypothesis that electronic interactions between individual solute fragments and given a solvent are relatively characteristic (i.e., independent of each other).

The GCS also finds that the ΔG^{chg} for a solute in a given solvent is proportional to the van der Waals surface area of the geometry-optimized solute for a given family of organic solutes. This relationship is found to have a nearly perfect correlation factor ($r^2 = 1.00$), and it presumably can be decomposed into a group contribution calculation method for any solute, for a given solvent. By using the quantum calculations to find linear free energy relationships such as these, the need to use *ab initio* calculations to solve every new problem is circumvented. *Ab initio* methods may only be necessary to optimize fragment contributions to ΔG^{chg} for solutes in a given solvent.

Because the GCS generalizes the behavior of the solvent, it is much easier to calculate partition coefficients than individual activity coefficients. This results from the fact that calculating a partition coefficient, say between octanol and water, does not require an understanding of the solute interaction behavior with itself in the pure phase. It only requires a parameterized relationship between the activities in the aqueous and octanol phases. For the infinite dilution partition coefficient of solute B in solvents o and w:

$$RT\ln(\gamma_w/\gamma_o) = RT\ln(\gamma_w(comb)/\gamma_o(comb)) + RTq_B(\tau_o - \tau_w) + \Delta G_w^{chg} - \Delta G_o^{chg} \qquad (4\text{-}19)$$

where γ_s = infinite dilution activity coefficient in solvent s,
$\gamma_s(comb)$ = combinatorial expression from the UNIQUAC equation,
q_B = van der Waals surface area of the solute B, and
τ_s = interaction energy parameter between solute molecule B and solvent molecule, s.

Unlike UNIFAC, the GCS model cannot be generally parameterized for any solvent or solvent mixture. Interaction parameters and ΔG^{chg} values for solute fragments must be separately determined for each solvent. The nature of the system suggests that empirical fitting methods may eventually be used to find these parameters, rather than computationally expensive quantum calculations.

Since the properties of the solvents have already been accurately evaluated (as in the case of water and octanol), the necessary input parameters for a partition coefficient calculation are only the molecular volume, molecular surface area, and ΔG^{chg}. Molecular volume and surface area are easily calculable with molecular simulations methods or software, and ΔG^{chg} may be determined from a group contribution method. The GCS model makes predicitions for the partitioning of alkanes, alkenes, alkynes, cyclic alkanes, alcohols, esters, nitrates, halogenated

alkanes, ketones, amines, nitriles, amides, and phenyl compounds in several mixture systems with an absolute average error of only 15% to 30% in the partition coefficient (Table 4-4) [31, 60]:

Table 4-4. Previous studies of the accuracy of GCS predicted partition coefficients [31, 60]

partition coefficient	N	AAE (factor of error in K_{ow})
K_{ow} (octanol-water)	226	0.26
K_{hw} (hexane-water)	18	0.22
K_{aw} (acetonitrile-water)	14	0.18
K_{ow} (octanol-water)	15	0.14

An important caveat in Lin and Sandler's work is that it has been parameterized using only homologous series' of solutes. It will not be well-validated until its efficacy with significantly more varied and complex structures has been established.

4-7. Conclusions and outlook

A number of approaches have been developed in an effort to explain and predict solvation energies and partition coefficients. Some generalizations can be made about the state of the science.

(1) Activity coefficient estimation for organic solutes in solvents of environmental interest (water, octanol, hexane) is becoming accurate and comprehensive.

(2) It is easier to predict a partition coefficient between two well-characterized solvents, than to predict an activity coefficient of an organic compound. This results from the fact that for a partition coefficient between solvents, e.g. hexane and water, the properties of the solvents remain constant during parameterization over a range of solutes. For the direct prediction of an activity coefficient on the other hand, computation of solvation effects in the pure solute must be incorporated in the model. Thus, a model for partition coefficients is actually more physically constrained than a model for activity coefficients. An exception may be the pure phase vapor pressure, which is rapidly becoming predictable with high accuracy for almost any organic compound [66-68].

(3) The unification of *ab initio* energetics computations with rigorous solvation theory is very recent, and it has additional room for development. The Group Contribution Solvation (GCS) model makes predictions of unprecedented accuracy using the Polarizable Continuum Model (PCM) solvation approximation and UNIQUAC. The Mobile Order and Disorder theory has not yet been developed with the use of *ab initio* calculations, however, and the GCS approach is not currently established as a rigorous solvation model.

(4) There is not a consensus on the best theoretical approach to modeling aqueous solvation. The use of *ab initio* computations to develop the investigation of the underlying physical chemistry will hopefully help to push this forward.

(5) The prediction of organic matter-water partition coefficients still involves significant uncertainty. This results largely from measurement inaccuracy in the experimental data, and the highly variable nature of organic matter. Some attempts are being made to improve predictive accuracy with characteristic factors related to the organic matter composition (ratio of C, H to N, O, S, for instance). No attempts have been made to involve highly theoretical computations such as those used in the GCS model, however.

(6) Linear solvation energy relationships (LSERs) are a highly accurate and robust tool for prediction of partition coefficients. However, they require prior knowledge or estimation of the molecular descriptors developed by Abraham et al. [35, 40].

4-8. Citations

1. Klopman, G., S. Wang, and D.M. Balthasar, *Estimation of aqueous solubility of organic molecules by the group contribution approach. Application to the study of biodegradation.* Journal of Chemical Information and Computer Sciences, 1992. **32**: p. 474-482.
2. Muller, M. and W. Klein, *Comparative evaluation of methods predicting water solubility for organic compounds.* Chemosphere, 1992. **25**: p. 769-782.
3. Bruggemann, R. and J. Altschuh, *A validation study for the estimation of aqueous solubility from n-octanol/water partition coefficients.* Science of the Total Environment, 1991. **109/110**: p. 41-57.
4. Lyman, W.J., *Solubility in Water*, in *Handbook of Chemical Property Estimation Methods*, W. Lyman, W. Reehl, and D. Rosenblatt, Editors. 1990, American Chemical Society: Washington D.C.
5. Leahy, D.E., *Intrinsic molecular volume as a measure of the cavity term in linear solvation energy relationships: octanol-water partition coefficients and aqueous solubilities.* Journal of Pharmaceutical Sciences, 1986. **75**: p. 629-636.
6. Reinhard, M. and A. Drefal, *Aqueous Solubility*, in *Handbook for Estimating Physicochemical Properties of Organic Compounds.* 1999, John Wiley & Sons: New York, NY. p. 118-135.
7. Myrdal, P.B., G.H. Ward, R.M. Dannenfelser, D. Mishra, and S.H. Yalkowsky, *AQUAFAC 1: aqueous functional group activity coefficients; application to hydrocarbons.* Chemosphere, 1992. **24**: p. 1047-1061.
8. Myrdal, P.B., G.H. Ward, P. Simamora, and S.H. Yalkowsky, *AQUAFAC: aqueous functional group activity coefficients.* SAR and QSAR in Environmental Research, 1993. **1**: p. 53-61.
9. Myrdal, P.B., A.M. Manka, and S.H. Yalkowsky, *AQUAFAC 3: aqueous functional group activity coefficients; application to the estimation of aqueous solubility.* Chemosphere, 1995. **30**: p. 1619-1637.
10. Lee, Y.C., P.B. Myrdal, and S.H. Yalkowsky, *Aqueous functional group activity coefficients (AQUAFAC) 4: applications to complex organic compounds.* Chemosphere, 1996. **33**: p. 2129-2144.
11. Pinsuwan, S., P.B. Myrdal, Y.C. Lee, and S.H. Yalkowsky, *AQUAFAC 5: aqueous functional group activity coefficients; application to alcohols and acids.* Chemosphere, 1997. **35**: p. 2503-2513.
12. Yalkowsky, S.H., *Mixing and Properties of Mixtures*, in *Solubility and Solubilization in Aqueous Media*, A.C. Society, Editor. 1999, Oxford University Press: New York, NY. p. 26, 44.
13. Giesen, D.J., C.J. Cramer, and D.G. Truhlar, *Entropic contributions to free energies of solvation.* Journal of Physical Chemistry, 1994. **98**: p. 4141-4147.
14. Hansch, C. and A.J. Leo, *Exploring QSAR.* 1995, Washington D.C.: American Chemical Society. p. 103-105.
15. Frank, H.S. and M.W. Evans, *Free volume and entropy in condensed systems. III. Entropy in binary liquid mixtures; partial molal entropy in dilute solutions; structure and thermodynamics in aqueous electrolytes.* Journal of Chemical Physics, 1945. **13**: p. 507-532.

16. Huyskens, P.L. and G.G. Siegel, *Fundamental questions about entropy II. The combinatorial entropy of mixing in liquids.* Bulletin des Societes Chimiques Belges, 1988. **97**(11-12): p. 815-819.
17. Huyskens, P.L. and G.G. Siegel, *Fundamental questions about entropy III. A kind of mobile order in liquids : preferential contacts between molecular groups.* Bulletin des Societes Chimiques Belges, 1988. **97**(11-12): p. 821-824.
18. Huyskens, P.L. and G.G. Siegel, *Fundamental questions about entropy IV. The hydrophobicity of alkanes : a nearly pure entropic effect.* Bulletin des Societes Chimiques Belges, 1988. **97**(11-12): p. 825-830.
19. Huyskens, P.L., *Mobile and static molecular disorder in liquids.* Journal of Molecular Structure, 1992. **274**: p. 223-246.
20. Ruelle, P. and U.W. Kesselring, *Aqueous solubility prediction of environmentally important chemicals from the mobile order thermodynamics.* Chemosphere, 1997. **34**(2): p. 275-298.
21. Ruelle, P., *Understanding the volume-solubility dependence: the mobile order and disorder view.* Journal of Physical Organic Chemistry, 1999. **12**: p. 769-786.
22. Ruelle, P., *The n-octanol and n-hexane/water partition coefficient of environmentally relevant chemicals predicted from the mobile order and disorder (MOD) thermodynamics.* Chemosphere, 2000. **40**: p. 457-512.
23. Constantinou, L., R. Gani, and J.P. O'Connell, *Estimation of the acentric factor and the liquid molar volume at 298 K using a new group contribution method.* Fluid Phase Equilibria, 1995. **103**: p. 11-22.
24. Fredenslund, A., R.J. Jones, and J.M. Praustnitz, *Group-contribution estimation of activity coefficients in nonideal liquid mixtures.* AIChE Journal, 1975. **21**(6): p. 1086-1099.
25. Abrams, D.S. and J.M. Prausnitz, *Statistical thermodynamics of liquid mixtures: a new expression for the excess Gibbs energy of partly or completely miscible systems.* AIChE Journal, 1975. **21**(1): p. 116-128.
26. Derr, E.L. and C.H. Deal. *Analytical solutions of groups: correlation of activity coefficients through structural group parameters.* 1969. London. p. 40-51.
27. Ronc, M. and G.A. Ratcliff, *Prediction of excess free energies of liquid mixtures by an analytical group solution model.* The Canadian Journal of Chemical Engineering, 1971. **49**: p. 825-830.
28. Gmehling, J., J. Li, and M. Schiller, *A modified UNIFAC model. 2. Present parameter matrix and results for different thermodynamic properties.* Industrial & Engineering Chemistry Research, 1993. **32**: p. 178-193.
29. Gmehling, J., J. Lohmann, A. Jakob, J.D. Li, and R. Joh, *A modified UNIFAC (Dortmund) model. 3. Revision and extension.* Industrial & Engineering Chemistry Research, 1998. **37**: p. 4876-4882.
30. Park, S.J. and J.M. Back, *Prediction of partition coefficients for some organic compounds using UNIFAC.* Journal of Industrial and Engineering Chemistry, 2000. **6**(2): p. 100-106.
31. Lin, S.T. and S.I. Sandler, *Prediction of octanol-water partition coefficients using a group contribution solvation model.* Industrial & Engineering Chemistry Research, 1999. **38**: p. 4081-4091.

32. Li, A., S. Pinsuwan, and S.H. Yalkowsky, *Estimation of solubility of organic compounds in 1-octanol.* Industrial & Engineering Chemistry Research, 1995. **34**: p. 915-920.
33. Kan, A.T. and M.B. Tomson, *UNIFAC prediction of aqueous and nonaqueous solubilities of chemicals with environmental interest.* Environmental Science & Technology, 1996. **30**(4): p. 1369-1376.
34. Hansch, C. and A.J. Leo, *Substituent constants for correlation analysis in chemistry and biology.* 1979, New York, NY: John Wiley & Sons.
35. Abraham, M.H., C.F. Poole, and S.K. Poole, *Classification of stationary phases and other materials by gas chromatography.* Journal of Chromatography A, 1999. **842**: p. 79-114.
36. Abraham, M.H. and G.S. Whiting, *XVI. A new solute solvation parameter, π_2^H, from gas chromatographic data.* Journal of Chromatography, 1991. **587**: p. 213-228.
37. Abraham, M.H., P.L. Grellier, D.V. Prior, P.P. Duce, J.J. Morris, and P.J. Taylor, *Hydrogen bonding. Part 7. A scale of solute hydrogen-bond acidity based on logK values for complexation in tetrachloromethane.* Journal of the Chemical Society - Perkins Transactions 2, 1989: p. 699-711.
38. Abraham, M.H., P.L. Grellier, D.V. Prior, J.J. Morris, and P.J. Taylor, *Hydrogen bonding. Part 10. A scale of solute hydrogen-bond basicity using logK values for complexation in tetrachloromethane.* Journal of the Chemical Society - Perkins Transactions 2, 1990: p. 521-529.
39. Abraham, M.H. and J.C. McGowan, *The use of characteristic volumes to measure cavity terms in reversed phase liquid chromatography.* Chromatographia, 1987. **23**(4): p. 243-246.
40. Abraham, M.H., H.S. Chadha, G.S. Whiting, and R.C. Mitchell, *Hydrogen-bonding. 32. An analysis of water-octanol and water-alkane partitioning and the delta-logP parameter of Seiler.* Journal of Pharmaceutical Sciences, 1994. **83**(8): p. 1085-1100.
41. Abraham, M.H., *Scales of solute hydrogen-bonding: their construction and application to physiochemical and biochemical processes.* Chemical Society Reviews, 1993: p. 73-83.
42. Abraham, M.H., J. Le, and W.E. Acree, *The solvation properties of the aliphatic alcohols.* Collection of Czechoslovak Chemical Communications, 1999. **64**(11): p. 1748-1760.
43. Abraham, M.H., J.A. Platts, A. Hersey, A.J. Leo, and R.W. Taft, *Correlation and estimation of gas-chloroform and water-chloroform partition coefficients by a linear free energy relationship method.* Journal of Pharmaceutical Sciences, 1999. **88**(7): p. 670-679.
44. Chiou, C.T., P.E. Porter, and D.W. Schmedding, *Partition equilibria of nonionic organic compounds between soil organic matter and water.* Environmental Science & Technology, 1983. **17**: p. 227-231.
45. Karickhoff, S.W., *Semi-empirical estimation of sorption of hydrophobic pollutants on natural sediments and soils.* Chemoshere, 1981. **10**: p. 833-846.
46. Gawlik, B.M., N. Sotiriou, E.A. Feicht, S. Schulte-Hostede, and A. Kettrup, *Alternatives for the determination of the soil adsorption coefficient, K_{OC}, of non-ionic organic compounds - a review.* Chemosphere, 1997. **34**(12): p. 2525-2551.

47. Schwarzenbach, R.P. and J. Westall, *Transport of nonpolar organic compounds from surface water to groundwater: Laboratory sorption studies.* Environmental Science & Technology, 1981. **15**: p. 1360-1367.
48. Schwarzenbach, R.P., P.M. Gschwend, and D.M. Imboden, *Environmental Organic Chemistry.* 1993, New York, NY: John Wiley & Sons. p. 267, 268, 272-276.
49. Gschwend, P.M. and S.C. Wu, *On the constancy of sediment-water partition coefficients of hydrophobic organic pollutants.* Environmental Science & Technology, 1985. **19**: p. 90-96.
50. Wienke, G. and J. Gmehling, *Prediction of octanol-water partition coefficients, Henry coefficients and water solubilities.* Toxicology and Environmental Chemistry, 1998. **65**: p. 57.
51. Kamlet, M.J., R.M. Doherty, M.H. Abraham, Y. Marcus, and R.W. Taft, *Linear solvation energy relationships. 46. An improved equation for correlation and prediction of octanol/water partition coefficients of organic nonelectrolytes (including strong hydrogen bond donor solutes).* Journal of Physical Chemistry, 1988. **92**: p. 5244.
52. Isnard, P. and S. Lambert, *Aqueous solubility and n-octanol/water partition coefficient correlations.* Chemosphere, 1989. **18**: p. 1837-1853.
53. Suzuki, T. and Y. Kudo, *Automatic logP estimation based on combined additive modeling methods.* Journal of Computer-Aided Molecular Design, 1990. **4**: p. 155-198.
54. Leo, A.J. and D. Hoekman, *Calculating logP(oct) with no missing fragments; the problem of estimating new interaction parameters.* Perspectives in Drug Discovery and Design, 2000. **18**: p. 19-38.
55. Leo, A.J. and C. Hansch, *Role of hydrophobic effects in mechanistic QSAR.* Perspectives in Drug Discovery and Design, 1999. **17**: p. 1-25.
56. Barone, V., M. Cossi, and J. Tomasi, *Geometry optimization of molecular structures in solution by the polarizable continuum model.* Journal of Computational Chemistry, 1998. **19**(4): p. 404-417.
57. Hawkins, G.D., C.J. Cramer, and D.G. Truhlar, *Universal quantum mechanical model for solvation free energies based on gas-phase geometries.* Journal of Physical Chemistry B, 1998. **102**(17): p. 3257-3271.
58. Dolney, D.M., G.D. Hawkins, P. Winget, D.A. Liotard, C.J. Cramer, and D.G. Truhlar, *Universal solvation model based on conductor-like screening model.* Journal of computational chemistry, 2000. **21**(5): p. 340-366.
59. Klamt, A., V. Jonas, T. Burger, and J.W.C. Lohrenz, *Refinement and parameterization of COSMO-RS.* Journal of Physical Chemistry A, 1998. **102**: p. 5047-5085.
60. Lin, S.T. and S.I. Sandler, *Infinite dilution activity coefficients from ab initio solvation calculations.* AIChE Journal, 1999. **45**(12): p. 2606-2618.
61. King, G. and A. Warshel, *Investigation of the free-energy functions for electron-transfer reactions.* Journal of Chemical Physics, 1990. **93**(12): p. 8682-8692.
62. Aqvist, J. and T. Hansson, *On the validity of electrostatic linear response in polar solvents.* Journal of Physical Chemistry, 1996. **100**(22): p. 9512-9521.
63. Marten, B., K. Kim, C. Cortis, R.A. Friesner, R.B. Murphy, M.N. Ringnalda, D. Sitkoff, and B. Honig, *New model for calculation of solvation free energies: Correction of self-consistent reaction field continuum dielectric theory for short-range hydrogen-bonding effects.* Journal of Physical Chemistry, 1996. **100**(28): p. 11775-11788.

64. Cossi, M., V. Barone, R. Cammi, and J. Tomasi, *Ab initio study of solvated molecules: a new implementation of the polarizable continuum model.* Chemical Physics Letters, 1996. **225**: p. 327-335.
65. Amovilli, C. and B. Mennucci, *Self-consistent-field calculation of Pauli repulsion and dispersion contributions to the solvation free energy in the Polarizable Continuum Model.* Journal of Physical Chemistry B, 1997. **101**: p. 1051.
66. Myrdal, P.B. and S.H. Yalkowsky, *Estimating pure component vapor pressures of complex organic molecules.* Industrial & Engineering Chemistry Research, 1997. **36**: p. 2494-2499.
67. Stein, S.E. and R.L. Brown, *Estimation of normal boiling points from group contributions.* Journal of Chemical Information and Computer Sciences, 1993. **34**(3): p. 581-587.
68. Simamora, P. and S.H. Yalkowsky, *Group contribution methods for predicting the melting points and boiling points of aromatic compounds.* Industrial & Engineering Chemistry Research, 1994. **33**: p. 1405-1409.

Chapter 5

Prediction Results of the Physical Property Estimation Methods and Subsurface Transport Model for Gasoline Constituents

5-1. Introduction

It has already been shown that gasoline contamination of community supply wells by leaking underground fuel tanks (LUFTs) depends heavily on the partitioning properties of the individual gasoline solutes. The ability to predict the water supply well contamination and environmental partitioning properties of gasoline constituents is therefore a critical exercise. In this chapter, the subsurface transport behaviors and associated partition coefficients of over twenty compounds found in gasoline were evaluated.

Several physical property estimation methods were used to predict the gasoline–water partition coefficients (K_{gw}), organic matter–water partition coefficients (K_{om}), and octanol–water partition coefficients (K_{ow}) of gasoline solutes. The K_{gw} and K_{om} values are critical parameters for modeling the subsurface transport behavior of individual organic compounds from a gasoline spill in the phreatic (saturated) zone. The K_{ow} was chosen because it is highly studied and can be accurately predicted, and very large databases make the K_{ow} convenient to relate to other solvation properties via LFERs (**l**inear **f**ree **e**nergy **r**elationships). Additionally, these properties reflect varying levels complexity of organic mixtures, and hence they may give insight into the limitations of modeling attempts to capture organic mixture–water partitioning behavior.

Where feasible, model predictions were tested against experimental data as a preliminary evaluation of accuracy and robustness using a common set of compounds found in gasoline. The data set is relatively diverse, including compounds that are large and small; polar and nonpolar; unsubstituted and highly substituted with moieties containing heteroatoms. It was hoped that this set, albeit small, would probe the weaknesses and strengths of the physical property models in informative ways.

The transport assessment method outlined in Chapter 3 was used to predict subsurface travel times and contaminant concentrations of gasoline components in proximate municipal water supply wells. Transport model results are useful for several reasons. First, these predictions provided a basis for evaluating the validity of the "ensemble" transport modeling approach (i.e., attempting to capture typical or average transport behavior). Additionally, the model results suggest other compounds which may currently pose significant risks to municipal drinking water wells in the U.S., thus guiding future studies. Finally, the transport model may be used to evaluate future gasoline additives or formulations *a priori* to ensure that these compounds will not pose large scale threats to national drinking water resources.

5-2. A proposed gasoline-water partitioning Linear Free Energy Relationship (LFER)

The simplest approach to predicting the gasoline–water partition coefficient (K_{gw}) is probably by use of a LFER with K_{ow}. The K_{ow} partitioning system is useful because it is a well-

characterized property for most organic compounds, from large databases and highly studied estimation methods (as described in Chapter 4). Additionally, K_{ow} values reflect the energetic contributions of solvation in both water and a mixture (water-saturated octanol) with both polar and non-polar functionalities. The water-saturated octanol mixture is therefore potentially useful to compare to gasoline, as both mixtures contain both polar and nonpolar functionalities.

Method: A regression of log K_{gw} and log K_{ow} was performed using 26 solutes found in gasoline. The solutes were qualitatively grouped as either "polar" and "nonpolar" based on the presence or absence of heteroatomic moieties (Table 5-1). They were additionally grouped by their ability to accept hydrogen bonds, based on the presence of outer shell lone pair electrons; or donate hydrogen bonds, based on the presence of acidic protons.

Table 5-1. Measured K_{ow} and K_{gw} data at 25 °C

	compound	K_{ow} [a]	K_{gw} [b]	polarity	hydrogen bonding
1	benzene	130	220 (220, 217, 350)	nonpolar	none
2	toluene	540	690 (690, 687, 1250)	nonpolar	none
3	ethylbenzene	1410	2200 (2200, 4500)	nonpolar	none
4	m-xylene	1580	2200 (2200, 4350)	nonpolar	none
5	o-xylene	1320	2200 (2200, 3630)	nonpolar	none
6	p-xylene	1410	2200 (2200, 4350)	nonpolar	none
7	naphthalene	2000	1500	nonpolar	none
8	methylbenzotriazole	13.4	2.7	polar	acceptor
9	thiophene	78	110	polar	acceptor
10	methyl-*tert*-butylether	8.7	16	polar	acceptor
11	benzothiophene	1320	1700	polar	acceptor
12	methanol	0.17	0.0051 (0.0051, 0.0055)	polar	acceptor + donor
13	ethanol	0.49	0.015 (0.0083, 0.022)	polar	acceptor + donor
14	benzotriazole	25.7	0.20	polar	acceptor + donor
15	aniline	7.9	3.1	polar	acceptor + donor
16	p-toluidine	24.5	12	polar	acceptor + donor
17	o-toluidine	20.9	12	polar	acceptor + donor
18	3,4-dimethylaniline	110	29	polar	acceptor + donor
19	2,6-dimethylaniline	69.2	39	polar	acceptor + donor
20	phenol	29.5	3.2	polar	acceptor + donor
21	p-cresol	87	9.3	polar	acceptor + donor
22	o-cresol	89	14	polar	acceptor + donor
23	3,4-dimethylphenol	170	22	polar	acceptor + donor
24	2,6-dimethylphenol	230	44	polar	acceptor + donor
25	3,4,5-trimethylphenol	777	53	polar	acceptor + donor
26	2,4,6-trimethylphenol	540	120	polar	acceptor + donor

[a] Data obtained from the database provided by BioByte Inc. with ClogP [1-3].

[b] Data obtained from Schmidt et al., Cline et al., Stephenson, and Heermann and Powers [4-7]. Where multiple values were found in the literature, they are all listed parenthetically. The K_{gw} value chosen here represents either data from one method or an average of listed data.

Results: A regression grouping all of the solutes revealed a relatively poor fit:

all compounds $\log K_{gw} = 1.33 \log K_{ow} - 1.13$ (5-1)
N = 26 AAE = 0.43 $r^2 = 0.87$

The absolute average error (AAE) of 0.43 log K_{gw} units corresponds to a factor of 2.7 in the K_{gw}. Separating compounds into different families yielded improved predictive relationships, but there were still significant outliers (Figure 5-1):

non-H bonders and H bond acceptors $\log K_{gw} = 1.11 \log K_{ow} - 0.21$ (5-2)
N = 11 AAE = 0.17 $r^2 = 0.992$

H bond donors and acceptors $\log K_{gw} = 1.18 \log K_{ow} - 1.16$ (5-3)
N = 15 AAE = 0.36 $r^2 = 0.88$

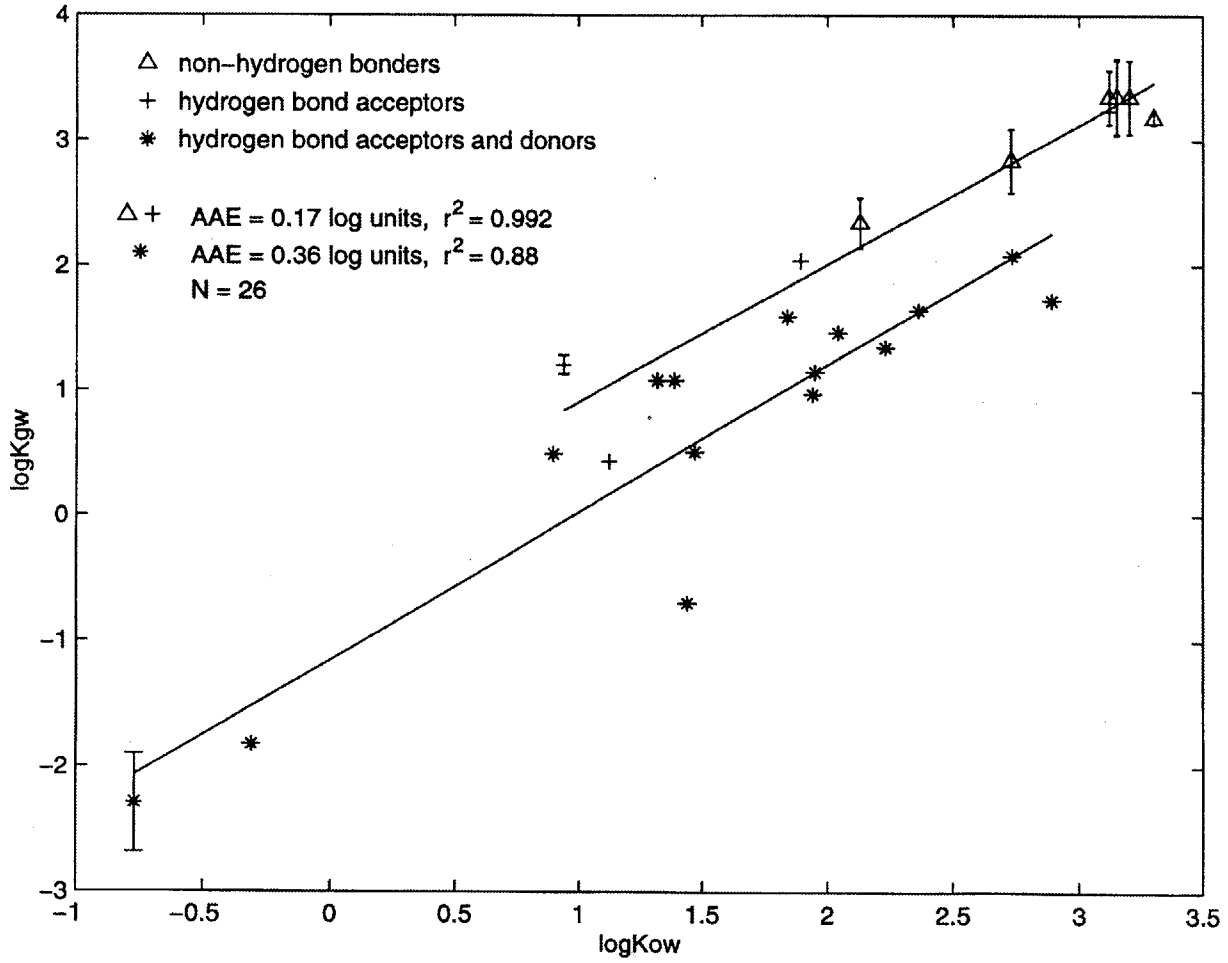

Figure 5-1. LFER between log K_{gw} and log K_{ow} for different compound families

Where multiple data were available (Table 5-1) or authors suggested measurement errors, error bars were estimated (Figure 5-1). The strong outliers in this dataset mostly fell below the existing regression lines and included the fused-ring aromatic compounds. Benzotriazole (log K_{gw} = -0.70), 1-methylbenzotriazole (log K_{gw} = 0.43), and naphthalene (log K_{gw} = 3.18) all fell significantly below the family-specific regressions. The only other fused-ring aromatic structure considered in the data set was benzothiophene. This suggests that the fused-ring aromatic structures may have an additional affinity for water-saturated octanol over gasoline than do the single-ring structures. This may reflect the ability of water-saturated octanol to interact better (than the gasoline mixture) with the increased density of π electrons that is found in fused-ring aromatic structures. It is important to bear in mind that the literature partition coefficient measurements used here had estimated measurement errors of much as 50 to 80%. In other words, some of the observed discrepancy in the LFER fit may simply be related to poor data. Alternatively, the observed outlier trend may reflect an important general limitation of the model: multiple types of solute-solvent interactions can undermine the predictive capability of single-variable LFERs [8].

The regression line for hydrogen bond donors and acceptors was shifted about 1 log K_{gw} unit lower than the regression line for non-hydrogen bonders and hydrogen bond acceptors. This corroborates the chemical intuition that compounds which can better facilitate hydrogen-bonding should have a higher affinity for water-saturated octanol than for gasoline.

Conclusions: It seems likely that a useful K_{gw} predictive tool may be developed from a larger dataset. Outliers suggested that, if the data are correct, predictive capability of the LFER for fused-ring aromatic structures may benefit from some type of correction factor. The log K_{gw} – log K_{ow} LFERs for individual groups gave more accurate predictions than UNIFAC, which is discussed in the next section (5-3). This is not a rigorous comparison, however, since the LFER prediction statistics were obtained using data from which they were fitted.

5-3. UNIFAC and AQUAFAC predictions of gasoline–water partitioning

UNIFAC is a generalized fragment-contribution method based on the statistical thermodynamics UNIQUAC solvation theory. UNIFAC has the advantage of being able to compute the activities for components of any hypothetical mixture at a range of temperatures. However, it has the disadvantage of requiring $6N^2$ parameters for a mixture containing N fragment types. In practice, the activity coefficients of many kinds of mixtures cannot be calculated, because many of the required UNIFAC parameters have not yet been fitted from laboratory measurements. UNIFAC is discussed further in Chapter 3.

Method: A hypothetical gasoline mixture was derived from components listed in Schubert and Johansen [9]. These authors obtained a finished motor gasoline representing the 1989 U.S. "industry average" composition and analyzed the gasoline mixture for hundreds of hydrocarbon components through several different laboratories. Gasoline compositions vary widely regionally, seasonally, and have changed during the last ten years. However, this composition is useful for predictive calculations, since it represents a relatively contemporary gasoline mixture that does not incorporate highly unusual chemical characteristics.

A hypothetical conventional (i.e., not oxygenated) gasoline mixture is hereafter referred to as *conventional syngas*, composed of the components that average greater than 1.8% by mass in the gasoline analyzed by Schubert and Johansen. The 17 components of conventional syngas consist of 48% hydrocarbons, 47% lightweight aromatics, and 5% olephins by mass (Table 5-2). The mole fraction concentrations and UNIFAC-predicted activity coefficients of the components were also calculated, showing that the syngas components experience near ideality in solution (activity coefficient ~ 1). This matches conventional expectations about mixtures of nonpolar hydrocarbons.

It is worth noting that current legislation imposes a limit of 1% vol/vol, or about 1.2% wt/ wt, benzene in gasoline and thus prohibits the formulation observed in syngas (4.3% wt/wt benzene). It might be argued that syngas is therefore less relevant because it does not realistically represent today's conventional finished motor gasoline. However, it should be kept in mind that the composition of gasoline continually changes in response to evolving demands from both automobile manufacturers and regulators. The important point is that the solvation properties of syngas should adequately represent the conventional gasolines of both 1989 and today.

Presumably, addition of an oxygenate to conventional gasoline may change the solvation properties of the mixture. 10% (vol/vol) MTBE was added to syngas, keeping other relative concentrations proportional, and a new composition was produced, hereafter referred to as *oxygenated syngas* (Table 5-3). Because the density of MTBE is nearly identical to that of

Table 5-2. Composition of the hypothetical gasoline mixture, "conventional syngas"

gasoline component	mass fraction abundance	mole fraction abundance	UNIFAC-calculated activity coefficient at 25 °C
butane	0.083	0.1275	1.05
pentane	0.075	0.0928	1.09
hexane	0.058	0.0601	1.10
heptane	0.022	0.0196	1.09
octane	0.020	0.0156	1.06
2-methylpentane	0.058	0.0601	1.10
2,3-dimethylbutane	0.040	0.0415	1.10
2,2,4-trimethylpentane	0.106	0.0828	1.08
methylcyclopentane	0.021	0.0223	1.07
2,-methyl-2-butene	0.018	0.0229	1.07
1-hexene	0.034	0.0361	1.02
benzene	0.043	0.0491	1.15
toluene	0.162	0.1570	1.15
xylenes	0.062	0.0521	1.08
ethylbenzene	0.073	0.0692	1.10
1,2,3-trimethylbenzene	0.092	0.0683	0.97
naphthalene	0.033	0.0230	1.56

typical conventional gasolines ($\rho_{gasoline}$ ~ 0.75), the mass abundance of MTBE in oxygenated syngas was also 10% (wt/wt).

Assuming Agamat's law applies to the syngas mixtures, the syngas molar volume was approximated as the mole fraction abundance-weighted average of the component molar volumes, based on literature pure liquid phase density data [10]:

$$V_{syngas} = 0.001 * \Sigma (X_i * mw_i / \rho_i) \qquad \text{for i = 1 to N mixture components} \qquad (5\text{-}4)$$

where V_{syngas} = the molar volume of syngas, L/mol,
X_i = mole fraction of component i,
mw_i = molecular weight of component i, g/mol, and
ρ_i = pure phase liquid density of component i, g/cm^3.

The calculated molar volumes were $V_{conv.\ syngas}$ = 0.1215 L/mol and $V_{oxyg.\ syngas}$ = 0.1212 L/mol.

After formulation of both conventional and oxygenated syngas, the partition coefficients of several heteroatom-containing solutes between syngas and water were predicted. Solutes were individually added to the syngas mixtures at realistic concentrations (Table 5-4) and their syngas activity coefficients were calculated using UNIFAC. Additionally, the aqueous activity coefficients of these compounds were calculated using both UNIFAC and AQUAFAC (both models are discussed in Chapter 3). Thus, both UNIFAC and AQUAFAC-based activity

Table 5-3. Composition of "oxygenated syngas"

gasoline component	mass fraction abundance	mole fraction abundance	UNIFAC-calculated activity coefficient at 25° C
butane	0.075	0.1150	1.06
pentane	0.067	0.0828	1.10
hexane	0.052	0.0538	1.12
heptane	0.020	0.0178	1.11
octane	0.018	0.0140	1.08
2-methylpentane	0.052	0.0538	1.12
2,3-dimethylbutane	0.036	0.0373	1.12
2,2,4-trimethylpentane	0.095	0.0736	1.10
methylcyclopentane	0.019	0.0201	1.09
2,-methyl-2-butene	0.016	0.0203	1.07
1-hexene	0.031	0.0328	1.04
benzene	0.039	0.0445	1.12
toluene	0.146	0.1413	1.14
xylenes	0.056	0.0470	1.08
ethylbenzene	0.066	0.0625	1.09
1,2,3-trimethylbenzene	0.083	0.0615	0.98
naphthalene	0.030	0.0208	1.51
methyl-*tert*-butylether	0.100	0.1011	1.21

coefficient predictions were used to compute syngas-water partition coefficients, from the relationship discussed in Chapter 3 (see eqn 3-2):

$$K_{gw} = (\gamma_{water} * V_{water})/(\gamma_{gasoline} * V_{gasoline}) \quad (5\text{-}5)$$

Table 5-4. Representative abundances of several compounds found in gasoline

	compound	concentration in gasoline
1	aniline	20 ppm[a]
2	p-toluidine	30 ppm[a]
3	o-toluidine	20 ppm[a]
4	3,4-dimethylaniline	15 ppm[a]
5	2,6-dimethylaniline	15 ppm[a]
6	phenol	150 ppm[a]
7	p-cresol	100 ppm[a]
8	o-cresol	100 ppm[a]
9	3,4-dimethylphenol	30 ppm[a]
10	2,6-dimethylphenol	30 ppm[a]
11	3,4,5-trimethylphenol	[b]
12	2,4,6-trimethylphenol	[b]
13	thiophene	150 ppm[c]
14	benzothiophene	300 ppm[c]
15	methyl-*t*-butylether	10.0% wt/wt[d]
16	methanol	10.6% wt/wt[d]
17	ethanol	10.5% wt/wt[d]
18	benzene	1.2% wt/wt[e]
19	toluene	16.2% wt/wt[e]
20	ethylbenzene	7.3% wt/wt[e]
21	n-propylbenzene	0.66% wt/wt[e]
22	naphthalene	3.3% wt/wt[e]
23	m-xylene	2.7% wt/wt[e]
24	o-xylene	2.7% wt/wt[e]
25	p-xylene	2.7% wt/wt[e]

[a] Based on measurements of several gasolines by Schmidt [4].

[b] Although these compounds have been identified in gasoline [4], their abundances have not yet been reported to my knowledge. Their activity coefficients were therefore calculated in UNIFAC at infinite dilution.

[c] These quantities represent high estimates based on measurements by Quimby et al. and Martin et al. [11, 12]. It should be noted that recent legislation has drastically reduced the allowable amount of sulfur in gasoline.

[d] Corresponds to 10% vol/vol.

[e] These quantities were based on data from Schubert and Johansen [9]. For the xylenes, only data for o-xylene were listed. The proposed abundances for p-xylene and m-xylene were therefore hypothetical.

Results: Activity coefficients were predicted for the 25 gasoline solutes (from Table 5-4) in both syngas and water (Table 5-5). Syngas activity coefficients were calculated using UNIFAC and aqueous activity coefficients were calculated using both UNIFAC and AQUAFAC. Note that both methanol and ethanol were treated here as hypothetically abundant solutes in syngas (10% vol/vol). Because these two solutes are very polar relative to the syngas mixture, their syngas activity coefficients depend highly on their concentrations in the syngas mixture. Methanol and ethanol were expected to partition mostly into the aqueous phase, therefore their activity coefficients in conventional syngas (Table 5-5) were calculated under infinite dilution conditions. The calculated and observed partition coefficients (Table 5-6) support this expectation. The MTBE activity coefficient for conventional gasoline (Table 5-6) was also calculated at infinite dilution.

Some activity coefficient values were not found, for varying reasons. UNIFAC lacked the interaction parameters between some of the different functional groups in the cases of the

Table 5-5. Syngas and aqueous activity coefficients for 25 gasoline solutes calculated using UNIFAC and AQUAFAC

gasoline solute	(conventional) $\gamma_{syngas,\ UNIFAC}$	(oxygenated) $\gamma_{syngas,\ UNIFAC}$	$\gamma_{water,UNIFAC}$	$\gamma_{water,AQUAFAC}$
aniline	6.4	-	120	270
p-toluidine	4.8	-	470	440
o-toluidine	4.8	-	470	440
3,4-dimethylaniline	3.7	-	1800	700
2,6-dimethylaniline	3.7	-	1800	700
phenol	8.8	3.3	11	65
p-cresol	6.9	2.6	43	110
o-cresol	6.9	2.6	43	110
3,4-dimethylphenol	5.5	2.1	170	170
2,6-dimethylphenol	5.5	2.1	170	170
3,4,5-trimethylphenol	4.4	1.7	680	270
2,4,6-trimethylphenol	4.4	1.7	680	270
thiophene	1.5	-	-	2200
benzothiophene	2.1	-	-	19000
methyl-*tert*-butylether	1.3	1.2	230	1200
methanol	17	-	2.3	1.5
ethanol	15	-	7.6	5.1
benzene	1.15	1.12	2400	4400
toluene	1.15	1.14	12000	7000
ethylbenzene	1.10	1.09	34000	23000
n-propylbenzene	1.06	1.05	110000	83000
naphthalene	1.6	1.5	140000	79000
m-xylene	1.08	1.08	56000	11000
o-xylene	1.08	1.08	56000	11000
p-xylene	1.08	1.08	56000	11000

sulfur and nitrogen containing compounds. For example, UNIFAC lacked sulfide-water interaction parameters, so only AQUAFAC could be used to calculate the aqueous activity coefficient for thiophene and benzothiophene. In addition, UNIFAC lacked sulfide-ether interactions parameters, so the sulfide activity coefficients could not be calculated in (MTBE) oxygenated syngas. As a result, only one type of prediction could be made for thiophene and benzothiophene (column 1 of Table 5-5). Similar problems limited the types of calculations that could be made for nitrogen-bearing compounds.

Table 5-6. Measured and calculated K_{gw} values for several compounds found in gasolines

gasoline solute	measured K_{gw}	U/A, conv.[a] calc. K_{gw}	U/U, conv.[b] calc. K_{gw}	U/A, oxyg.[c] calc. K_{gw}	U/U, oxyg.[d] calc. K_{gw}
aniline	3.1	6.4	2.9	-	-
p-toluidine	12	14	14	-	-
o-toluidine	12	14	14	-	-
3,4-dimethylaniline	29	28	72	-	-
2,6-dimethylaniline	39	28	72	-	-
phenol	3.2	1.1	0.19	3.0	0.5
p-cresol	9.3	2.3	0.93	6.0	2.5
o-cresol	14	2.3	0.93	6.0	2.5
3,4-dimethylphenol	22	4.6	4.65	12	12
2,6-dimethylphenol	44	4.6	4.65	12	12
3,4,5-trimethylphenol	53	9.3	23	24	59
2,4,6-trimethylphenol	120	9.3	23	24	59
thiophene	110	220	-	-	-
benzothiophene	1700	1400	-	-	-
methyl-*t*-butylether	16	140	27	150	28
methanol	0.0051	0.013	0.020	-	-
ethanol	0.015	0.051	0.075	-	-
benzene	220	570	310	580	320
toluene	690	900	1600	910	1600
ethylbenzene	2200	3200	4600	3200	4600
naphthalene	1500	7600	13000	7800	14000
m-xylene	2200	1500	7400	1500	7400
o-xylene	2200	1500	7400	1500	7400
p-xylene	2200	1500	7400	1500	7400

[a] "U/A, conv" refers to a K_{gw} calculated from a conventional syngas activity coefficient calculated using UNIFAC and an aqueous activity coefficient calculated using AQUAFAC.

[b] "U/U, conv" refers to a K_{gw} calculated from a conventional syngas activity coefficient and an aqueous activity coefficient both calculated using UNIFAC.

[c] "U/A, oxyg" refers to a K_{gw} calculated from an oxygenated syngas activity coefficient calculated using UNIFAC and an aqueous activity coefficient calculated using AQUAFAC.

[d] "U/U, oxyg" refers to a K_{gw} calculated from a oxygenated syngas activity coefficient and an aqueous activity coefficient both calculated using UNIFAC.

Using the UNIFAC- and AQUAFAC-calculated activity coefficients (Table 5-5), the gasoline–water partition coefficients of gasoline solutes were computed (using eqn 5-5) for both conventional and oxygenated gasoline (Table 5-6). The partition coefficient calculations were conducted using a syngas molar volume of 0.12 L/mol as given by eqn 5-4, and an aqueous molar volume of 0.0180 L/mol. Ethanol and methanol have no entries for columns 4 and 5 (Table 5-6) because they were presumed to replace MTBE at 10% vol/vol, rather than be added with it. Consequently they were only modeled in conventional syngas as a 10% vol/vol mixture.

Experimentally measured K_{gw} values compared reasonably with K_{gw} predictions for both conventional and oxygenated syngas (Figures 5-2, 5-3, 5-4, and 5-5). The dotted line signifies a factor of two in the error of the predictions, demonstrating that this modeling approach was useful but inaccurate.

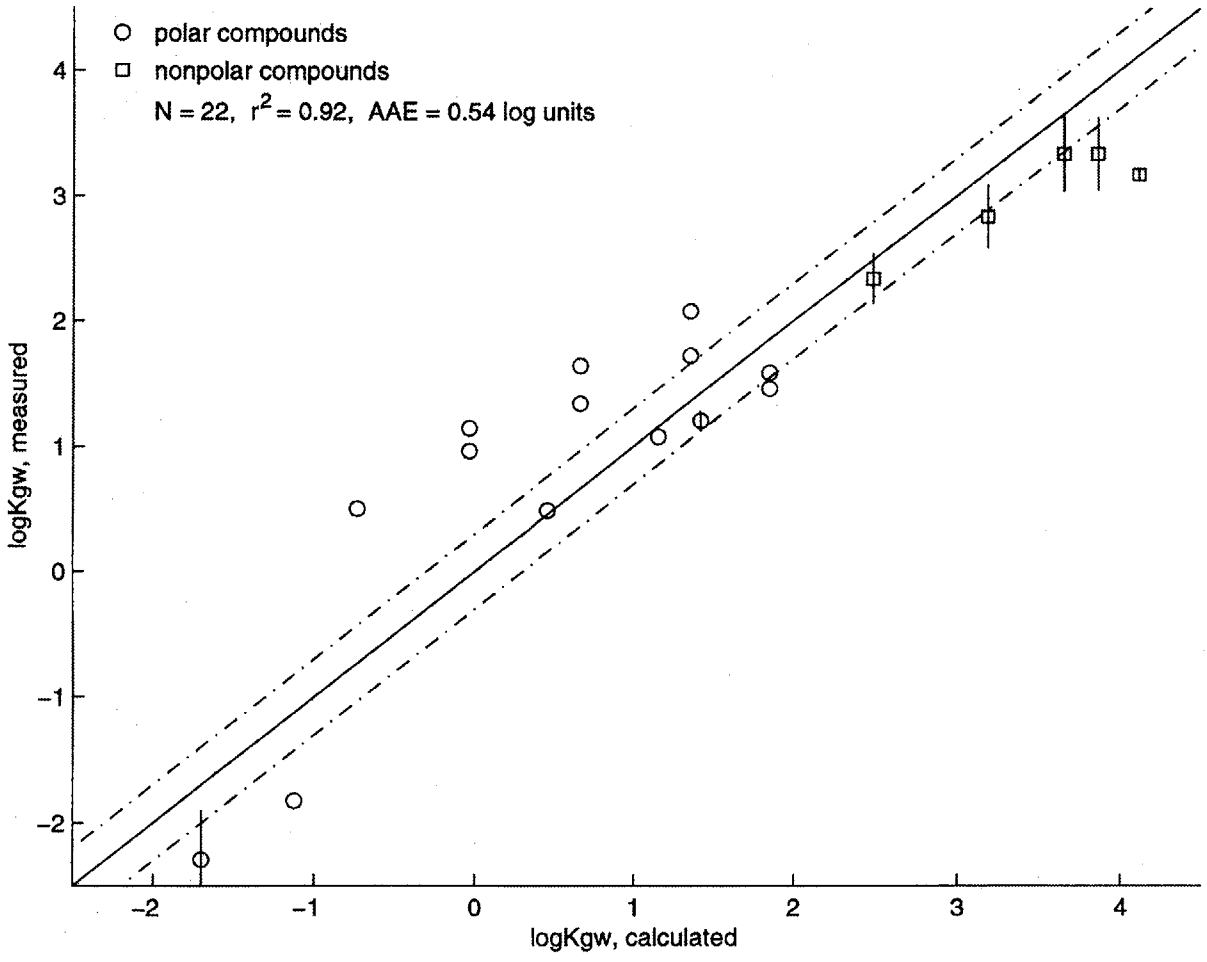

Figure 5-2. Partition coefficients between conventional syngas and water, calculated using UNIFAC for activity coefficients in both conventional syngas and water

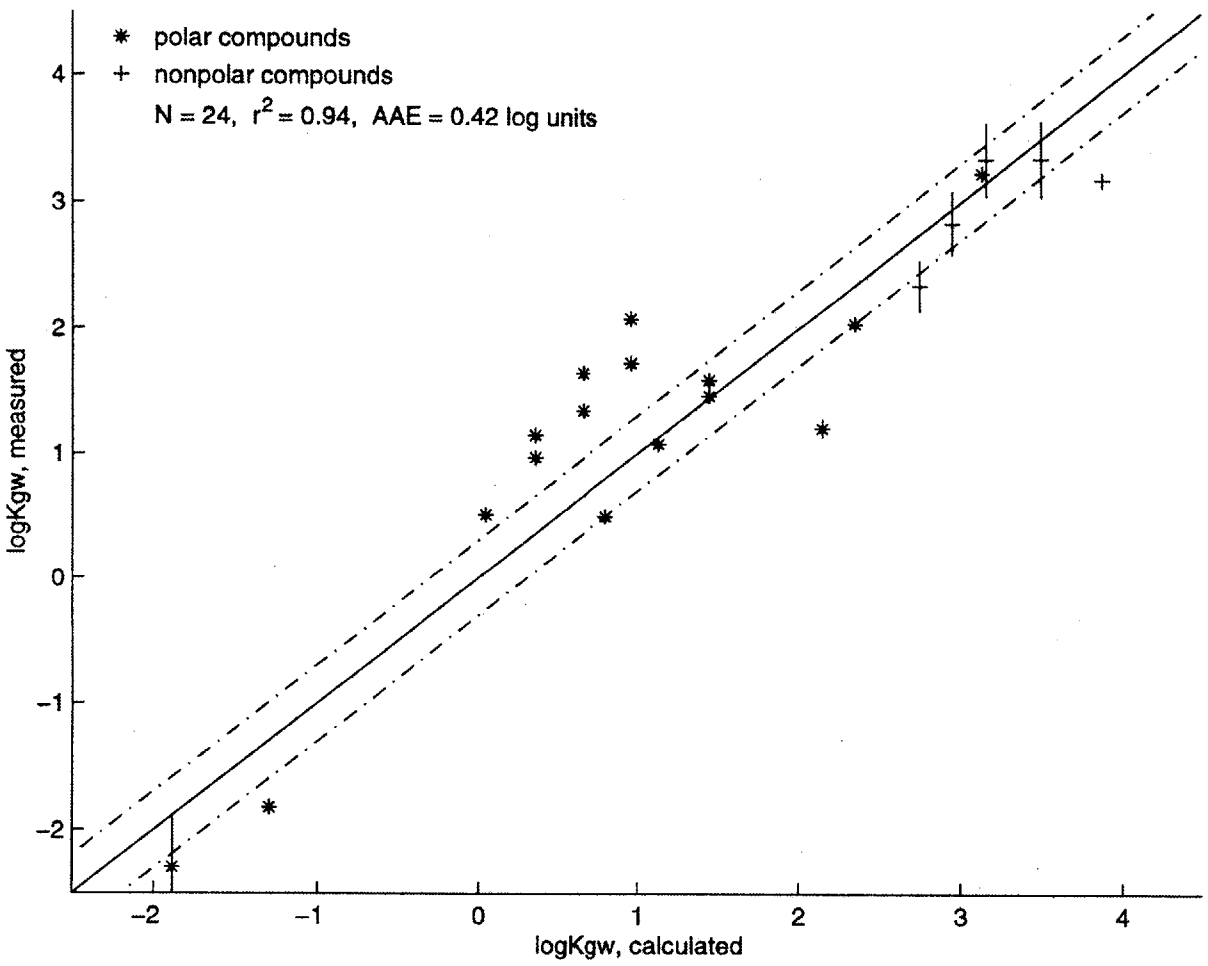

Figure 5-3. Partition coefficients between conventional syngas and water, calculated using UNIFAC (for activity coefficients in syngas) and AQUAFAC (for activity coefficients in water)

The UNIFAC/AQUAFAC modeling approach captured the trend of the measurement data, but still displayed significant error (Figures 5-2, 5-3). Inspection of the data revealed that the K_{gw} for substituted phenols was consistently underpredicted, regardless of whether AQUAFAC or UNIFAC was used to calculate the aqueous activity coefficient. This suggests that the UNIFAC gasoline activity coefficient computation for phenols was overpredicted (i.e., the phenols are more "comfortable" in the gasoline solution environment than the computations suggest). The K_{gw} values for methanol, ethanol, MTBE and naphthalene were all significantly overpredicted. Other K_{gw} predictions were within a factor of two of measured values. There did not appear to be a clear trend in differences between predictions based on AQUAFAC and UNIFAC calculation of the aqueous activity coefficient. The model statistics were slightly better if AQUAFAC was used to calculate the aqueous activity coefficient (the K_{gw} average absolute error factor was ~ 2.6), rather than UNIFAC (K_{gw} AAE factor of 3.5).

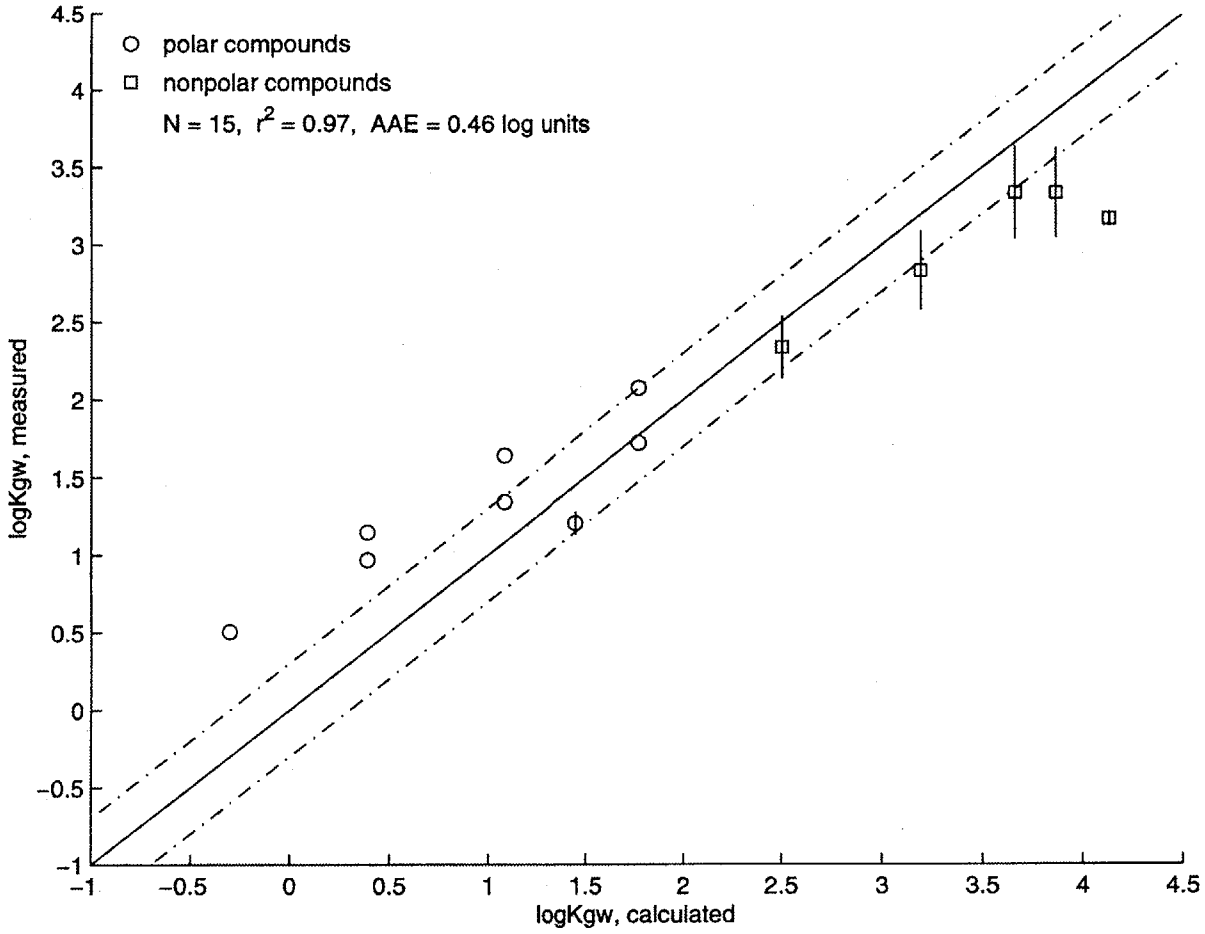

Figure 5-4. Partition coefficients between oxygenated (10% MTBE) syngas and water, calculated using UNIFAC for activity coefficients in both oxygenated syngas and water

When MTBE was added to the syngas mixture, fewer compounds could be modeled, but prediction errors decreased (Figures 5-4, 5-5). K_{gw} calculations for phenols improved notably when MTBE was added to the syngas mixture. Anilines and aromatic sulfides were not included in this dataset, because of the limitations of the UNIFAC parameter set. Other K_{gw} predictions were similar to calculations made for conventional gasoline (Figures 5-2, 5-3). As with conventional gasoline, the model statistics were slightly better when AQUAFAC was used to calculate the aqueous activity coefficient (K_{gw} AAE factor of 2.3) rather than UNIFAC (K_{gw} AAE factor of 2.9).

Hence, UNIFAC provided useful but inaccurate predictions of K_{gw}. Trends between the errors and solute chemical structures did not clarify UNIFAC's failure to give better results.

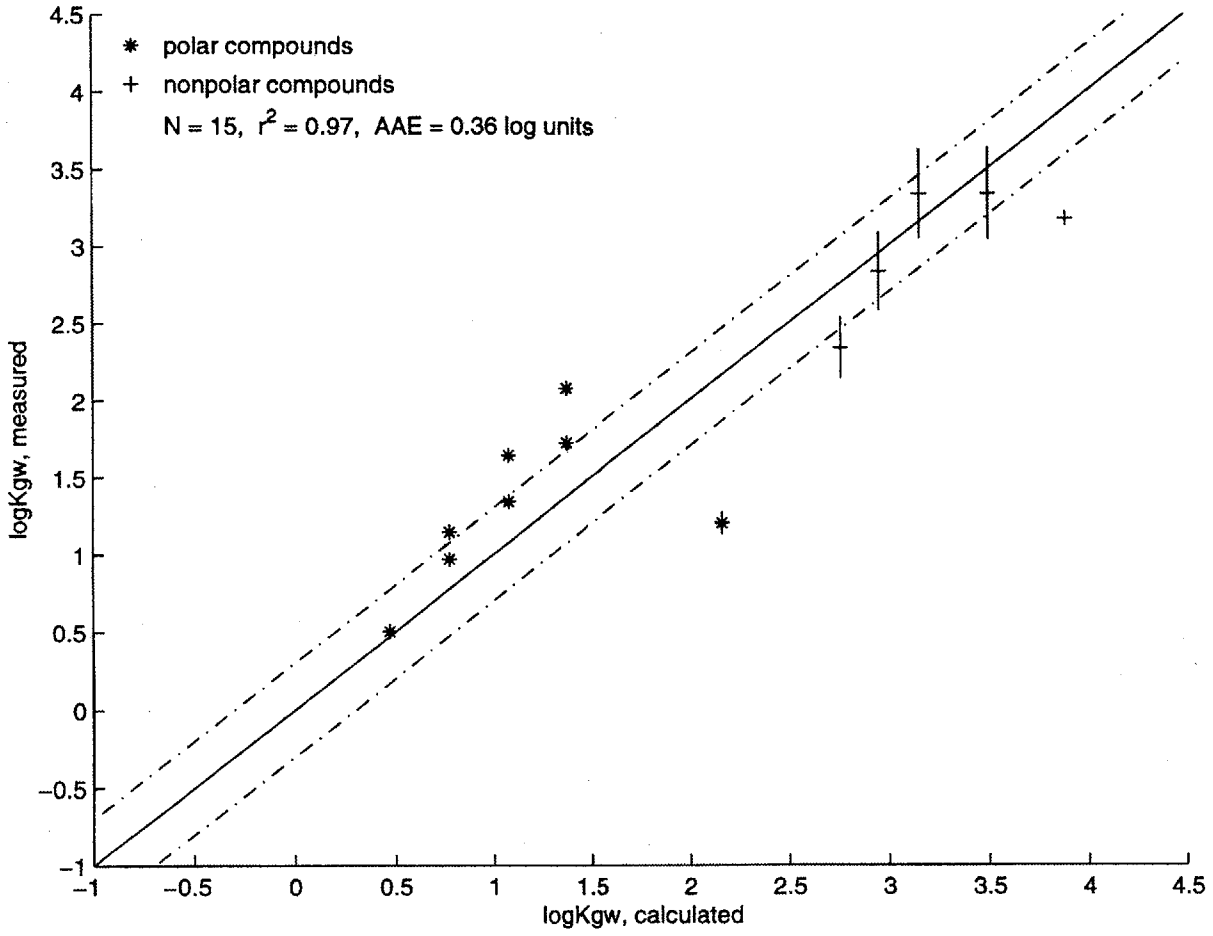

Figure 5-5. Partition coefficients between oxygenated (10% MTBE) syngas and water, calculated using UNIFAC (for activity coefficients in syngas) and AQUAFAC (for activity coefficients in water)

5-4. Linear Solvation Energy Relationship predictions of gasoline–water partitioning

Linear solvation energy relationships (LSERs) have been used to predict partition coefficients for many systems. Solvation parameters (R_2, π^H, $\Sigma\alpha^H$, $\Sigma\beta^H$, and V_x) that are characteristic for individual solutes are linearly combined to find the log transformed partition coefficients for different gas-liquid and liquid-liquid systems (see section 4-3):

$$\log K_{gw} = \Delta c + \Delta r^* R_2 + \Delta s^* \pi^H + \Delta a^* \Sigma\alpha^H + \Delta b^* \Sigma\beta^H + \Delta m^* V_x \qquad (5\text{-}6)$$

The appropriate multipliers (Δc, Δr, Δs, Δa, Δb, and Δm) to the solvation parameters for individual partitioning systems are generally determined by least squares multiple regression [13].

Method: Using the published K_{gw} values of 29 gasoline solutes and the estimated K_{gw} values of 9 n-alkanes, the multipliers to five LSER solvation parameters [14-16] were determined. The smallest 9 n-alkanes (n = 1, 2, ... 9) were assumed to have a gasoline activity coefficient of approximately 1.0 (Tables 5-2, 5-3), based on the observation that gasoline mixtures are composed of mostly hydrocarbons [9]. The alkane K_{gw} values were therefore determined from eqn 5-5 using published aqueous activity coefficients (based on hypothetical liquid phase solubilities) [17], a gasoline activity coefficient of unity, a gasoline molar volume of 0.12 L/mol (from eqn 5-4), and aqueous phase molar volume of 0.018 L/mol. K_{gw} values for the rest of the solutes (Table 5-8) were obtained from measurements performed using real or simulated gasolines by Heerman and Powers, Schmidt et al., Cline et al., and Stephenson [4-7]. Singular value decomposition [13] was used to perform the least squares multiple regression between the solvation parameters and log K_{gw} values of the solutes.

Results: Regression of the LSER gave very good fit statistics:

$$\log K_{gw} = 0.11 - 0.38R_2 - 0.25\pi^H - 1.50\Sigma\alpha^H - 6.47\Sigma\beta^H + 4.84V_x \qquad (5\text{-}7)$$

N = 38
AAE = 0.11 log units (error factor of 1.30 in the partition coefficient)
$r^2 = 0.998$

The uncertainty in the regression multipliers, however, was significant. Assuming that the population of possible multiplier values is normally distributed, the standard error of the individual multipliers can be estimated from the matrices used in the singular value decomposition method [18]. Although a good fit was found, only two of the regressed multipliers, Δb and Δm, were statistically significant in the current formulation of the LSER (Table 5-7).

Table 5-7. Estimated uncertainties of the LSER solvation parameter multipliers

multiplier	affected solvation parameter	estimated multiplier value	estimated standard error of multiplier
Δc	none (intercept)	0.1	+/– 1.2
Δr	R_2	– 0.4	+/– 2.4
Δs	π^H	– 0.3	+/– 2.7
Δa	$\Sigma\alpha^H$	– 1.5	+/– 2.0
Δb	$\Sigma\beta^H$	– 6.5	+/– 2.6
Δm	V_x	4.8	+/– 1.2

Accordingly, the four extraneous solvation parameters (the intercept, R_2, π^H, and $\Sigma\alpha^H$) were individually applied in a three-variable LSER with the only two statistically significant parameters ($\Sigma\beta^H$ and V_x):

$$\log K_{gw} = \Delta x^*X + \Delta b^*\Sigma\beta^H + \Delta m^*V_x \qquad (5\text{-}8)$$

where X = the tested solvation parameter.

Table 5-8. Measured or estimated K_{gw} values and solvation parameters used in the LSER regression

K_{gw}	R_2	π^H	α^H	β^H	V_x	solute
20 (est.)	0.000	0.00	0.00	0.00	0.2495	methane
100 (est.)	0.000	0.00	0.00	0.00	0.3904	ethane
630 (est.)	0.000	0.00	0.00	0.00	0.5313	n-propane
3200 (est.)	0.000	0.00	0.00	0.00	0.6722	n-butane
$1.5*10^4$ (est.)	0.000	0.00	0.00	0.00	0.8131	n-pentane
$5.6*10^4$ (est.)	0.000	0.00	0.00	0.00	0.9540	n-hexane
$2.7*10^5$ (est.)	0.000	0.00	0.00	0.00	1.0949	n-heptane
$1.3*10^6$ (est.)	0.000	0.00	0.00	0.00	1.2358	n-octane
$7.2*10^6$ (est.)	0.000	0.00	0.00	0.00	1.3767	n-nonane
3.1	0.955	0.96	0.26	0.41	0.816	aniline
12	0.923	0.95	0.23	0.45	0.957	p-toluidine
12	0.966	0.92	0.23	0.45	0.957	o-toluidine
29	0.972	0.89	0.20	0.46	1.098	2,6-dimethylaniline
3.2	0.805	0.89	0.60	0.30	0.775	phenol
9.3	0.820	0.87	0.57	0.31	0.916	p-cresol
14	0.840	0.86	0.52	0.30	0.916	o-cresol
22	0.830	0.86	0.56	0.39	1.057	3,4-dimethylphenol
44	0.860	0.79	0.54	0.39	1.057	2,6-dimethylphenol
53	0.830	0.88	0.55	0.44	1.198	3,4,5-trimethylphenol
120	0.860	0.79	0.37	0.44	1.198	2,4,6-trimethylphenol
0.0051	0.278	0.44	0.43	0.47	0.308	methanol
0.015	0.246	0.42	0.37	0.48	0.449	ethanol
0.059	0.212	0.36	0.33	0.56	0.590	isopropanol
0.14	0.180	0.30	0.31	0.60	0.731	tert-butanol
16	0.024	0.19	0.00	0.45	0.872	MTBE
5.9	0.106	0.62	0.00	0.45	0.747	ethylacetate
110	0.687	0.56	0.00	0.15	0.641	thiophene
1700	1.323	0.88	0.00	0.20	1.010	benzothiophene
220	0.610	0.52	0.00	0.14	0.716	benzene
690	0.601	0.52	0.00	0.14	0.857	toluene
2200	0.613	0.51	0.00	0.15	0.998	ethylbenzene
18500	0.604	0.50	0.00	0.15	1.139	n-propylbenzene
2200	0.623	0.52	0.00	0.16	0.998	m-xylene
2200	0.663	0.56	0.00	0.16	0.998	o-xylene
2200	0.613	0.52	0.00	0.16	0.998	p-xylene
13800	0.728	0.61	0.00	0.19	1.139	1,2,3-trimethylbenzene
12500	0.630	0.51	0.00	0.18	1.139	4-ethyltoluene
1500	1.340	0.92	0.00	0.20	1.085	naphthalene

In this way, the LSER was reconstructed so as to minimize the number of necessary parameters and reduce the overall uncertainty of the regression. It is important to note that the multiplier

values are only physically meaningful to the extent that they explain the relative importance of the solvation parameters. In other words, the significance of the solvation parameters in gasoline–water partitioning is what was tested in this series of regressions.

Table 5-9. Estimated standard error of isolated LSER multipliers

Δb	σ_{Δ_b}	Δm	σ_{Δ_m}	Δc	Δr	Δs	Δa	σ_{Δ_x}	σ_{model}
–8.06	+/– 0.85	4.76	+/– 0.38	-	-	-	-	-	0.28
–8.22	+/– 1.23	4.49	+/– 0.94	0.29	-	-	-	+/– 0.93	0.27
–7.57	+/– 0.98	5.04	+/– 0.50	-	–0.69	-	-	+/– 0.72	0.21
–6.98	+/– 1.28	5.05	+/– 0.45	-	-	–1.03	-	+/– 0.99	0.20
–6.76	+/– 1.45	4.71	+/– 0.46	-	-	-	–1.74	+/– 1.37	0.20

Absence of a multiplier entry, denoted "-" in Table 5-9, indicates that the corresponding parameter was not included in the regression (the multiplier was set to zero). The estimated standard deviation of the multipliers is denoted $\sigma_{\Delta x}$, and the estimated standard deviation of the predicted log K_{gw} under the constraints of the applied multipliers is denoted σ_{model}.

The first row in Table 5-9 shows that application of only the solute basicity parameter ($\Sigma\beta^H$) and volume parameter (V_x) provided an adequate description the behavior of the system, generating a model standard error of only 0.28 in the log K_{gw}. The uncertainties of the Δc, Δr and Δs multipliers were equivalent to or larger than the multiplier values themselves, demonstrating that the LSER constant, solute excess molar refraction, and solute polarity parameters did not contribute significantly to model performance. The solute acidity multiplier (Δa) uncertainty was nearly 80% of the acidity multiplier value. However, it was the third most statistically significant variable in the model fit (after Δb and Δm). This trend agrees with previous work on LSERs describing partition coefficients between nonpolar phases such as hexadecane or cyclohexane and water. In these studies, the solute volume term (V_x) and basicity term ($\Sigma\beta^H$) are resolved as the dominant model parameters with the acidity term ($\Sigma\alpha^H$) third in importance [14-16].

Note that as the number of parameters in the model was increased, the multiplier uncertainties increased (i.e., the validity of the model fit decreased). In the effort to achieve a balance between minimalist parameterization and inclusion of physically significant processes, three solvation parameters were chosen to describe an optimal predictive LSER for gasoline–water partitioning:

$$\log K_{gw} = -1.74\Sigma\alpha^H - 6.76\Sigma\beta^H + 4.71V_x \qquad (5\text{-}9)$$

N = 38
AAE = 0.20 log units (a factor of 1.58 in the partition coefficient)
$r^2 = 0.994$

Although the total number of fitted parameters has been halved, the regression statistics were very similar to those given by the original LSER (eqn 5-7). Thus, the multiplier uncertainty was substantially decreased (Table 5-9 vs Table 5-7).

A final test was conducted on the improved K_{gw} LSER (eqn 5-9) in order to validate its predictive capability. The predictive capability of a model is most robustly validated with an independent data set that was not used in the fitting of the model itself. Therefore, 37 data points were regressed with eqn 5-9 to generate model multiplier values, and this model fit was used to predict the remaining (38^{th}) data point. This procedure was iterated in round robin fashion 38 times, each time using a subset of 37 fitting points to predict a different 38^{th} point. In this way, all of the data could be used to test the model from an independent regression set. The model predictive error found in the round robin validation test was only slightly greater than the model error found in the original regressions, demonstrating the robustness of the model (Figure 5-6).

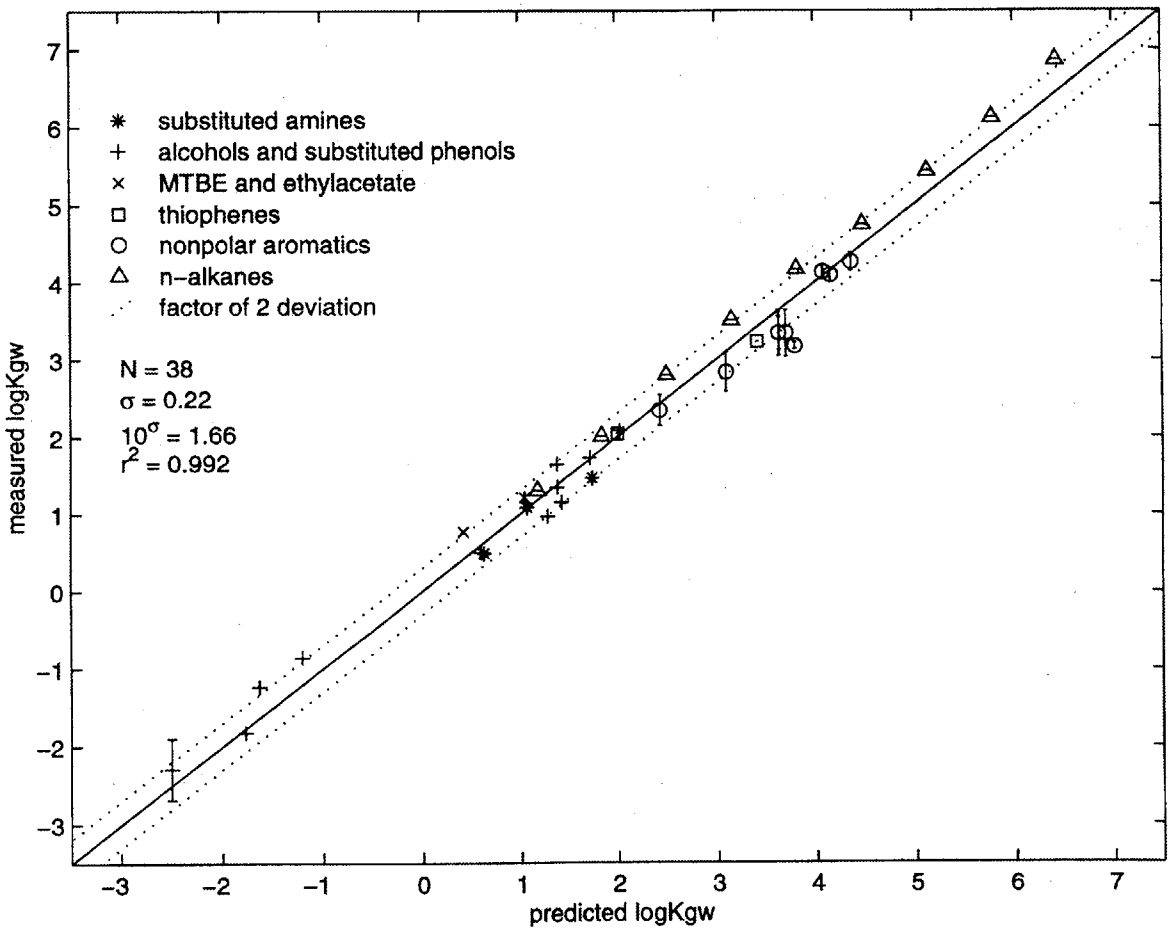

Figure 5-6. Round robin prediction test of the derived gasoline–water LSER using independent data

5-5. ClogP v. 4.0 predictions of octanol–water partitioning

In this section, a traditional fragment/factor contribution method was used to estimate K_{ow} values for a set of compounds found in gasoline. ClogP has been parameterized using a database of over 10,000 compounds [1, 2].

Method: The ClogP predicted log K_{ow} values were compared to experimentally measured values (Table 5-10). Experimental values were obtained from the ClogP database.

Results: ClogP is highly accurate and is continually revised, based on improved data sets and data analysis. It is able to make predictions for a very wide variety of complex compounds and is highly accurate, making it a powerful modeling tool [2]. It demonstrates the usefulness that an empirical partition constant model can attain with decades of well-guided effort. Unfortunately, the factors and fragments of the ClogP algorithm are not explicitly published, so it was difficult to make specific interpretations of the model results shown here. Only one prediction out of the set, for 3,4-dimethylphenol, approached an error of 25% in the K_{ow}. This probably represents the best accuracy that can be expected inside of laboratory measurement error.

Table 5-10. Experimentally measured and ClogP calculated K_{ow}'s at 25° C

compound	calc. logK_{ow}	meas. logK_{ow}
benzotriazole	1.41	1.44
1-methylbenzotriazole	1.064	1.13
aniline	0.915	0.90
p-toluidine	1.41	1.39
o-toluidine	1.36	1.32
2,6-dimethylaniline	1.81	1.84
phenol	1.47	1.47
p-cresol	1.97	1.94
o-cresol	1.97	1.95
3,4-dimethylphenol	2.42	2.23
2,6-dimethylphenol	2.47	2.36
thiophene	1.79	1.89
benzothiophene	3.17	3.12
methyl-*tert*-butylether	1.05	0.94
methanol	-0.76	-0.77
ethanol	-0.24	-0.31
benzene	2.14	2.13
toluene	2.67	2.73
o-xylene	3.09	3.12
m-xylene	3.14	3.20
p-xylene	3.14	3.15
ethylbenzene	3.17	3.15
naphthalene	3.32	3.30

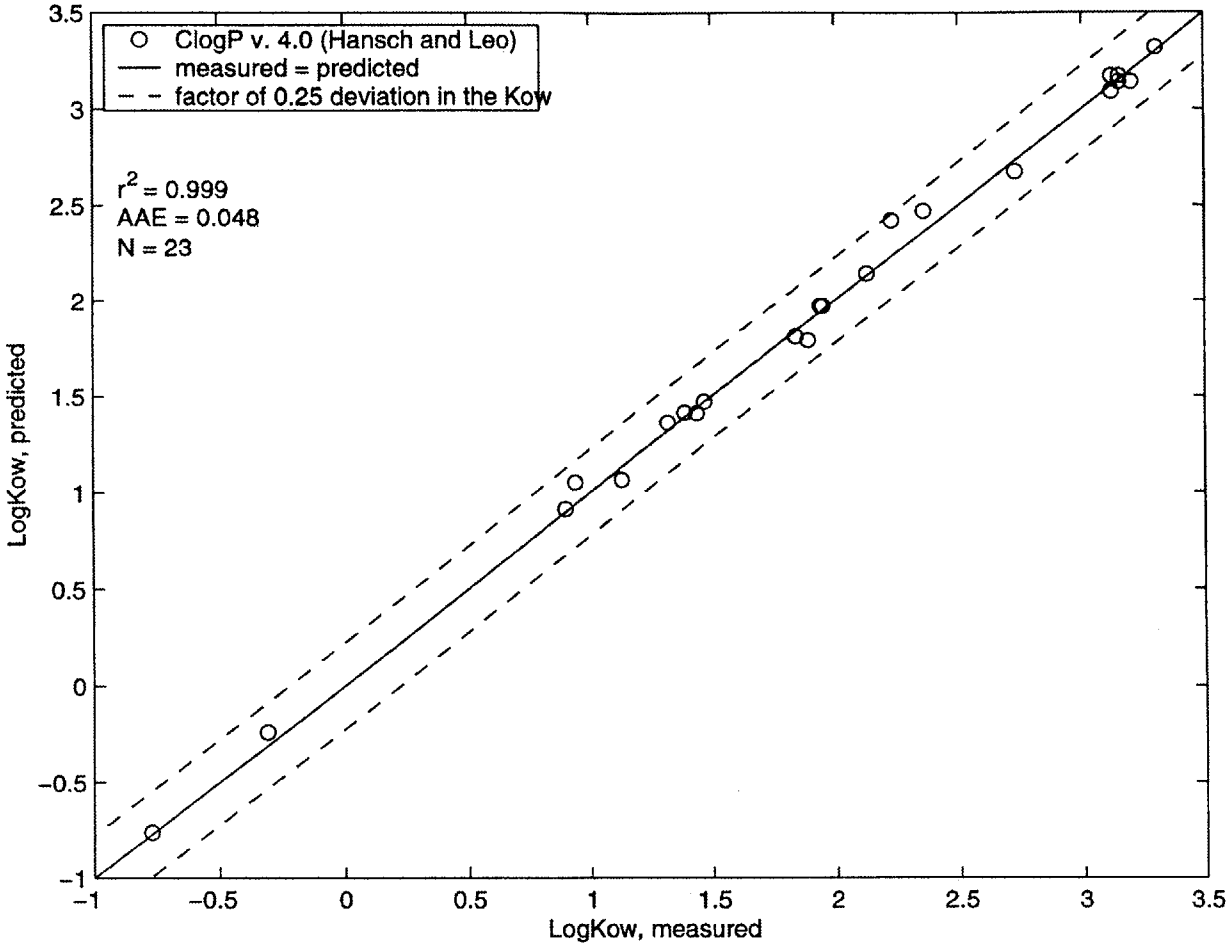

Figure 5-7. Measured vs ClogP predicted logK_{ow} values for 23 gasoline solutes

Conclusions: ClogP is clearly a powerfully accurate, empirical prediction tool (Figure 5-7). This makes the K_{ow} an attractive system with which to build correlations with other properties such as K_{gw} or K_{om}.

5-6. Results of the organic matter–water partition coefficient estimation method

Unlike other physical properties, the K_{om} solvent environment is highly variable. As a result, K_{om} values for the same compound in different systems (such as sediment organic matter vs soil organic matter) may vary up to a factor of two or more [17]. In this section, a LFER was used to estimate K_{om} values in place of real K_{om} data.

Method: A series of log K_{ow} – log K_{om} LFERs derived by Schwarzenbach et al. [17] was used to estimate the K_{om} values of 21 compounds found in gasoline:

aromatic hydrocarbons $\log K_{om} = 1.01 \log K_{ow} - 0.72$ (5-10a)
N = 10 $r^2 = 0.99$

chlorinated hydrocarbons $\log K_{om} = 0.88 \log K_{ow} - 0.27$ (5-10b)
N = 12 $r^2 = 0.97$

chloro-s-triazines $\log K_{om} = 0.37 \log K_{ow} + 1.15$ (5-10c)
N = 6 $r^2 = 0.93$

phenyl ureas $\log K_{om} = 1.12 \log K_{ow} + 0.15$ (5-10d)
N = 6 $r^2 = 0.93$

general correlation (all compounds) $\log K_{om} = 0.82 \log K_{ow} + 0.14$ (5-11)
N = 34 $r^2 = 0.93$

Where appropriate, compound family specific LFERs (eqn 5-10) were used to estimate the K_{om} values of gasoline constituents; otherwise the general correlation (eqn 5-11) was used (Table 5-11). K_{ow} values were taken from experimental data and ClogP-predicted K_{ow} values were used where measured values were not available (Table 5-10).

Table 5-11. LFER-estimated K_{om} values for 21 compounds found in U.S. gasolines

compound	log K_{om}	K_{om}
aniline	0.88	7.6
p-toluidine	1.28	19
o-toluidine	1.22	17
3,4-dimethylaniline	1.67	46
2,6-dimethylaniline	1.62	42
phenol	1.35	22
p-cresol	1.73	54
o-cresol	1.74	55
3,4-dimethylphenol	1.97	93
2,6-dimethylphenol	2.08	120
N,N'-disalicylidene-1,2-diaminopropane	1.42	26
thiophene	1.69	49
benzothiophene	2.70	500
MTBE	0.91	8.1
di-sec-butyl-*p*-phenylenediamine	3.31	2100
methanol	-0.49	0.33
ethanol	-0.11	0.77
benzene	1.43	27
toluene	2.04	110
ethylbenzene	2.46	290
naphthalene	2.61	410

5-7. Transport calculations of compounds found in gasoline

The subsurface transport model was used to predict the transport times of 21 gasoline constituents from LUFTs to community supply wells and to calculate the expected constituent concentrations in the wells. These compounds represent the subset of polar gasoline constituents tabulated in Chapter 2 for which gasoline concentration data are available. Additionally, common aromatic hydrocarbon contaminants are included for comparison. As described in Chapter 3, the transport model calculated solute partitioning into groundwater from gasoline NAPL pooled on the water table; individual solute advection towards the groundwater well and dispersion in three dimensions; and solute sorption to aquifer sediment (retardation).

Method: Degradative (reaction) processes were presumed nonexistent, and transport behavior was controlled by fuel concentration, fuel–water partition coefficient and organic matter–water partition coefficient of each gasoline solute. Environmental parameters reflecting the "standard" subsurface transport scenario formulated in chapter were considered (Table 5-12). Besides the standard case, three additional transport parameter sets were tested to assess the sensitivity of the transport system to important changes in hydrogeologic and contamination characteristics. These included a parameter set with increased sediment organic matter content (0.5% instead of 0.1%); a parameter set with decreased well pumping rate (80 gal/min instead of 400 gal/min); and a parameter set with increased gasoline spill size (1000 gallons instead of 100 gallons).

Table 5-12. Subsurface transport parameters for the standard case

NAPL volume [m^3]	0.38 (100 gallons)
NAPL lens thickness [m]	0.05
sediment fraction of organic matter (f_{om})	0.001
sediment porosity	0.25
sediment density [g/cm^3]	2.5
groundwater velocity [m/day]	1
aquifer saturated thickness [m]	25
dispersivity (x) [m]	10
dispersivity (y) [m]	1
dispersivity (z) [m]	0.1
well pumping rate [m^3/day]	2180 (400 gal/min)
well distance from LUFT [m]	1000

Compound fuel concentrations were taken from literature measurements or estimates (Table 5-13). Fuel–water partition coefficients were taken from literature or were calculated. Organic matter–water partition coefficients were taken from estimated values calculated in the previous section. It should also be noted that some compounds under consideration can ionize via acid-base chemistry under normal aquifer pH conditions (pH ~ 5 to 9). If a contaminant is partly ionized in groundwater, it will have an enhanced effective aqueous concentration, because the ionic species will not partition appreciably into fuel or natural organic matter. In other words, ionization of fuel contaminants can facilitate their subsurface transport by increasing their effective aqueous concentration. Additionally, however, ionized species are subject to

Table 5-13. Physical property inputs for the subsurface transport calculation

gasoline solute	concentration in fuel [ppm]	pK_a [k]	K_{fw}	(calc.) K_{om}
aniline	20[a]	4.6	3.1[a]	7.8
p-toluidine	30[a]	5.2	12[a]	19
o-toluidine	20[a]	4.5	12[a]	17
3,4-dimethylaniline	15[a]	5.2	29[a]	46
2,6-dimethylaniline	15[a]	3.9	39[a]	42
phenol	150[a]	9.9	3.2[a]	22
p-cresol	100[a]	10.3	9.3[a]	54
o-cresol	100[a]	10.3	14[a]	55
3,4-dimethylphenol	30[a]	10.4	22[a]	93
2,6-dimethylphenol	30[a]	10.6	44[a]	120
N,N'-disalicylidene-1,2-diaminopropane	12[b]	11.8	940[a]	26
thiophene	150[j]	-	110[a]	49
benzothiophene	300[j]	-	1700[a]	500
methyl-*tert*-butylether	100000[d]	-	16[f]	8.1
di-sec-butyl-*p*-phenylenediamine	20[b]	?	11000000[g]	2100
methanol	106000[e]	15.3	0.0051[f]	0.33
ethanol	105000[e]	15.9	0.015[h]	0.77
benzene	12000[i]	-	220[f]	27
toluene	162000[c]	-	690[f]	110
ethylbenzene	73000[c]	-	2200[f]	290
naphthalene	33000[c]	-	1500[f]	410

[a] Schmidt [4].
[b] Owen [19].
[c] Schubert and Johansen [9].
[d] Johnson et al. [20].
[e] corresponds to 10% vol/vol.
[f] Cline et al. [5].
[g] calculated from AQUAFAC estimation of the aqueous activity coefficients and UNIFAC estimation of the gasoline activity coefficient, with 10% MTBE.
[h] Heerman and Powers [6].
[i] corresponds to 1% vol/vol, as imposed by current legislation.
[j] Quimby et al. [12].
[k] Howard and Meylan [21].

cation exchange with aquifer sediments. Acid-base chemistry was not treated quantitatively here since it is highly dependent on groundwater pH.

Results: The transport method was used to predict plume types, front arrival times, municipal well water concentrations, and plume spreading for the standard case and three perturbation tests (Tables 5-14, 5-15, 5-16, and 5-17; Figures 5-8, 5-9, 5-10, and 5-11). The

Table 5-14. Transport model results for the standard case

compound	plume type	front arrival time [days]	well concentration [ppb]	[M]	plume spread [m] x	y	z
aniline	slug	920	0.0093	1.0E-10	130	42	13
p-toluidine	slug	990	0.013	1.2E-10	130	42	13
o-toluidine	slug	980	0.088	8.2E-11	130	42	13
3,4-dimethylaniline	slug	1200	0.0055	4.5E-11	130	42	13
2,6-dimethylaniline	slug	1100	0.0056	4.6E-11	130	42	13
phenol	slug	1000	0.064	6.8E-10	130	42	13
p-cresol	slug	1200	0.035	3.3E-10	130	42	13
o-cresol	slug	1200	0.035	3.2E-10	130	42	13
3,4-dimethylphenol	slug	1500	0.0087	7.1E-11	130	42	13
2,6-dimethylphenol	slug	1600	0.0078	6.4E-11	130	42	13
N,N'-disalicylidene-1,2-diaminopropane	steady state	1000	0.0053	1.9E-11	-	42	13
thiophene	slug	1200	0.054	6.4E-10	130	42	13
benzothiophene	slug	4100	0.03	2.2E-10	140	42	13
methyl-*tert*-butylether	slug	920	47	5.3E-7	130	42	13
di-sec-butyl-*p*-phenylenediamine	steady state	15000	7.6E-07	3.4E-15	-	42	13
methanol	slug	870	52	1.6E-6	130	42	13
ethanol	slug	870	52	1.1E-6	130	42	13
benzene	slug	1000	4.9	6.2E-8	130	42	13
toluene	slug	1600	41	4.5E-7	140	42	13
ethylbenzene	steady state	2800	14	1.3E-7	-	42	13
naphthalene	slug	3500	3.8	2.9E-8	140	42	13

plume "spread" refers to the square root of the spatial variance induced by dispersion during transport (i.e., one standard deviation of the plume distribution). The location of the solute front refers to one standard deviation (one unit of plume spread) in front of the plug flow front, corresponding to a solute concentration roughly 1/3 that of the plume concentration near the centroid. The calculated well concentration is the expected value (average) contaminant concentration in the well water when the centroid nears the well. The plume "type" was determined by the initial length of the plume relative to the longitudinal spreading that occurs during transport. If the initial plume length was less than two units of dispersion-induced plume spread, the plume was treated as a slug. Otherwise, the plume was treated as a steady state source.

Presuming that the transport model reasonably captured the quantitative behavior of organic compounds in these types of subsurface systems, transport calculation results using the four parameter sets studied here should indicate probable observations for non-degraded compounds at numerous sites in the U.S. These kinds of results should reveal research and policy needs for large scale well-testing for individual compounds in gasoline and further biodegradability research. Eventually, such screening could lay the foundations for informed decision-making in

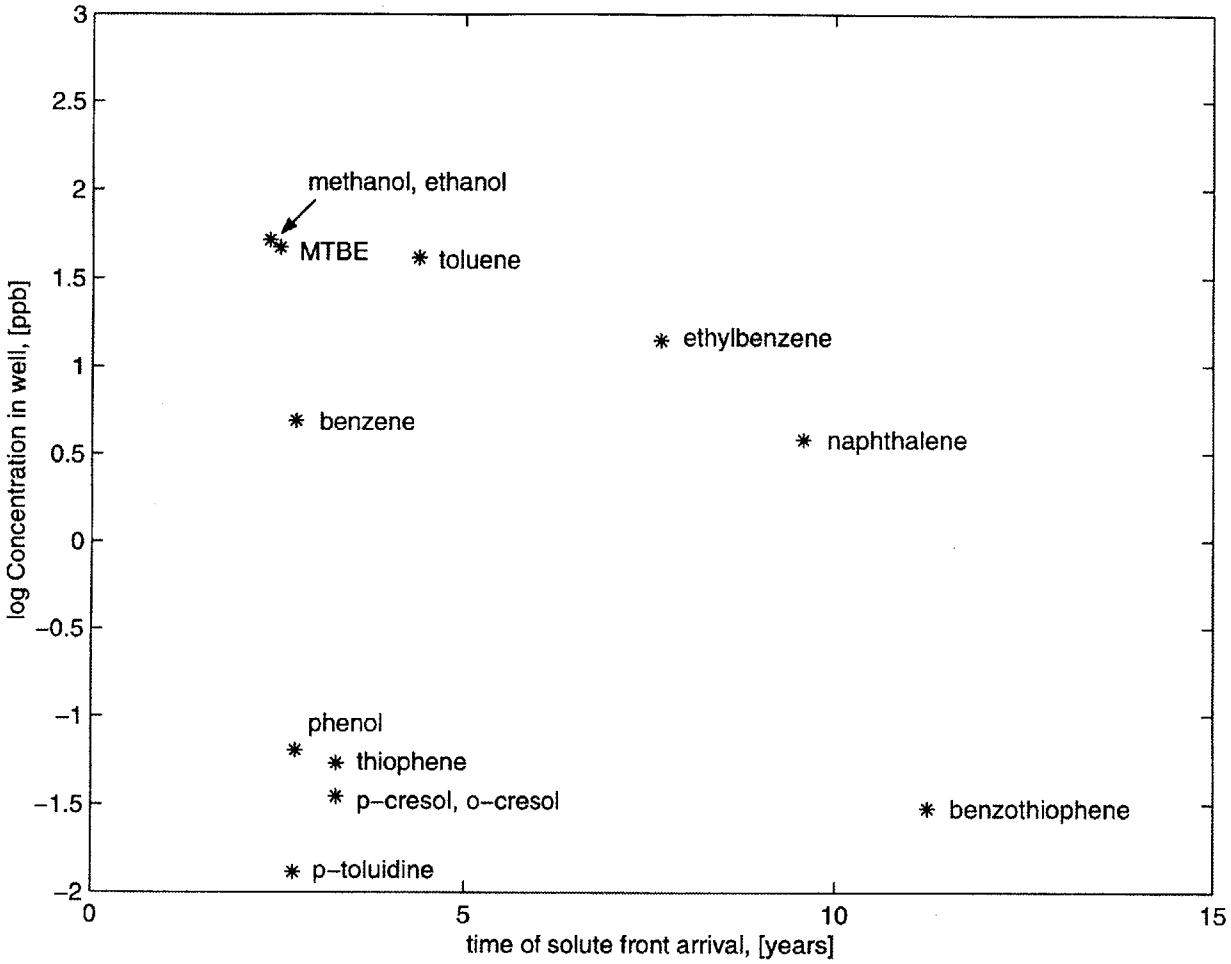

Figure 5-8. Arrival time of solute front vs well water concentration: the standard case

U.S. EPA (Environmental Protection Agency) and API (American Petroleum Institute) policy directing the industry-wide use of gasoline additives.

A. The standard case

The proposed standard transport case gave credible results (Table 5-14, Figure 5-8). The predicted MTBE well concentrations (about 50 ppb) were very comparable to community supply well concentrations observed in nationwide surveys [20]. Methanol and ethanol behaved very similarly to MTBE, partitioning quickly into the groundwater (experiencing "slug" transport) and arriving at the receptor well 2.5 to 4 months sooner than the average groundwater flow (as a result of longitudinal dispersion). Many other compounds (benzene, phenol, aniline, cresols, toluidines) also experienced nearly non-retarded transport in the model. The predicted concentrations of these compounds in the municipal well water were significantly lower than the concentrations of MTBE, however, since they are much less abundant in gasoline. Notably, toluene is predicted to contaminate the well in concentrations comparable to that of MTBE and

Table 5-15. Transport model results for the increased sediment organic matter content (0.5%) case

compound	plume type	front arrival time [days]	well concentration [ppb]	[M]	plume spread [m] x	y	z
aniline	slug	1100	0.0076	8.2E-11	130	42	13
p-toluidine	slug	1500	0.0087	8.1E-11	130	42	13
o-toluidine	slug	1400	0.006	5.6E-11	130	42	13
3,4-dimethylaniline	slug	2400	0.0027	2.2E-11	130	42	13
2,6-dimethylaniline	slug	2200	0.0029	2.4E-11	130	42	13
phenol	slug	1600	0.041	4.3E-10	130	42	13
p-cresol	slug	2600	0.016	1.5E-10	130	42	13
o-cresol	slug	2700	0.016	1.5E-10	130	42	13
3,4-dimethylphenol	slug	3900	0.033	2.7E-11	130	42	13
2,6-dimethylphenol	slug	4800	0.0027	2.2E-11	130	42	13
N,N'-disalicylidene-1,2-diaminopropane	slug	1700	0.0027	9.7E-12	140	42	13
thiophene	slug	2500	0.026	3.1E-10	130	42	13
benzothiophene	slug	17000	0.0075	5.6E-11	130	42	13
MTBE	slug	1100	38	4.3E-7	130	42	13
di-sec-butyl-*p*-phenylenediamine	steady state	69000	7.6E-7	3.4E-15	-	42	13
methanol	slug	880	52	1.6E-6	130	42	13
ethanol	slug	890	50	1.1E-6	130	42	13
benzene	slug	1700	2.9	3.8E-8	130	42	13
toluene	slug	4400	15	1.7E-7	130	42	13
ethylbenzene	slug	10000	3.0	2.8E-8	130	42	13
naphthalene	slug	14000	0.99	7.7E-9	130	42	13

ethanol (neglecting biodegradation), but toluene is expected to require roughly twice as much transport time (4.4 years).

The model predicted high concentrations of both benzene and toluene in the municipal supply well water on a relatively short time frame (less than 5 years). This elicits a need for closer examination, since MTBE has contaminated wells on a widespread basis, whereas benzene and toluene have contaminated a much smaller fraction of municipal wells [20, 22]. Several investigations strongly suggest that BTEX (benzene, toluene, ethylbenzene and xylenes) are relatively degradable under typical aquifer conditions, whereas MTBE degrades very slowly in most aquifers [23-26]. Since degradability was not considered for the purposes of the "screening" model proposed here, the results did not capture this observation. The degradability of BTEX explains the observation that these compounds rarely contaminate water supplies. Nevertheless, the utility of the model is evident. Had a screening transport model been used to assess the potential for groundwater damage from either BTEX or MTBE before they were substantially investigated by scientists and regulators, the results would have clearly advised further study of the biodegradability of these compounds in aquifers.

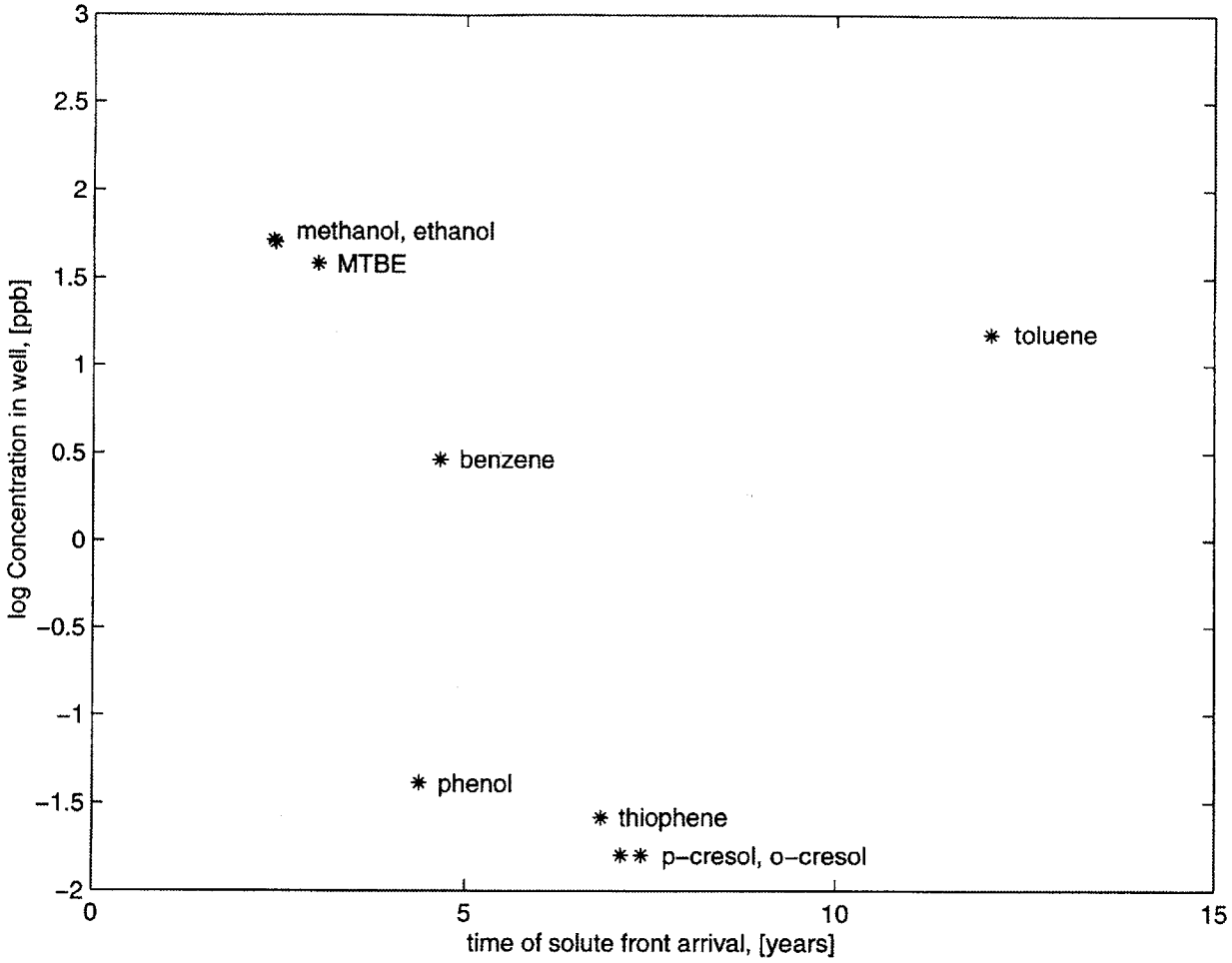

Figure 5-9. Arrival time of solute front vs well water concentration: increased sediment organic matter

Field study results corroborate predicted subsurface retardation values for benzene and MTBE. In a plume characterization by Landmeyer et al., in a silty sand aquifer (sediment organic matter not reported) with an ambient groundwater flow of 0.1 to 0.4 m/day, benzene travelled about 1.25 times more slowly than MTBE (which was considered non-retarded) [27]. Other studies document a retardation factor of 1.2 to 1.3 for benzene in aquifers [28]. Given an aquifer sediment organic matter of 0.1% (the standard case), the transport model computed a retardation factor of 1.15 for benzene and about 1.06 for MTBE, in general agreement with the field study observations.

Several highly polar compounds were predicted in the municipal well water at concentrations an order of magnitude lower than benzene. Phenol, aniline and their methylated analogues approached concentrations of 0.1 ppb in the municipal water. If the groundwater also happened to have a pH near the pK_a of one of these contaminants (< 5 in the case of the substituted anilines and > 9 in the case of the phenols), the contaminant would significantly ionize. However, since the compounds under consideration are experiencing relatively non-

Table 5-16. Transport model results for the decreased well pumping rate (80 gal/min) case

compound	plume type	front arrival time [days]	well concentration [ppb]	[M]	plume spread [m] x	y	z
aniline	slug	920	0.047	5.0E-10	130	42	13
p-toluidine	slug	990	0.065	6.1E-10	130	42	13
o-toluidine	slug	980	0.044	4.1E-10	130	42	13
3,4-dimethylaniline	slug	1200	0.028	2.3E-10	130	42	13
2,6-dimethylaniline	slug	1100	0.028	2.3E-10	130	42	13
phenol	slug	1000	0.32	3.4E-9	130	42	13
p-cresol	slug	1200	0.18	1.6E-9	130	42	13
o-cresol	slug	1200	0.18	1.6E-9	130	42	13
3,4-dimethylphenol	slug	1500	0.044	3.6E-10	130	42	13
2,6-dimethylphenol	slug	1600	0.039	3.2E-10	130	42	13
N,N'-disalicylidene-1,2-diaminopropane	steady state	1000	0.027	9.4E-11	-	42	13
thiophene	slug	1200	0.27	3.2E-9	130	42	13
benzothiophene	slug	4100	0.15	1.1E-9	140	42	13
MTBE	slug	920	230	2.6E-6	130	42	13
di-sec-butyl-*p*-phenylenediamine	steady state	15000	3.8E-6	1.7E-14	-	42	13
methanol	slug	870	260	8.2E-6	130	42	13
ethanol	slug	870	260	5.6E-6	130	42	13
benzene	slug	1000	24	1.3E-7	130	42	13
toluene	slug	1600	210	2.2E-6	140	42	13
ethylbenzene	steady state	2800	69	6.5E-7	-	42	13
naphthalene	slug	3500	19	1.5E-7	140	42	13

retarded slug transport, their subsurface travel times and well concentrations probably would not be significantly affected under these conditions. Therefore, the expected well concentrations of the minor polar constituents are probably too low to be of interest to regulators. However, they are near a concentration range that may pose risks under different conditions (i.e., increased gasoline spill size, decreased well pumping rate of household wells, etc). It is also important to bear in mind that the reported model concentrations reflect a longitudinally averaged plume since uncertainty in hydrogeologic characteristics prevents us from incorporating better resolution of physical processes into the model [29]. The actual risks posed by these compounds was beyond the scope of this work, however, since a review of their known biodegradability in aquifer conditions was not conducted here.

B. Increased sediment organic matter ($f_{om} = 0.005$)

In some water supply aquifers, the retardation of compounds in the subsurface may be underestimated by the standard case. It was thus deemed useful to test the sensitivity of the transport predictions to increased levels of organic matter (Table 5-15, Figure 5-9). By inflating the sediment organic matter abundance 5-fold, the retardation factor was substantially increased

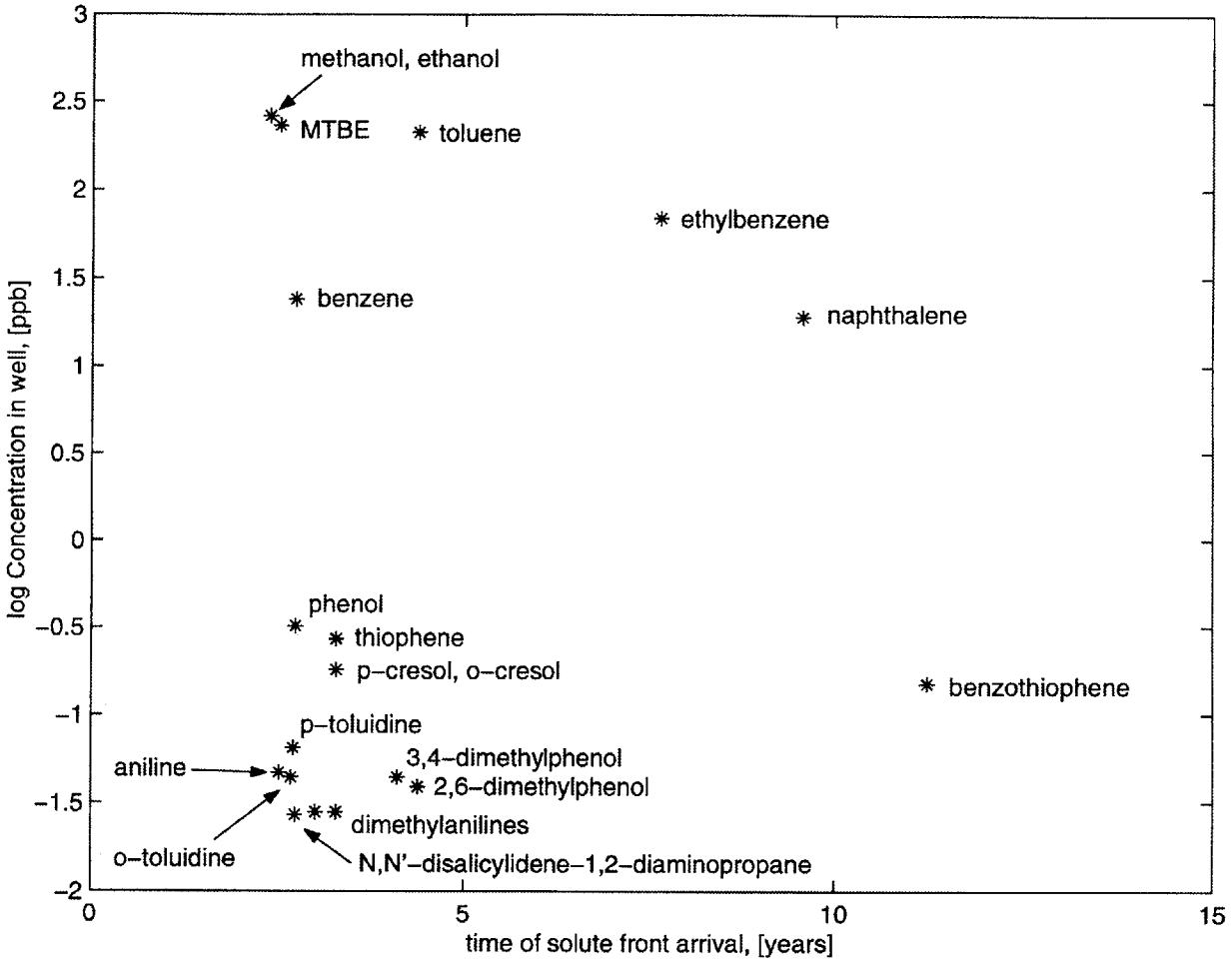

Figure 5-10. Arrival time of solute front vs well water concentration: decreased well pumping rate

for nonpolar compounds such as BTEX and benzothiophene. The expected transport times of benzene and toluene were increased to 5 years and 12 years, respectively. This reflects a retardation factor for benzene of about 2.0, significantly higher than the values of 1.2 to 1.3 previously observed in field studies [27, 28]. The transport behavior of highly soluble compounds such as ethanol and methanol was unaffected by the increased abundance of sediment organic matter. The model predicted a retardation factor of 1.26 for MTBE.

An increased but realistic abundance of sediment organic matter substantially reduced the predicted risk of contamination by nonpolar compounds such as BTEX. However, the predicted arrival times of highly polar fuel components were changed by only months.

C. Decreased well pumping rate (80 gal/min)

The standard transport case represented a system in which the municipal well was of considerable size (400 gal/min), although significantly larger (e.g., ~1000 gal/min) wells are

Table 5-17. Transport model results for the increased spill size (1000 gal) case

compound	plume type	front arrival time [days]	well concentration [ppb]	[M]	plume spread [m] x	y	z
aniline	slug	920	0.093	1.0E-9	130	43	13
p-toluidine	slug	990	0.13	1.2E-9	130	43	13
o-toluidine	slug	980	0.088	8.2E-10	130	43	13
3,4-dimethylaniline	slug	1200	0.055	4.5E-10	130	43	13
2,6-dimethylaniline	slug	1100	0.056	4.6E-10	130	43	13
phenol	slug	1000	0.64	6.8E-9	130	43	13
p-cresol	slug	1200	0.35	3.3E-9	130	43	13
o-cresol	slug	1200	0.35	3.2E-9	130	43	13
3,4-dimethylphenol	slug	1500	0.087	7.1E-10	130	43	13
2,6-dimethylphenol	slug	1600	0.078	6.4E-10	130	43	13
N,N'-disalicylidene-1,2-diaminopropane	steady state	1000	0.030	1.2E-10	-	43	13
thiophene	slug	1200	0.54	6.4E-9	130	43	13
benzothiophene	slug	4100	0.27	2.0E-9	150	43	13
MTBE	slug	920	470	5.3E-6	130	43	13
di-sec-butyl-*p*-phenylenediamine	steady state	15000	4.3E-6	1.9E-14	-	43	13
methanol	slug	870	520	1.6E-5	130	43	13
ethanol	slug	870	520	1.1E-5	130	43	13
benzene	slug	1000	47	6.0E-7	140	43	13
toluene	steady state	1600	550	6E-6	-	43	13
ethylbenzene	steady state	2800	78	7.3E-7	-	43	13
naphthalene	steady state	3500	51	4.0E-7	-	43	13

frequently also implemented. In general, an increased pumping rate was hypothesized to decrease the well water pollutant concentration, because the plume was believed to constitute a small fraction of the capture zone cross-sectional area. In other words, a high pumping rate draws water from a large area, effectively diluting the plume. The calculated transverse plume spread in table 5-16 (42 m) may be compared to a representative capture zone width (350 m, for the standard case) in order to establish the validity of this assumption for a 400 gal/min well.

Similarly, a decreased pumping rate will result in an increased pollutant concentration in the well water, as the contamination plume likely constitutes a larger proportion of the subsurface water drawn into the well. It was important to consider how the transport system would respond to decreased well pumping rate, as this more closely reflects the risks experienced by small communities or household municipal wells (Figure 5-10, Table 5-14). If the well pumping rate was decreased 5-fold to 80 gal/min, the transport model predicted increased solute concentrations by about a factor of 5 relative to the standard case. All other transport characteristics were similar to those predicted in the standard case. This presents the potential for contamination of small wells by possibly relevant concentrations of minor gasoline components such as phenol, the cresols, or thiophene (predicted C_{well} ~ 0.1 to 0.3 ppb).

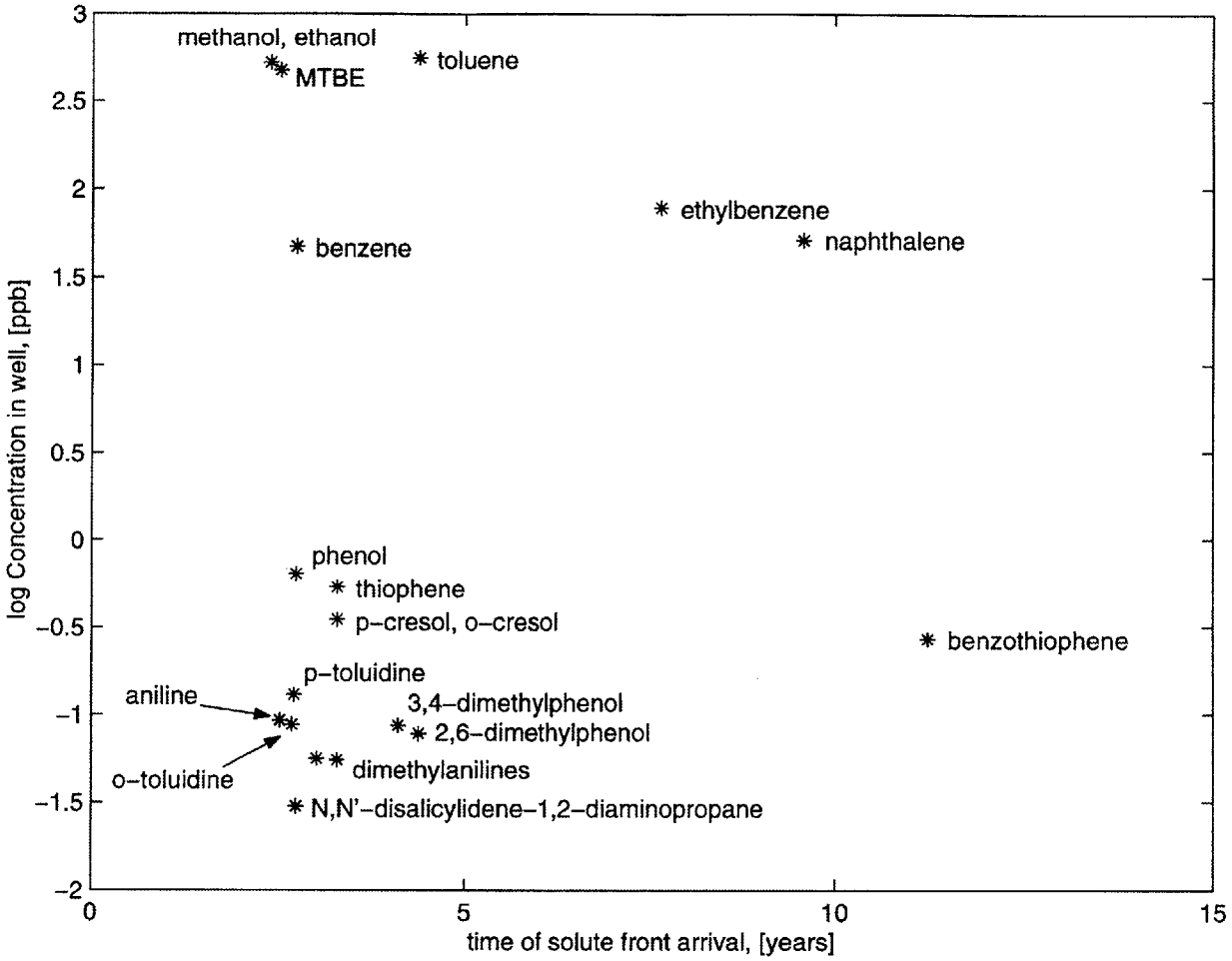

Figure 5-11. Arrival time of solute front vs well water concentration: increased spill size

D. Increased gasoline spill volume (1000 gallons)

If a 10-fold larger NAPL spill was considered, the transport model predicted results similar to the standard case except with solute concentrations increased by a factor of 10 (Table 5-17, Figure 5-11). As discussed previously, this increases the risk posed by minor polar gasoline components that may otherwise appear relatively benign. Phenol, the cresols and thiophene have predicted supply well concentrations approaching 1 ppb and short calculated transport times (less than 3 years) under these conditions.

Discussion and Conclusions: It is important to bear in mind that the pollutant concentrations calculated here reflect uniform hydrogeology and spatial averaging of the plume, as well as many other averaged parameters. The calculated concentrations were therefore useful as order-of-magnitude screening indicators rather than specific predictions. Nevertheless, some important conclusions may be drawn from the results.

Preliminary analyses suggested that the transport model approach was accurate for nondegraded compounds. Several studies suggest that in either aerobic or anaerobic conditions, MTBE degradation in saturated soils is generally slow relative to the transport time of MTBE considered here (900 to 1000 days) [24-26]. MTBE contamination data is therefore useful for validation of the transport model. Inspection of the literature by Johnson et al. shows that municipal wells in the U.S. have been contaminated by as much as 600 ppb MTBE, although this appears rare [20]. However, a substantial number of US community supply wells have documented MTBE levels above 20 ppb. Additionally, studies in Maine suggest that thousands of regional household wells may contain in excess of 35 ppb MTBE contamination [30].

Evidence suggests that most of the household well contamination in Maine may be related to small spills related to homeowner releases or even automobile accidents [20]. The transport model generally predicted the correct range of observed MTBE contamination, calculating 40 to 500 ppb MTBE in community supply wells, depending on conditions (well pumping rate, spill size, etc). It was difficult to draw more specific conclusions about contamination of household wells, since the parameterization of the hydrogeologic model in Chapter 3 was conducted specifically for municipal well supply aquifers. It is clear, however, that the low pumping rates associated with private wells should result in a lower dilution factor and therefore high contaminant concentrations relative to municipal wells, other factors being equal.

While the transport model apparently predicted a similar order of magnitude of MTBE contamination as is observed in nationwide municipal well surveys, the level of uncertainty in the predictions was not quantitatively treated here. As outlined in Chapter 3, the "ensemble" transport model approach was originally aimed at capturing an expected value or average description of gasoline contaminant transport behavior at thousands of potential or existing community supply wells in the US. Accordingly, the physical description and parameters of the transport system were given representative or average characterizations, based on review of relevant literature. However, the information presented did not relate a detailed study of the variability in the model parameters. The next logical step in the analysis developed here would be estimation of variability in the transport model parameters and a detailed study of the resulting overall variability in the model predictions. This might allow the model to reflect the probability distribution of expected outcomes in the transport system; a result that could not be resolved at the current level of analysis.

The general implications of the model predictions regarding different gasoline constituents were clear. The transport model predicted that, if undegraded, oxygenates such as MTBE, ethanol, or methanol will contaminate municipal wells at significant (40 to 500 ppb) levels within short time frames (less than 3 years). Model predictions additionally suggested that benzene and toluene may also create a substantial contamination risk, arriving at wells within 3 to 10 years at well water concentrations of 3 to 50 ppb (for benzene) or 15 to 550 ppb (for toluene). However, past experience with benzene and toluene shows that they are generally degradable in aquifer conditions on such time frames. As a result, these compounds do not pose a large scale contamination risk of the same order as MTBE.

Model predictions also suggested that minor gasoline constituents such as thiophene, phenol, and the cresols, dimethylphenols, and toluidines are less likely than MTBE to present

contamination risks as a result of their lower concentrations in gasoline. However, these minor constituents still approach significant contamination levels under certain conditions. Very realistic changes in parameter values (e.g., increased spill size or low pumping rates of household wells) may easily result in substantial contamination risks from these (minor constituent) compounds if they degrade slowly in the environment. Further analysis of the potential for minor gasoline constituents to contaminate drinking water supplies would therefore constitute a worthwhile future effort.

5-8. Conclusions

The physical property estimation methods demonstrate that with guided effort, partition coefficients can be computed highly accurately for complex solvent systems such as octanol and water. For the more complicated gasoline–water and organic matter–water systems, partitioning can be closely correlated to the K_{ow} for individual compound families. This suggests that, like the K_{ow}, the K_{om} may eventually be predicted with much higher accuracy as well. The estimation methods examined here were sufficiently accurate to be used as a screening tool with a subsurface transport model.

LSERs constitute a promising approach to partition coefficient estimation. A derived K_{gw} LSER modeled known partitioning data with good accuracy, although further validation with a broader range of compound types is needed.

The transport calculations predicted municipal well MTBE concentrations that fall within the same order of magnitude as those observed in nationwide surveys. The preliminary predictions are encouraging, because the model was not "fitted" in any way and was completely derived and parameterized using fundamental physical and chemical transport principles. The accuracy of its results should therefore motivate further validation tests with MTBE and other compounds found in gasoline. Insights gained from MTBE and BTEX predictions led to the conclusion that some previously unstudied minor gasoline constituents, such as thiophene, phenol, p-cresol, o-cresol, p-toluidine, o-toluidine, and dimethylphenols may also pose contamination risks to many U.S. drinking water supplies.

5-9. Citations

1. Leo, A.J. and D. Hoekman, *Calculating logP(oct) with no missing fragments; the problem of estimating new interaction parameters.* Perspectives in Drug Discovery and Design, 2000. **18**: p. 19-38.
2. Leo, A.J. and C. Hansch, *Role of hydrophobic effects in mechanistic QSAR.* Perspectives in Drug Discovery and Design, 1999. **17**: p. 1-25.
3. Hansch, C. and A.J. Leo, *Hydrophobic Parameters*, in *Substituent Constants for Correlational Analysis in Chemistry and Biology.* 1979, Wiley, Inc: New York, NY. p. 13-43.
4. Schmidt, T.C., P. Kleinert, C. Stengel, and S.B. Haderlein, *Polar fuel constituents - compound identification and equilibrium partitioning between non-aqueous phase liquids and water.* 2001.
5. Cline, P.V., J.J. Delfino, and P.S.C. Rao, *Partitioning of aromatic constituents into water from gasoline and other complex solvent mixtures.* Environmental Science & Technology, 1991. **25**: p. 914-920.
6. Heermann, S.E. and S.E. Powers, *Modeling the partitioning of BTEX in water-reformulated gasoline systems containing ethanol.* Journal of Contaminant Hydrology, 1998. **34**: p. 315-341.
7. Stephenson, R.M., *Mutual solubilities: water-ketones, water-ethers, and water-gasoline-alcohols.* Journal of Chemical Engineering Data, 1992. **37**: p. 80-95.
8. Goss, K.U. and R.P. Schwarzenbach, *Linear free energy relationships used to evaluate equilibrium partitioning of organic compounds.* Environmental Science & Technology, 2001. **35**: p. 1-9.
9. Schubert, A.J. and N.G. Johansen, *Cooperative study to evaluate a standard test method for the speciation of gasolines by capillary gas chromatography.* Society of Automotive Engineering, 1993(930144).
10. CRC, *Physical Constants of Organic Compounds*, in *Handbook of Chemistry and Physics*, D. Lide, Editor. 1997, CRC Press, Inc: Boca Raton, FL.
11. Martin, P., F. McCarty, U. Ehrmann, L.D. Lima, N. Carvajal, and A. Rojas, *Characterization and deposit-forming tendency of polar compounds in cracked components of gasoline. Identification of phenols and aromatic sulfur compounds.* Fuel Science and Technology International, 1994. **12**(2): p. 267-280.
12. Quimby, B.D., V. Giarrocco, J.J. Sullivan, and K.A. McCleary, *Fast analysis of oxygen and sulfur compounds in gasoline.* Journal of High Resolution Chromatography, 1992. **15**: p. 705-709.
13. Heath, M.T., *Scientific Computing.* 1997, Boston, MA: McGraw Hill. p. 134.
14. Abraham, M.H., C.F. Poole, and S.K. Poole, *Classification of stationary phases and other materials by gas chromatography.* Journal of Chromatography A, 1999. **842**: p. 79-114.
15. Abraham, M.H., A.-H. J, G.S. Whiting, A. Leo, and R.S. Taft, *Hydrogen bonding. Part 34. The factors that influence the solubility of gases and vapours in water at 298 K, and a new method for its determination.* Journal of the Chemical Society, Perkins Transactions 2, 1994: p. 1777-1791.

16. Abraham, M.H., H.S. Chadha, G.S. Whiting, and R.C. Mitchell, *Hydrogen-bonding. 32. An analysis of water-octanol and water-alkane partitioning and the delta-logP parameter of Seiler.* Journal of Pharmaceutical Sciences, 1994. **83**(8): p. 1085-1100.
17. Schwarzenbach, R.P., P.M. Gschwend, and D.M. Imboden, *Environmental Organic Chemistry.* 1993, New York, NY: John Wiley & Sons. p. 271-272, 291, 618.
18. Press, W.H., S.A. Teukolsky, W.T. Vetterling, and B.P. Flannery, *Numerical Recipes in C: The Art of Scientific Computing.* 1993, Cambridge: Cambridge University Press. p. 676-681.
19. Owen, K., *Gasoline and Diesel Fuel Additives*, ed. T.S.o.C. Industry. 1989: John Wiley & Sons.
20. Johnson, R., J.F. Pankow, D. Bender, C. Price, and J.S. Zogorski, *MTBE, To what extent will past releases contaminate community water supply wells?* Environmental Science & Technology, 2000. **34**(9): p. 2A-9A.
21. Howard, P.H. and W.M. Meylan, *Handbook of Physical Properties of Organic Chemicals.* 1997, Boca Raton: CRC Press.
22. Squillace, P.J., M.J. Moran, W.W. Lapham, C.V. Price, R.M. Clawges, and J.S. Zogorski, *Volatile organic compounds in untreated ambient groundwater of the United States.* Environmental Science & Technology, 1999. **33**: p. 4176-4187.
23. Rifai, H.S., R.C. Borden, J.T. Wilson, and C.H. Ward, *Intrinsic bioremediation for subsurface restoration*, in *Intrinsic Bioremediation*, R. Hinchee, J. Wilson, and D. Downey, Editors. 1995, Batelle Press: Columbus, OH. p. 1-29.
24. Yeh, C.K. and J.T. Novak, *Anaerobic biodegradation of gasoline oxygenates in soils.* Water Environment Research, 1994. **66**(5): p. 744-752.
25. Horan, C.M. and E.J. Brown. *Biodegradation and inhibitory effects of methyl-tertiary-butyl ether (MTBE) added to microbial consortia.* in *10th Annual Conference on Hazardous Waste Research.* 1995. Kansas State University, Manhattan, KS. p. 11-19.
26. Hubbard, C.E., J.F. Barker, S.F. O'Hannesin, M. Vandegriendt, and R.W. Gillham, *Transport and Fate of Dissolved Methanol, Methyl-tertiary-butyl Ether, and Monoaromatic Hydrocarbons in a Shallow Sand Aquifer.* 4601, American Petroleum Institute, 1994.
27. Landmeyer, J.E., F.H. Chapelle, P.M. Bradley, J.F. Pankow, C.D. Church, and P.G. Tratnyek, *Fate of MTBE relative to benzene in a gasoline-contaminated aquifer.* Groundwater Monitoring and Remediation, 1998(Fall): p. 93-102.
28. Knox, R.C., D.A. Sabatini, and L.W. Canter, *Subsurface Fate and Transport Processes.* 1993, Boca Raton, FL: Lewis Publishers.
29. Kitanidis, P.K., *The concept of the dilution index.* Water Resources Research, 1994. **30**(7): p. 2011-2026.
30. Maine, *The presence of MTBE and other gasoline compounds in Maine's drinking water: preliminary report*, Bureau of Health, Bureau of Waste Management and Remediation, Maine Geological Survey, 1998.

Chapter 6
Summary and Conclusions

The goal of this work was to characterize the subsurface transport of gasoline solutes from leaking underground fuel tanks (LUFTs) and the corresponding national impact on drinking water wells. The transport model provided a preliminary screening assessment of the need for biodegradability testing, health screening tests, and more extensive environmental impact studies of compounds added to or found in gasoline. This approach is proposed as a general screening tool for future gasoline additives and reformulations. Additionally, a similar approach could be used to assess the possible risks associated with JP (aviation) and diesel fuels. If proposed fuel additives (such as alkylates, recently proposed for use in gasoline) were methodically screened before implementation, nationwide drinking water contamination events such as that caused by MTBE could be easily avoided.

In Chapter 2, gasoline was reported to include a number of polar organic compounds at concentrations ranging from a few ppm to mass percent levels. Many of these compounds are highly water-soluble and are therefore likely to transport large distances rapidly in the subsurface. However, they are neither studied in environmental literature nor mentioned in community or government agency regulatory guides as potential contamination threats to drinking water. Consequently, like MTBE, they are useful test subjects for developing a subsurface transport screening methodology.

In Chapter 3, it was proposed that the hydrogeological parameters which describe subsurface transport near shallow drinking water wells are not highly variable when the large majority of sites in the U.S. is considered. Aquifers chosen as community drinking water supplies require a substantial pumping capacity and are usually composed of porous, highly conductive, unconsolidated sediments. As a result, the characteristics of these aquifers can be generalized for transport calculation purposes. Combined with information about typical distances between community supply wells and LUFTs and groundwater flow rates, preliminary transport calculations can be conducted for novel organic compounds added to gasoline.

After establishing the subsurface hydrogeology of the system, contaminant physical properties were needed to parameterize the transport model. Environmentally relevant partition coefficients for the vast majority of compounds that are used in industry or commerce have not been measured. In the interest of developing the model as a screening tool, it was assumed that the partition coefficients of future or proposed gasoline additives or reformulations may not be known *a priori* and therefore must be estimated. Chapter 4 outlined the current state of partition coefficient estimation for organic compounds in gasoline–water (K_{gw}), octanol–water (K_{ow}), and organic matter–water (K_{om}) mixture pairs. Traditional empirical group contribution calculations such as UNIFAC and AQUAFAC demonstrate accuracy within an order of magnitude for K_{gw} and K_{ow}. Quantum mechanically based calculation methods are rapidly becoming competitive, but require further validation before they may be considered comprehensively accurate.

Linear solvation energy relationships (LSERs) have been suggested as models for partitioning in a number of liquid mixture and gas phase systems. They appear more accurate than

any other method reviewed for finding partition coefficients in general. However, LSER calculations require both regression parameters for individual partitioning systems and independently derived solute solvation parameters. Solvation parameters have been compiled for hundreds of compounds [1, 2], but their measurement or derivation for novel compounds is not necessarily trivial, as is discussed elsewhere [3].

In Chapter 5, subsurface transport calculations and physical property estimation methods were applied to 21 solutes found in gasoline. Linear free energy relationship regressions between K_{gw} and K_{ow} produced good fits only for individual compound families, and therefore may not be generally applicable for other types of organic compounds. A linear solvation energy relationship was derived for K_{gw}, providing an additional tool for future calculations. The estimated K_{gw} LSER standard error of 0.22 log K_{gw} units was determined from a validation test of model predictions against independent data. The LSER regression suggested that, similar to previously studied hexadecane–water and cyclohexane–water systems, partitioning in the gasoline–water system was controlled primarily by solute volume, solute basicity, and solute acidity.

The transport model calculated a municipal well MTBE concentration range of 40 to 500 ppb, depending on parameter settings. These calculations agree with observations in nationwide community water supply surveys, which report observed municipal supply well MTBE concentrations of 20 to 600 ppb. The model demonstrated good predictive capability considering that it was not fitted in any way and was derived only from physical and chemical transport principles. The expected variability in the transport model predictions resulting from parameter variability was not analyzed, however. Therefore, insight into the probability distribution of predicted transport outcomes was not resolved.

The transport model predicts essentially unretarded migration of MTBE, methanol and ethanol in the subsurface, calculating municipal well concentrations of 40 to 500 ppb for these solutes. This is a realistic result for MTBE, which has been found highly resistant to biodegradation in a range of subsurface environments. It seems likely that methanol and ethanol may experience significant biodegradation on the time scale of interest in the transport model (850 to 950 days). However, the potential health impact of methanol contamination of drinking water wells may still be substantial. The transport model predicts retarded migration of benzene, toluene and ethylbenzene to municipal wells, with significant expected concentrations (10 to 500 ppb). Large scale surveys do not generally support this prediction [4]. This should not be a surprising result, as BTEX are believed relatively biodegradable on the time scale of transport in the model (3 to 10 years) [5].

Transport predictions for oxygenates should be interpreted carefully. If future oxygenates or other highly mobile compounds added to fuels are reasonably biodegradable on transport time scales (unlike MTBE), these compounds may quickly consume the available dissolved oxygen in the path of the plume. In this case, other compounds which are difficult to degrade under anaerobic conditions (such as benzene) may suddenly pose a much more significant threat [6].

According to the transport model, other studied solutes may be found in municipal wells at environmentally relevant concentrations. Cresols, toluidines, and thiophene are predicted to contaminate municipal wells at low ppb levels, depending on model parameter settings. These

transport predictions may not appear to constitute an important risk. However, if any of these minor gasoline constituents are persistent (non-degraded) in the subsurface and toxic to human health, widespread and hazardous exposures could quickly result. Additionally, such exposures could remain undetected for years, even if they occurred on a large scale. The transport model results demonstrate that minor gasoline constituents can and should be screened as possible drinking water pollutants. These compounds are not "obvious" culprits as large scale contaminants and are therefore unlikely to receive due attention.

The combined physical property estimation and transport model approach was both feasible and useful as a screening tool for predicting gasoline additive exposures resulting from subsurface spills. Predictions of MTBE contamination of drinking water wells showed good agreement with field observations. The transport model was poor as a site-specific model of subsurface transport, relative to the current state of the science. Rather, it was designed to assess the potential exposures related to subsurface contamination from thousands of gasoline spills. Thus, it could quantitatively guide regulators and industry in understanding a critical aspect of the social and environmental costs of individual gasoline formulations and additives.

Citations

1. Abraham, M.H., H.S. Chadha, G.S. Whiting, and R.C. Mitchell, *Hydrogen-bonding. 32. An analysis of water-octanol and water-alkane partitioning and the delta-logP parameter of Seiler.* Journal of Pharmaceutical Sciences, 1994. **83**(8): p. 1085-1100.
2. Abraham, M.H., A.-H. J, G.S. Whiting, A.J. Leo, and R.S. Taft, *Hydrogen bonding. Part 34. The factors that influence the solubility of gases and vapours in water at 298 K, and a new method for its determination.* Journal of the Chemical Society, Perkins Transactions 2, 1994: p. 1777-1791.
3. Abraham, M.H., C.F. Poole, and S.K. Poole, *Classification of stationary phases and other materials by gas chromatography.* Journal of Chromatography A, 1999. **842**: p. 79-114.
4. Squillace, P.J., M.J. Moran, W.W. Lapham, C.V. Price, R.M. Clawges, and J.S. Zogorski, *Volatile organic compounds in untreated ambient groundwater of the United States.* Environmental Science & Technology, 1999. **33**: p. 4176-4187.
5. Rifai, H.S., R.C. Borden, J.T. Wilson, and C.H. Ward, *Intrinsic bioremediation for subsurface restoration*, in *Intrinsic Bioremediation*, R. Hinchee, J. Wilson, and D. Downey, Editors. 1995, Batelle Press: Columbus, OH. p. 1-29.
6. Chapelle, F.H., *Bioremediation of petroleum hydrocarbon-contaminated ground water: the perspectives of history and hydrology.* Ground Water, 1999. **37**: p. 122-132.

Appendix

Transport program C++ code

This code and the compiled executables (for Windows and Unix (Solaris) systems) are available in electronic format from the author.

```
#include <iostream.h>

#include <math.h>

#include <fstream.h>

#include <string>

#include <iomanip.h>


void WELCOME(void);


double ROUND(double, int);


void READ_SPILL_DATA(char *, double &, double &, double &, double &, double &, double &);


void READ_ENV_DATA(char *, double &, double &, double &, double &, double &, double &, double &, double &, double
&, double &);


double PLUME_INIT(double &, double &);


void WRITEFILE(char *, string, double, double, double, double, double, double);


int main()
{
 const double Pi = 3.14159265;
 char *datafile = "transport_parms.dat";


 WELCOME();
 // cout << "Please enter a one-word abbreviation for the compound name\n"
 //    << "in ten letters or less:\n? ";
 // cin >> compoundname;


 double Cf, Kfw, Kom;     // partition constants, fuel concentration
 double mw;               // molecular weight
 double V_NAPL, H_NAPL;     // NAPL spill volume, NAPL spill thickness
 double fuel_density = 0.75;


 READ_SPILL_DATA(datafile, mw, Cf, Kfw, Kom, V_NAPL, H_NAPL);


 double fom, porosity, sed_density;  // aquifer sediment properties
 double v, H;             // groundwater velocity, aquifer thickness
 double ax, ay, az;       // dispersivities
 double Qwell, Lx;        // well pumping rate, distance from spill


 READ_ENV_DATA(datafile, fom, porosity, sed_density, v, H, ax, ay, az, Qwell, Lx);


 // DATA CHECK:
```

```
cout << "\n\n      - - - PRELIMINARY DATA CHECK - - -\n";
cout << "\n solute molec wt = " << mw << endl;
cout << " solute fuel concentration = " << Cf << " ppm\n";
cout << " solute Kfw = " << Kfw << endl;
cout << " solute Kom = " << Kom << endl;
cout << " NAPL volume = " << V_NAPL << " m^3 = "
    << ROUND(264.2*V_NAPL,3) << " gallons\n";
cout << " NAPL thickness = " << H_NAPL << " m\n";
cout << " fraction of organic matter = " << fom << endl
    << " porosity = " << porosity << endl
    << " sediment density = " << sed_density << " g/cm^3\n"
    << " groundwater longitudinal velocity = " << v << " m/day\n"
    << " aquifer saturated thickness = " << H << " m\n"
    << " dispersivities (in meters) = " << ax << " [x]  " << ay << " [y]  " << az << " [z]" << endl
    << " well pumping rate = " << Qwell << " m^3/day\n"
    << " distance to the supply well = " << Lx << " m\n";


// MAIN PROGRAM ALGORITHM


double mass = Cf*fuel_density*V_NAPL;  // total mass of compound, in [g]


double Ex, Ey, Ez;  // dispersion coefficients


Ex = ax*v;
Ey = ay*v;
Ez = az*v;


double Cw;    // aqueous equilibrium concentration with fuel, mol/L
double R;     // retardation factor


Cw = (Cf*fuel_density/(mw*1000))/Kfw;          // Cw is in mol/L
double Cwppm = Cw*mw*1000;                     // Cwppm is in ppm


R = 1 + fom*Kom*sed_density*(1-porosity)/porosity;


double r;     // radius of NAPL spill


r = sqrt(V_NAPL/(Pi*H_NAPL));


double az_spill = 0.002;  // vertical dispersivity on a 10 m scale, (Gelhar)


// Estimation of the initial plume cross_section
double A = PLUME_INIT(r, az_spill);


double t_depletion = -porosity*V_NAPL*Kfw*log(0.25)/(A*v);


double length_init = v*t_depletion/R;     // initial length in x direction


if (length_init < 2*r)     // lower bound is size of spill
  length_init = 2*r;



double DEVy_init = 2*r;
```

```
double DEVz_init = sqrt(2*az*2*r);



double Tarr;  // arrival time of the front of the solute plume

Tarr = (R/v)*(Lx + Ex/v - sqrt(Ex*Ex/(v*v) + 2*Ex*Lx/v));



double Tarr_plugflow = Lx*R/v;  // arrival time for plug flow front


double DEVx_final = sqrt( pow(length_init,2)/12 + 2*Ex*Tarr/R );
double DEVy_final = sqrt( pow(DEVy_init,2) + 2*Ey*Tarr/R );
double DEVz_final = sqrt( pow(DEVz_init,2) + 2*Ez*Tarr/R );


string transport_type;
double dmdt_well;


if ( length_init < 2*sqrt(2*ax*Lx))     //  slug type transport
{
 dmdt_well = mass*v/(2*DEVx_final*R);        // units: g/day
 transport_type = "slug";
}
else                                 // steady state type transport
{
 dmdt_well = (A/porosity)*v*mass/(V_NAPL*Kfw);  // units: g/day
 transport_type = "steady state";
}


double Cwellppm = dmdt_well/Qwell;                  // units: mg/L
double Cwell = Cwellppm/(1000*mw);                   // units: mol/L


double b = Qwell/(v*H*porosity);          // capture zone width


// SUMMARY AND RESULTS


string go;

cout << "\npress any key followed by a return to continue\n";
cin >> go;


cout << "\n    - - - TRANSPORT.C FULL RESULTS - - -\n";


cout << "\nThe time of arrival of the solute front is "
    << ROUND(Tarr,2) << " days."
    << "\nThe plug-flow time of arrival is "
    << ROUND(Tarr_plugflow,2) << " days.\n"
    << "\nThe initial plume length is "
    << ROUND(length_init,2) << " meters\n"
    << "\nThe initial spread of the plume is:\n"
    << "\t[y] " << ROUND(DEVy_init,2) << " meters\n"
    << "\t[z] " << ROUND(DEVz_init,2) << " meters\n"
    << "\nThe plume transport type is '" << transport_type << "'.\n";
```

```
  cout << "\nThe final spread of the plume is:\n";
  if (transport_type == "slug")
    cout << "\t[x] " << ROUND(DEVx_final,2) << " meters\n";
  cout << "\t[y] " << ROUND(DEVy_final,2) << " meters\n"
       << "\t[z] " << ROUND(DEVz_final,2) << " meters\n"
       << "\nThe width of the well capture zone is " << ROUND(b,2)
       << " meters.\n"
       << "\nThe aqueous concentration at the spill is:\n"
       << "\t" << ROUND(Cw,2) << " mol/L     "
       << " or    " << ROUND(Cwppm,2) << " ppm\n"
       << "\nThe aqueous concentration in the well is:\n"
       << "\t" << ROUND(Cwell,2) << " mol/L     "
       << " or    " << ROUND(Cwellppm,2) << " ppm\n\n";


  // DEBUGGING CODE
  //  cout << "The final dev(x) should be " << sqrt(pow(DEVx_init,2) + 2*Ex*Tarr/R)  << endl;
  //  cout << "The Tarr should be " << (Lx - sqrt(2*(Ex/R)*Tarr))*R/v << endl;


  char* outfilename = "transport.out";


  string writebool;


  cout << "Write results to file " << outfilename << " ? [y or n]: ";
  cin >> writebool;


  if (writebool == "y")
  {
    WRITEFILE(outfilename, transport_type, Tarr, Cwell, Cwellppm, DEVx_final, DEVy_final, DEVz_final);
  }


  return 0;
}



void WELCOME()
{
  cout << "                          * * *  * * * *"
       << "\nNOTE TO USER:  Welcome to transport.c, a program designed to "
       << "characterize\nthe contamination plume created by gasoline "
       << "components.  Change inputs\nusing the transparms.dat parameter "
       << "file.  This program is not exception-\nhandled and will bail "
       << "if the parameter file is incorrectly modified.";
}


double ROUND(double x, int sigfigs)  // round double to int sigfigs
{
  double x_rounded = 0;
  double mag = ceil(log10(fabs(x)));


  //  if (floor(x/pow(10,mag-2)) <= 15)  // if 1st digit < 1.5, increase sigfigs
  //    sigfigs = sigfigs + 1;


  x_rounded = pow(10,mag-sigfigs)*floor(x/pow(10,mag-sigfigs) + 0.5);


  return x_rounded;
}
```

```
}


void READ_SPILL_DATA(char *datafile, double &mw, double &Cf, double &Kfw, double &Kom, double &V_NAPL, double
&H_NAPL)
{
 ifstream infile(datafile, ios::in);
 if (!infile)
 {
  cerr << "\nWhere the heck is '" << datafile << "'?!!  "
       << "I can't find it.\nA program needs data to run, you know..."
       << "\nExiting.\n\n";
  exit(1);
 }


 string dummy, dummy2;


 while (infile >> dummy)
 {
  if (dummy2 == "molecular" && dummy == "weight")
    infile >> mw;
  if (dummy2 == "fuel" && dummy == "concentration")
  {
    infile >> dummy;
    infile >> Cf;
  }
  if (dummy == "Kfw")
    infile >> Kfw;
  if (dummy == "Kom")
    infile >> Kom;
  if (dummy2 == "NAPL" && dummy == "volume")
  {
    infile >> dummy;
    infile >> V_NAPL;
  }
  if (dummy2 == "lens" && dummy == "thickness")
  {
    infile >> dummy;
    infile >> H_NAPL;
  }

  dummy2 = dummy;
 }
}


void READ_ENV_DATA(char *datafile, double &fom, double &porosity, double &density, double &v, double &H, double
&ax, double &ay, double &az, double &Qwell, double &Lx)
{
 ifstream infile(datafile, ios::in);
 if (!infile)
 {
  cerr << "\nWhere the heck is '" << datafile << "'?!!  "
       << "I can't find it.\nA program needs data to run, you know..."
       << "\nExiting.\n\n";
  exit(1);
 }


 string dummy, dummy2;


 while (infile >> dummy)
 {


  if (dummy == "fom")
    infile >> fom;
```

```
    if (dummy == "porosity")
      infile >> porosity;
    if (dummy2 == "sediment" && dummy == "density")
    {
      infile >> dummy;
      infile >> density;
    }
    if (dummy2 == "groundwater" && dummy == "velocity")
    {
      infile >> dummy;
      infile >> v;
    }
    if (dummy2 == "saturated" && dummy == "thickness")
    {
      infile >> dummy;
      infile >> H;
    }
    if (dummy == "a(x)")
    {
      infile >> dummy;
      infile >> ax;
    }
    if (dummy == "a(y)")
    {
      infile >> dummy;
      infile >> ay;
    }
    if (dummy == "a(z)")
    {
      infile >> dummy;
      infile >> az;
    }
    if (dummy2 == "pumping" && dummy == "rate")
    {
      infile >> dummy;
      infile >> Qwell;
    }
    if (dummy2 == "well" && dummy == "distance")
    {
      infile >> dummy;
      infile >> Lx;
    }

    dummy2 = dummy;
  }
}


double PLUME_INIT(double &r, double &az)
{
  double Area = 0;
  int N = static_cast<int>(r*1000);
  double del = static_cast<int>(r*1000)/(1000*static_cast<double>(N));


  for (int i = 0; i < N; i++)
    Area += del*pow((r*r - pow((i*del + del/2),2)),0.25);


  Area = 2*2*sqrt(az)*Area;


  return Area;
}


void WRITEFILE(char *filename, string transport_type, double Tarr, double Cwell, double Cwell_ppm, double DEVx_final,
double DEVy_final, double DEVz_final)
{
  int newfile_flag = 0;
```

```
ifstream findfile(filename, ios::in);
if (!findfile)
  newfile_flag = 1;


if (newfile_flag == 0)
{
  findfile >> dummy;
  findfile >> dummy2;

  if (dummy != "***" || dummy2 != "TRANSPORT.C")
  {
    cerr << "             *** ERROR ***\n"
         << "You have designated the file '" << filename << "' for "
         << "another use.\nTransport.c will not produce an output summary "
         << "file until the filename\n'" << filename << "' is available for "
         << "writing.\nExiting.\n";
    exit(1);
  }
}


if (newfile_flag == 0)
{
  while (findfile >> dummy)
    if (dummy == "slug" || dummy == "steady")
      runs_counter++;
}


findfile.close();


ofstream outfile(filename, ios::app);


if (newfile_flag == 1)
{
  cout << "This is run # 1\n";
  outfile << setw(55) << "*** TRANSPORT.C RESULTS SUMMARY **\n\n"
    //          << setw(5) << "trial"
          << setw(13) << " t_arr "
          << setw(10) << "C_well"
          << setw(10) << "C_well"
          << setw(25) << "plume dispersion, [m]"
          << setw(14) << "transport" << endl
          << setw(6) << "run#  "
          << setw(7) << "[days]"
          << setw(10) << "[ppb] "
          << setw(10) << "[M] "
          << setw(7) << "x"
          << setw(7) << "y"
          << setw(7) << "z"
          << setw(15) << "type" << endl;
}


if (newfile_flag == 0)
  cout << "This is run # " << runs_counter << endl;


outfile << setw(2) << runs_counter
        << setw(10) << ROUND(Tarr,2)
        << setw(10) << ROUND(Cwell_ppm*1000,2)
        << setw(11) << ROUND(Cwell,2);
if (transport_type == "steady state")
  outfile << setw(8) << "- ";
else
  outfile << setw(8) << ROUND(DEVx_final,2);
```

```
  outfile << setw(7) << ROUND(DEVy_final,2)
        << setw(7) << ROUND(DEVz_final,2)
        << "       " << transport_type << endl;


}
```